UNIVERSITY OF CALIFORNIA,
IRVINE

Using Murine Bone Marrow Transplantation to Understand Hematopoietic Stem Cell Development and to Explore Possible Treatments for Blood Disorders

DISSERTATION

submitted in partial satisfaction of the requirements
for the degree of

DOCTOR OF PHILOSOPHY

in Biological Sciences

by

Erika Synthie Varady

Dissertation Committee:
Professor Matthew Inlay, Chair
Professor Matthew Blurton-Jones
Professor Craig Walsh

2021

DEDICATION

To my loving parents, Ann and Gabriel,

my Grandmother Ilona,

and my best friend Nyles.

TABLE OF CONTENTS

LIST OF FIGURES

Page

LIST OF SUPPLEMENTAL FIGURES AND TABLES

ACKNOWLEDGEMENTS

I would like to express my appreciation for everything Dr. Matthew Inlay did for me. He is an amazing and helpful PhD advisor who has guided me through graduate school. His mentoring style allowed me to become an independent scientist and tackle challenges on my own and I am very grateful for that. Dr. Inlay is also a great friend and I appreciate all the life advice he has given me. His wife, Dr. Connie Inlay, is also an amazing person who positively impacted my graduate experience by encouraging me, being kind and understanding, and helping me find a job after graduate school. Thank you, Matt and Connie. I wish you and your family all the happiness and good fortune for the future.

I would like to thank my PhD committee members, Dr. Craig Walsh and Dr. Mathew Blurton-Jones for giving me great scientific advice and suggestions that pushed my projects forward in the right direction. They are also very kind and patient mentors which made my committee meetings very enjoyable. In addition, I have had many great collaborators throughout my graduate career. Working with the Blurton-Jones lab and the Walsh lab was a joyful experience, and I am grateful for their advice and friendship. I want to give a special thanks to Alborz Karimzadeh for training me during my rotation and first year as a graduate student. I appreciate him taking the time to teach me invaluable laboratory techniques.

I am thankful for the Oxnard Foundation for their generous financial contribution to my research. Their donation funded my graduate stipend and materials throughout my graduate career. I appreciate their motivation to help people who struggle with challenging life-altering diseases such as Idiopathic Thrombocytopenic Purpura (ITP).

Vanessa Scarfone is a great colleague who not only has helped me with flow cytometry but has also been a magnificent friend. I would like to thank her for caring about my mental well-being and for inspiring me to have strength. I would also like to express my deep gratitude to me dear friend Pauline Nguyen. She has contributed much needed joy and laughter into my PhD life. Mentoring her was one of my greatest honors. Vanessa and Pauline have brought light to my graduate experience.

I would like to thank the previous Inlay lab members Tannaz Faal, Yasamine Ghorbanian, and Karin Grathwohl for their friendship and support in my early PhD years. These women have provided a positive laboratory environment which made me look forward to going into lab every day.

I would not be here if it was not for the guidance and support from my previous mentors Dr. Mi-Jeong Kim, Dr. Georgios Vidalakis, Dr. Greg Douhan, Dr. Sohrab Bodaghi, Dr. Tom Serwold, Dr. Anupama Dahanukar, Dr. Venkatesh Sivanandam, and Dr. A.L.N. Rao. I am indebted to these scientists for taking the time to teach and train me when I was a starting scientist. The University of California Riverside honors program community has also helped me achieve my goals by pushing me intellectually and giving me a great support system as an undergraduate student. Finally, I would like to express my deepest gratitude towards my close friends and family for giving me courage to get through my PhD and for supporting me throughout this journey.

VITAE

Erika S. Varady

PROFESSIONAL PROFILE

- Immunologist and stem cell biologist trained in preclinical research to treat blood disorders including autoimmune disease and Graft-vs-host-disease (GvHD) using mouse models
- Spearheaded project on treating T cells with a glucocorticoid to create immunogenic tolerance and reduce GvHD in allogeneic bone marrow transplantation (BMT)
- Highly motivated to improve patients' lives by better understanding and improving immunotherapies
- Experienced in mentoring junior scientists and providing guidance throughout their research

AREAS OF EXPERIENCE

Flow Cytometry

12+ color analyzer (BD Fortessa and LSRII)

Cell sorter (BD Aria II and AutoMACs)

Immunology and Molecular Biology

T cell *in vitro* and in *vivo* assays (MLR, T cell activation, expansion, adoptive transfer), cell culture, ELISA, qPCR (QuantStudio 6 & 7), PCR, cloning, western blot, CRISPR mouse model design (ITP), human PBMC isolation and culture.

Stem Cell Biology

Murine hematopoietic stem cell culture, isolation and sorting (embryonic and adult), small molecule co-cultures, migration assays, and *in vivo* transplantation assays (adult and neonatal), some mouse surgery.

Mouse models

Tissue harvesting and processing, blood collection, embryo harvesting and dissections, irradiation, injection, animal husbandry, disease models (ITP, GvHD), use of transgenic and immunodeficient mice

Microscopy and Histology

Cryostat, microtome, H&E staining, immunofluorescence/ immunohistochemistry, Olympus FV3000, Keyence, Nikon SMZ1500.

Software

FlowJo, BD FACSDiva, FCS Express, GraphPad Prism, Adobe Photoshop, Microsoft Office.

Mentoring

Undergraduate students (3), Graduate students (2)

EDUCATION

UNIVERSITY of CALIFORNIA, IRVINE, Irvine, CA 2016-2021

Ph.D., Molecular Biology and Biochemistry, Projected graduation August 2021

UNIVERSITY of CALIFORNIA, RIVERSIDE, Riverside, CA 2012-2016

B.S., Biology

EXPERIENCES

UNIVERSITY of CALIFORNIA, IRVINE Irvine, CA

Ph.D. in Molecular Biology and Biochemistry, Inlay lab 2016- 2021

- For my thesis project, I have successfully improved BMT in mice by increasing murine hematopoietic stem cell bone marrow engraftment and decreasing GvHD after mouse allogeneic transplantation.
- Developing and characterizing a novel mouse model for idiopathic thrombocytopenic purpura.
- Identified a surface marker signature to select for hematopoietic stem cells and its embryonic precursor cell, using flow cytometry, cell sorting, stem cell transplantation and lineage tracing in mice.
- Collaborated with a neuroscience lab to use BMT to recapitulate T cells in the mouse brain.
- Led a project on characterizing a potentially novel primitive T cell progenitor from mouse embryo.

JOSLIN DIABETES CENTER, Harvard Medical School Boston, MA

Summer Undergraduate Internship Summer 2015

Department of Immunobiology, Serwold Lab

- Screened a panel of proteins to differentiate murine common lymphoid progenitors into mature T cells *in vitro*.

UNIVERSITY of CALIFORNIA, RIVERSIDE Riverside, CA

Undergraduate Research 2013- 2016

Department of Microbiology and Plant Pathology, Vidalakis Lab and Rao Lab, and Department of Molecular Cell and Systems Biology, Dahanukar Lab

- University honors program thesis project where I isolated, identified and characterized DNA microsatellite markers in the *Penicillium digitatum* genome (Vidalakis Lab).
- Worked with a team to characterize and screen amino acid taste receptors in *Drosophila melanogaster* by knocking out potential receptors and conducting feeding choice assays (Dahanukar Lab).

- Worked alongside a graduate student to test if the *Tomato aspermy virus* replicase could repair the *Cucumber mosaic virus* satellite RNA using molecular cloning and agroinfiltration when infecting *Nicotiana benthamiana (Rao Lab).*

PUBLICATIONS

1. **E.S. Varady**, L.A. Ayala, P.U. Nguyen, M.A. Inlay. Fluticasone Propionate (Flonase) improve stem cell transplantation in mice by increasing hematopoietic stem cell engraftment and decreasing graft vs host disease severity. (Manuscript in preparation).
2. A. Karimzadeh, **E.S. Varady**, V.M. Scarfone, C. Chao, K. Grathwohl, P.U. Nguygen, Y. Ghorbanian, I.L. Weissman, T. Serwold, M.A. Inlay. Absence of CD11a expression identifies embryonic hematopoieic stem cell precursors via competitive neonatal transplantation assay. (Manuscript in Press).
3. **E.S. Varady**, S. Bodaghi, G. Vidalakis, G.W. Douhan. (2019). Microsatellite characterization and marker development for the fungus Penicillium digitatum, causal agent of green mold of citrus. *MicrobiologyOpen,* e788.
4. T. Faal, D.T. Phan, H. Davtyan, V.M. Scarfone, **E. Varady**, M. Blurton-Jones, C.W. Hughes & M.A. Inlay. (2019). Induction of Mesoderm and Neural Crest-Derived Pericytes from Human Pluripotent Stem Cells to Study Blood-Brain Barrier Interactions. *Stem Cell Reports*, 12(3), 451-460.
5. A. Karimzadeh, V.M. Scarfone, **E. Varady**, C. Chao, K. Grathwohl, J.W. Fathman, D.A. Fruman, T. Serwold, M.A. Inlay. (2018) The CD11a and endothelial protein C receptor marker combination simplifies and improves the purification of mouse hematopoietic stem cells. *Stem cells translational medicine*, 7(6), pp.468-476.
6. A. Ganguly, L. Pang, V.K. Duong, A. Lee, H. Schoniger, **E. Varady**, & A. Dahanukar. (2017) A molecular and cellular context-dependent role for Ir76b in detection of amino acid taste. *Cell reports*, 18(3), 737-750.
7. V. Sivanandam, **E. Varady**, and A. L. N. Rao. (2015) "Heterologous replicase driven 3′ end repair of Cucumber mosaic virus satellite RNA." *Virology* 478, 18-26.
8. E. Romero, B. Nguyen, J. Sanabria, **E. Varady**, I-Chieh Wang and T. H. Morton. (2014) "Two Faces of Dimethoxyalkanes: Steric Repulsion and Hyperconjugative Stabilization" *University of California, Riverside Undergraduate Research Journal*, Volume VIII page 57.

PRESENTATIONS

- 4th Annual UC Hematologic Malignancies Consortium Research Symposium, **Invited Speaker.** Sept. 2019, "*Improving Bone Marrow transplantation with Flonase"*
- SoCal Flow Summit 2019. **Oral**. "*Bone Marrow Transplantation, a Possible Therapy for Idiopathic Thrombocytopenic Purpura (ITP*
- UCI Immunology Fair, Dec. 2019. **Oral**. "*Improving bone marrow transplantation in mice to treat novel ITP mouse model"*
- International Society of Experimental Hematology (ISEH) 2018 & 2019. **Poster**. "*Treating Idiopathic Thrombocytopenia Purpura with Bone Marrow Transplantation"*

- LaJolla Immunology Conference 2018. **Poster**. "*Treating Idiopathic Thrombocytopenia Purpura with Bone Marrow Transplantation"*
- SoCal Flow Summit 2017. **Poster**. "*Characterizing a Primitive Lymphocyte Progenitor from the Mouse Embryo"*
- UCI Immunology Fair, 2017. **Poster**. "*Characterizing a Primitive Lymphocyte Progenitor from the Mouse Embryo"*

GRANTS/AWARDS

UCI SCRC Helios Seed grant on thesis topic	April 2021
NIH Immunology Training Grant T32 AI 0602573	2018- 2020
Travel award: 4th Annual UCHMC Research Symposium	Sept. 2019
Excellence in Cytometry: SoCal Flow Summit	April 2019
UC Riverside Honors Program Scholarship	**2015**

MENTORSHIP

Luis Angel Ayala January 2021- present, PhD graduate student at UCI, currently in the Inlay Lab

Iris Wong July 2020-present, Master student at UCI, currently in the Inlay Lab

Pauline Nguyen October 2017- August 2019, Undergraduate at UCI; received the Undergraduate Research Opportunities Program fellowship; Currently working at the UCI SCRC flow cytometry core.

Anne Del Rosario September 2019- March 2020, Undergraduate at UCI

Paulina Martinez February 2019- March 2020, Undergraduate at UCI

TEACHING EXPERIENCE

Molecular Biology Teaching Assistant, Spring 2018

Immunology Lab Teaching Assistant, Spring 2018

Biochemistry Teaching Assistant, Winter 2018

Immunology Teaching Assistant, Winter 2018

ABSTRACT OF THE DISSERTATION

Using Murine Bone Marrow Transplantation to Understand Hematopoietic Stem Cell Development and to Explore Possible Treatments for Blood Disorders

By

Erika Synthie Varady

Doctor of Philosophy in Biological Sciences

University of California, Irvine, 2021

Associate Professor Matthew Inlay, Chair

Blood cells keep us alive by fighting off infection and providing oxygen to every cell in our body. Every blood cell is derived from hematopoietic stem cells (HSCs) which can self-renew to maintain a constant HSC pool throughout a lifetime, engraft long-term in a conditioned recipient, and give rise to all the lineage blood cells. These characteristics are key for carrying out the lifesaving therapy HSC transplantation (HSCT), also known as hematopoietic cell transplantation (HCT) or bone marrow transplantation (BMT). A form of HCT called allogeneic HCT (allo-HCT) is a therapeutic strategy that eradicates a defective blood system, often with radiation therapy or chemotherapy conditioning, then replaces it with a healthy one using non-identical donor HSCs. It is effective against hematological malignancies like leukemia, and lymphoma, the 7th and 8th leading cause of death among cancers. Unfortunately, allo-HCT is used as a last resort treatment due to the complications associated with it including suboptimal allo-HSC recipient engraftment and the major complication Graft-vs-Host disease (GvHD). Resolving these limitations could increase the shortage of much needed donor cells and expand the patient pool to patients with milder blood cancer cases and other diseases such as autoimmune diseases.

GvHD occurs when donor immune cells, or graft cells, recognize the host as a foreign threat, thus engendering host tissue damage and organ failure. Many have strived to prevent GvHD after allo-HCT, however, there is still a high incidence of GvHD seen in the clinic. Currently, we face the complex challenge of minimizing GvHD while conserving the benefit of the Graft-vs-Leukemia (GvL) effect elicited by donor immune cells. There is currently no strategy that fully satisfies all these issues plaguing allo-HCT. There is a need for a new approach to safely and efficiently eliminate GvHD while preserving GvL and HSC engraftment in allo-HCT.

Here we explore a new proof-of-principle method that prevents GvHD after allo-HCT by using the glucocorticoid fluticasone propionate (Flonase) on a mouse model. We treated donor cells isolated from spleen and bone marrow with the glucocorticoid fluticasone propionate (Flonase) then transplanted them into lethally irradiated fully major histocompatibility complex (MHC) mismatched allogeneic recipients to prevent GvHD. We provide evidence on Flonase efficacy that addresses multiple issues associated with allo-HCT. Here we show that Flonase treatment increases HSC chemotaxis to the bone marrow through increased C-X-C chemotactic receptor type 4 (CXCR4) expression. We also show that pre-treating donor cells with Flonase decreases GvHD in allo-HCT and creates donor T cell immune tolerance. Our results demonstrate a possible mechanism underlying Flonase-induced immune tolerance involving regulatory T cell suppression of alloreactive cells. We also utilize HCT to learn more about pre-HSCs, the HSC precursor. Altogether, we explore potential ways of improving HCT by shedding light on the pre-HSC and showing proof of concept that Flonase donor cell pre-treatment can prevent GvHD. We also investigate using HCT to treat the autoimmune disease Idiopathic Thrombocytopenic Purpura (ITP) by first developing a new mouse model to allow us to test HCT.

CHAPTER 1: INTRODUCTION

Hematopoietic Stem Cells

Hematopoietic stem cells (HSCs) are self-renewing multipotent cells that give rise to mature cells of the blood system including red blood cells, white blood cells and platelets. Our knowledge of HSCs has increased monumentally after the discovery of blood forming cells by Dr. Ernest A. McCulloch and Dr. James E. Till.[1] These blood forming cells would later be called HSCs, however Till and McCulloch knew there was a stem cell that could give rise to hematopoietic cell lineages after experimenting with mice. The method they used to discover these blood stem cells involved collecting bone marrow cells from donor mice then injecting them intravenously into lethally irradiated recipients. They found that there was a linear increase of visible splenic nodules or colonies containing a heterogenous mixture of hematopoietic cells corelated to the number of bone marrow cells injected. They also showed that HSCs could self-renew after finding newly formed spleen colonies after performing multiple successful secondary transplants from a single spleen colony.[2]

Till, McCulloch and the graduate student at the time, Dr. Andy Becker, cemented the identification of the stem cell that gave rise to splenic colony formation. They showed that each colony was derived from one stem cell clone by inducing unique chromosomal breakage in donor bone marrow cells using radiation to mark and distinguish clones from one another.[3]

The heterogenous mixture of hematopoietic cells from these spleen colonies from Till and McCulloch's early work contained cells of the myeloid lineage, however Wu et. al. (1968) showed that lymphocytes are also derived from the same clone origin as the myeloid cells.[4] This clarified that blood cells share a multipotent progenitor. HSC isolation was then pioneered by the Irving Weissman lab at Stanford University. Using mice, they showed that the cell population containing HSCs expressed the cell surface marker stem cell antigen-1 (Sca-1), lowly expressed Thy-1 and was negative for hematopoietic lineage cell markers.[5] They also discovered that these cells were able to sustain long-term self-renewal in mice by lineage tracing methods carried out 14 weeks post transplantation.[6] This sparked the growth of the HSC field which would later uncover how HSCs develop and how they could be utilized for therapeutic use.

Most of what we know about HSC development comes from murine embryonic studies that carried out experiments on hematopoietic cells contained in embryonic tissues. HSCs develop in the embryo from hemogenic endothelial cells in the aorta-gonad-mesonephros (AGM). HSCs arise around 12.5 days post conception (d.p.c.), however it is preceded by HSC independent development of primitive blood cells from the blood islands in the extraembryonic yolk sac (YS) at 7.5 d.p.c., which gives rise to primitive erythroid cells that carry oxygen to embryonic tissues at 8.5 d.p.c. when the blood circulatory system is first formed.[7,8] Erythro-myeloid progenitors are later formed at 8.5 d.p.c. and give rise to red blood cells and myeloid cells that make up the innate immune system including tissue resident cells. There is also a lymphocyte precursor that exists prior to HSC development derived from the YS at 9.5 d.p.c.[9]

HSCs are derived from a precursor cell named the "pre-HSC" which develops from hemogenic endothelium around day 10 d.p.c.[10,11] The pre-HSC was uncovered by a transplantation experimentation methodology that involves injecting cells from the YS, AGM, placenta (PL) and

fetal liver (FL), at early embryonic stages before definitive HSCs arise, into neonatal immunodeficient NOD scid gamma mice (NSG) then lineage tracing donor cell lineage output in recipients. We use that method in Chapter 2 to identify specific cell surface markers to phenotype pre-HSCs. Inlay, et. al. used the markers Sca-1+, c-kit+, CD41+, VE-Cadherin+, CD11a- to isolate pre-HSCs in the early embryo.[11] One distinct difference between definitive HSCs and pre-HSCs is that HSCs can engraft into the bone marrow in adult mice and pre-HSCs cannot. However, these precursor cells are still multipotent and can self-renew. Understanding pre-HSC development can potentially allow us to manipulate induced pluripotent stem cells to make HSCs in a dish which has proven to be challenging in the scientific community thus far.

Studying pre-HSCs can also shed light on what enables HSC engraftment to the bone marrow. Many groups, including us, have studied the chemotactic pathway involving C-X-C chemotactic receptor type 4 (CXCR4), a G-protein coupled receptor, on HSCs that enables them to follow a chemotactic gradient of the chemokine CXCL12, also known as stromal derived factor 1 alpha (SDF-1α) released by the bone marrow stromal cells, into the bone marrow through the blood.[12] CXCR4 and CXCL12 is needed for HSC-bone marrow colonization during fetal development and $CXCL12^{-/-}$ and $CXCR4^{-/-}$ mice die perinatally.[13,14] Additionally, when CXCR4 is conditionally deleted in mice using tamoxifen activated Cre recombinase, HSCs lose their retention in the bone marrow niche.[15] HSCs need CXCR4-CXCL12 to retain their long term self-renewal, to maintain a constant pool of HSCs and to differentiate into lineage cells.[16-18]

Hematopoietic Cell Transplantation

The CXCR4 chemotactic pathway is a well sought-after target for improving HSC bone marrow engraftment efficiency to increase the number of HSCs that seed the bone marrow. HSC-bone marrow chemotaxis and engraftment is critical for the success of hematopoietic stem cell

transplantation (HSCT) also referred to as hematopoietic cell transplantation (HCT), bone marrow transplantation (BMT) or blood and marrow transplantation, a curative therapy for many life-threatening blood disorders. This therapy is used to reset a diseased blood system using chemotherapy or radiation therapy then replaces it with a healthy one using donor HSCs. This is an important therapy especially for hematological malignancies such as Leukemia, and Lymphoma, the 7th and 8th leading cause of death among cancers respectively. CXCR4 has been induced on mobilized human peripheral blood HSCs (also referred to CD34+ cells) and human cord blood (CB) HSCs using CXCR4 transgene expression and glucocorticoid treatment respectively.[19,20] Increasing CXCR4 expression on these human HSCs increased their ability to home to the bone marrow when transplanted in NSG mice. An important reason to improve CXCR4 expression on human HSCs is to enhance the bone marrow engraftment efficiency for HCT. This is especially important when working with low numbers of HSCs collected from CB. CXCR4 expression also decreases on HSCs after *ex vivo* culture, making it challenging to modify or expand donor HSCs *in vitro* for HCT.[21]

HCT treats many different blood disorders such as multiple myeloma, Non-Hodgkin's Lymphoma, acute myeloid leukemia, acute lymphoblastic leukemia, myeloproliferative neoplasms, chronic myeloid leukemia, aplastic anemia and severe combined immunodeficiency disorder to name a few. Approximately 23,000 HCTs were performed in the US in 2019 and has grown by about 5% per year.[22] There are two types of HCT including autologous and allogeneic transplantation where recipients receive donor cells containing HSCs from either themselves or from another donor respectively. Donor cells are collected from mobilized peripheral blood, bone marrow, or CB. Peripheral blood is the most popular source of donor cells for transplantation

followed by the bone marrow.[22] Clinics have recently reduced their use of CB due to low numbers of HSCs extracted from each cord.[23]

HSCs are essential for HCT due to their ability to home to and seed the bone marrow, self-renew to maintain a constant stem cell pool, and give rise to all blood lineage cells including red blood cells, platelets, and immune cells/ white blood cells. Therefore, donor cells harvested from either the bone marrow or mobilized peripheral blood are an amalgam of HSCs and all of the lineage blood cells. In allogeneic transplantation, mature single positive T cells within the donor cell population are essential for eliciting an immune response called a graft-vs-leukemia/tumor (GVL) response to eliminate host cancer cells and prevent disease relapse. Interestingly, T cells also help facilitate donor HSC engraftment, therefore they are needed within the donor cell pool.[24] There is a fine balance between eliciting a GVL response while preventing graft-vs-host disease (GvHD), a major complication of allogeneic HCT (allo-HCT). Donor T cells are needed to fight cancer cells for GVL; however, they can also damage host tissues as they are recognized as non-self and cause GvHD. HCT is only reserved for patients who are in dire need of one due to the chances of GvHD. Other lethal complications can also arise from this therapy including disease relapse, organ failure, hemorrhage, and graft rejection.

About 10% of the total injected donor T cells are alloreactive and undergo proliferation and activation within the host.[25,26] These alloreactive T cells have specific T cell receptors (TCRs) that bind strongly to host human leukocyte antigen (HLA) on the surface of host cells. Strong donor TCR-host HLA binding causes T cell activation and a damaging immune response. Approximately 70% of patients do not have the choice of receiving donor cells from an HLA matched sibling and have to look to another relative or an unrelated donor. Typically for these allogeneic transplants, HLAs between donor and host are as closely matched as possible to prevent

GvHD, also known as high-resolution matching. There are 8 HLA proteins that need to be matched including 3 major histocompatibility complex I (MHC I) alleles A, B, and C and 5 major histocompatibility complex II (MHC II) alleles -DRB1, -DQA1, -DQB1, - DPA1 and -DPB1. Those that find an 8/8 match from an unrelated donor has a higher chance of survival and transplantation success than a recipient that receives 7/8 matched donor cells.[27,28] aGvHD and cGvHD can also be caused by sequence differences in host and donor minor histocompatibility antigens, or MiHAs, the peptides that are presented by MHC class I and II.[29,30]

GvHD, including both aGvHD and the chronic form (cGvHD), accounts for about 6% of deaths for acute myeloblastic leukemia, 5% of myeloproliferative neoplasms and acute lymphoblastic leukemia.[22] A larger percent (~30-70%) of patients who received an allo-HCT developed cGvHD where 66% of these cases had prior aGvHD.[31-33] cGvHD severely impacts patients' quality of life and damages not only the skin, gut, and liver, but also the eyes, genitals, muscles, joints, mouth and lungs.[34,35] cGvHD was historically distinguished from aGvHD by manifesting after 100 days post transplantation, however the NIH has since identified a late-onset aGvHD that persists 100 days post HCT.[36] There are many factors that are taken into consideration for a proper diagnosis for human cGvHD and late-onset aGvHD that makes it difficult to distinguish them. There are many overlapping symptoms such as skin jaundice, skin rash, nausea, vomiting, diarrhea, however the most apparent difference is that cGvHD affects other tissues besides the skin, gut and liver due to donor lymphocyte infiltration.[36]

In allo-HCT, pre-transplant conditioning regiments including total body irradiation (TBI), and chemotherapy drugs like busulfan and cyclophosphamide cause tissue damage that facilitates a strong systemic inflammatory reaction, also known as a cytokine storm, that initiates aGvHD.[37-39] After conditioning, damage-associated molecular patterns (DAMPs), such as high mobility

group box 1 (HMGB-1) and adenosine triphosphate (ATP), and pathogen-associated molecular patterns (PAMPs), such as lipopolysaccharide (LPS), and β-D-glucan, are released by damaged host tissue and commensal pathogens respectively.[40,41] These DAMPs and PAMPs activate host and/or donor antigen presenting cells (APCs) like dendritic cells (DCs), monocytes and macrophages to release proinflammatory cytokines like tumor necrosis factor alpha (TNF-α), interleukin 1 beta (IL-1β), interleukin 2 (IL-2), interleukin 6 (IL-6), and interferon gamma (IFN-γ).[42] This cytokine storm induces APC expansion and MHC class I and class II upregulation.[43,44] Subsequently, T cells are primed for activation and proliferation after TCR binding to MHCs on donor and host APCs.[45] Neutrophils also contribute to early induction of aGvHD by releasing reactive oxygen species after infiltration into the damaged gut.[46] Cytokine storms that augment aGvHD are mostly localized in the gut, skin and liver due to high amounts of microbiota that release PAMPs.[47,48] This would explain why donor T cells traffic to these tissues and cause tissue damage and cytotoxicity during GvHD.[49]

aGvHD tends to favor a Th1 helper cell response when naïve donor T cells develop into helper CD4+ T cells that produce Th1 cytokines such as IL-2, IFN-γ, and IL-12. These cytokines activate APCs to amplify antigen presentation and tissue damage. Th1 cells also activate cytotoxic CD8+ T cells (CD8 T cells) that release damaging soluble mediators like perforin and granzymes that disrupt host cell membrane integrity. Activated CD8 T cells also promote host tissue cell death through the Fas-Fas ligand (FasL) pathway.[50] However, it is shown that both CD4 and CD8 T cells have elevated Fas and FasL during GvHD.[51]

cGvHD has a different immunopathology than aGvHD in that aGvHD is mainly caused by a T helper 1 (Th1) immune response and cGvHD by a T helper 2 (Th2) response.[42] cGvHD mostly occurs at later stages of GvHD due to a prolonged exposure to non-self MHC antigens or MiHAs.

This long-term exposure elicits an antibody mediated Th2 response and resembles an autoimmune reaction. In cGvHD, Th2 cells secrete IL-4, IL-5, IL-6 and IL-10 and activates host and donor B cell antibody production.[52] These antibodies can cause host tissue damage as they are specific to host tissue. There are also increased levels of B cell activating factor (BAFF) in patients with cGvHD.[53]

GvHD mouse models

Most of what we know about the molecular and cellular pathogenesis of GvHD is from mouse models of allogeneic transplantation. There are more established mouse models for aGvHD, and models for cGvHD have been imperfect. All of the different mouse models for aGvHD involve transplanting bone marrow cells and splenocytes from a donor mouse into a lethally irradiated MHC-mismatched, also known as the H2 complex or haplotype, recipient mouse. Mismatching MHCs or haplotypes between donor and recipient mice is critical for eliciting aGvHD and is needed for the donor cells to recognize host tissue as foreign. Donors and recipients can be fully MHC mismatched, for example the mouse model used in Chapter 3 is fully mismatched for MHCI, MHC II and MiHAs where the donor mice (mouse strain C57/Bl6) bare a H-2^b haplotype and recipients (mouse strain Balb/cJ) have H-2^d.[54] There are other aGvHD mouse models that are also fully MHCI, MHC II and MiHA mismatched that use C3H/HeJ (H-2^k) and C57/Bl6 (H-2^b) donors and C57/Bl6 (H-2^b) and B10.BR (H-2^k) recipients respectively.[55-57] These fully mismatched mouse models show lethality after day 10 and have symptoms of GvHD.

Other aGvHD models use partially mismatched models which are broken up into four categories: Only MHCI is mismatched, only MHCII is mismatched, only MiHAs are mismatched, or half mismatched also known as haploidentical transplants. Haploidentical mouse models have been a recent popular model for human haploidentical allo-HCT mainly to improve allo-HCT and

treat GvHD. Haploidentical transplants use a parent as a hematopoietic cell donor, therefore it is only a half-matched transplant. Human haploidentical allo-HCT is becoming the new gold standard for allo-HCT due to increased efficacy and safety of allo-HCT from post-transplant cyclophosphamide treatment. Cyclophosphamide treatment will be covered in more detail in the GvHD therapy portion of this introduction. Haploidentical mismatched mouse models develop aGvHD symptoms and/ or lethality at day 30 post-transplant. These transplants involve parental donor cell transplantation into offspring that express two different MHC haplotypes passed down from each parent. For example, in haploidentical transplantation, recipient B6D2F1 (H-$2^{b/d}$) mice are created by crossing donor C57/Bl6 (H-2^{b}) with DBA/2 (H-2^{d}) mice.[58] There are two additional haploidentical transplant models that cross donor C57/Bl6 (H-2^{b}) mice with C3H/HeN (H-2^{k}) and A/J (H-2^{a}) to create B6C3F1 (H-$2^{k/b}$) and B6AF1 (H-$2^{b/a}$) recipients respectively.[59,60]

MiHA mismatched aGvHD models are also used mostly to understand the role of MiHAs in GvHD, and the immunologic consequences of MiHA mismatched transplantation. These models often develop mild aGvHD with lethality as late as 80 days post transplantation.[61] One of the most important aGvHD, or xenogeneic GvHD (X-GvHD) mouse models involve xenotransplantation of human PBMCs into the following immunocompromised mice: NSG, Balb/c (Rag2, IL2rγ knockout), and NOD/SCID β2m-null (mice that have higher human cell engraftment due to lower NK cell activity). These mice do not have T or B cells which is important for avoiding human cell graft rejection.[62-65] These xenograft models are more translational for human research, however the donor cell engraftment efficiency is significantly lower than mouse-mouse engraftment due to rejection and species incompatibility. The reason we chose a fully mismatched aGvHD mouse model for our study is that it elicits a more severe version of GvHD that is easily detected at day

10 post-transplant. This model elicits the worst outcome of aGvHD and if reduced with experimental treatment, the less severe forms would most likely benefit even more from treatment.

The immunopathology and cause of cGvHD is not as well understood, with some contribution of imperfect mouse models. Mouse models used for cGvHD mimic autoimmune disease pathology, for example, a frequently used cGvHD model is also that of scleroderma, an autoimmune disease of the skin and connective tissue. These models made from MiHA mismatch transplantation tend to develop skin lesions, progressive lung and liver fibrosis and have high levels of alloantibodies and alloreactive B cells.[66-68] Many older existing cGvHD mouse models overlap with aGvHD models, making it difficult to distinguish cGvHD, however, a more recent promising model induces bronchiolitis obliterans, a distinct symptom of cGvHD, using cyclophosphamide conditioning.[69]

It is important to understand the intricacies and discrepancies of different disease mouse models to help one chose the best fit for their research.

Regulatory T cells in GvHD

Typically, regulatory T cells (Tregs) prevent healthy tissue damage from alloantibody-mediated destruction or host T cell cytotoxicity in autoimmunity; however, in allo-HCT and GvHD, there are reduced levels of Tregs.[70,71] Tregs are known to reduce GvHD severity by suppressing alloreactive T cell function and creating immune tolerance after allo-HCT.[72,73] In addition, transplanting *in vitro* expanded Tregs at the same time as allo-HCT prevents aGvHD.[74] Recently, there has been a gain in momentum in research for the use of Tregs in allo-HCT to prevent GvHD that even sparked an ongoing clinical trial in Spain treating patients who have

steroid refractory cGvHD with Tregs in hopes to eliminate cGvHD.[75] Many groups aim to control or regulate immune dysregulation in GvHD either by depleting alloreactive T cells or increasing the number of Tregs in the system, however, it is difficult to expand Tregs *in vitro*.

Tregs suppress alloreactive conventional CD4 (non-Treg cells) and CD8 T cells from activating and proliferating. The mechanism in which Tregs suppress dysfunctional T cells is not fully clear, however there is evidence that it is mediated through cell-to-cell contact or cytokine signaling. Tregs suppress autoreactive T cells by producing anti-inflammatory cytokines such as IL-10, transforming growth factor β (TGF-β), and IL-35.[76-78] They also use proteins like CTLA-4, CD39, LAG-3, and granzymes to suppress dysfunctional immune cells.[79-82] CTLA-4 is a well-known protein receptor that blocks conventional T cell co-stimulation through CD28 by competing for B7 binding. CTLA-4 expression on Tregs is upregulated in GvHD, however, overexpressing CTLA-4 does not prevent GvHD in allo-HCT recipient mice.[83] However, blocking CLTA-4 expression exacerbates conventional CD4 T cell induced GvHD in allo-HCT in mice, therefore CLTA-4 is needed to reduce GvHD.[84] Data has been consistent with showing reduced Tregs within the CD4 T cell population in aGvHD.[70,71] Treg therapy is an important area of research for creating immune tolerance in allogeneic donor cells to alleviate GvHD. However, there is a delicate balance of preventing GvHD while keeping the beneficial GVL response. It was demonstrated through mouse tumor models that transplanting a 1:1 ratio of CD4+, CD25+ Tregs to conventional CD4 T cells did not eliminate tumor clearance, however thresholds higher than that started to impair GVL.[71] Treg therapy shows promise for reducing and preventing GvHD and advancing technology could help achieve it.

Current GvHD Treatments

There are many treatments for GvHD given before and after the onset of symptoms. The old standard of care was pre-treatment with the calcineurin inhibitors like cyclosporine and tacrolimus immediately after allo-HCT to eliminate alloreactive lymphocytes. Calcineurin inhibitors are used less in recent years due to the deleterious side effects like kidney damage and neurotoxicity. Antithymocyte immunoglobulin (ATG), polyclonal antibodies specific for T cells, is given prior to allo-HCT to eliminate donor T cells.[85] These antibodies lead to T cell depletion through antibody dependent phagocytosis and the complement system. These antibodies also hinder myeloid cell function but induce regulatory T cell function. There are also many immunosuppressive drugs that inhibit important pathways required for lymphocyte activity such as methotrexate, mycophenolate mofetil, rapamycin, corticosteroids (methylprednisolone and prednisone), alemtuzumab, and cyclophosphamide. These drugs have significantly reduced the death rates and occurrence of GvHD; however, they do elicit damaging side effects, especially if taken in multiple courses over a prolonged period of time.

Post-transplant cyclophosphamide treatment in combination with haploidentical transplantation is becoming the new gold standard that reduced the GvHD-related death tole by approximately half that of normal unrelated donor allo-HCT.[22] A phase 2 clinical trial compared patients receiving post-transplant cyclophosphamide treatment, after haploidentical transplant, with the standard of care treatment that used tacrolimus and methotrexate and found that there was a 2% incidence of severe aGvHD and a GvHD free survival of 53% for cyclophosphamide treatment compared to 13% and 37% respectivley.[86] Post-haploidentical cyclophosphamide treatment is a recent breakthrough treatment to prevent GvHD, with the first 13 therapies given in 1999 then significantly increased in number after 2013.[87] Alas, there is still a lack of data for this

new treatment due to smaller numbers of treatments given compared to the standard of care. Nonetheless this therapy holds promise for increased HCT safety for a larger recipient pool.

Idiopathic Thrombocytopenic Purpura

In theory HCT can treat any blood disorder including autoimmune diseases. If improved, HCT can be available to patients who suffer from autoimmune diseases like Idiopathic thrombocytopenic purpura (ITP). ITP is a rare platelet autoimmune disorder that results in increased bleeding due to platelet destruction by the immune system. This is caused primarily by autoreactive antibodies but can also involve cytotoxic T cells in platelet destruction.[88] Lower platelet concentrations in the blood can increase internal bleeding and the chance of organ and brain hemorrhaging, therefore patients who have this disease live a different lifestyle of avoiding highly intensive sports and activities. There are treatment options that can alleviate ITP symptoms, albeit temporarily, for example, intravenous immunoglobulin therapy (IVIG) prevents antibody dependent phagocytosis of platelets by splenic macrophages for a limited time period. This treatment, along with immunosuppressive drugs like glucocorticoids is the standard of care to temporarily treat flare ups, or bleeding episodes caused by ITP.

The cause of ITP is still unclear. Sometimes patients develop ITP after a viral infection, for example after acquiring hepatitis C virus, which supports the theory that the antibodies created against viruses can also bind platelets in virus-associated ITP.[89] There could also be a genetic predisposition to ITP.[90] More information is needed to elucidate the cause and cellular immune dysfunction of ITP. There is currently one established mouse model for ITP with two renditions that is created by immunizing CD61 or CD41 knock out mice with platelets from wild type mice

to create immunity against these platelet surface proteins.[91,92] Splenocytes from these immunized mice are then adoptively transferred into wild type recipient mice to elicit an immune response and eliminate platelets. These mouse models have limitations in that CD61 knockout mice have a high percentage of embryonic lethality and CD41 is very important for hematopoietic stem cell development, therefore immune dysfunction is expected in these knockout mice. Furthermore, 67% of mice die after inducing ITP in the CD61 knock out model which prevents any long-term studies using this model. New ITP mouse models are needed to test possible therapies and to expand our basic knowledge on this disease.

Conclusion

In this dissertation, I explore and discuss the concept of improving hematopoietic cell transplantation (HCT). Four topics cover the importance and improvement of HCT. First, we explore HCT, or bone marrow transplantation, in a basic research setting where we use it to understand HSC development modeled in mice. In Chapter 3, I show data on improving HCT through HSC engraftment and I present a proof-of-concept drug therapy that reduced GvHD after allo-HCT. Finally, I discuss an alternative HCT application for the autoimmune disease ITP and explore a new ITP mouse model to test this application. HCT is a potentially curative treatment for deadly hematological malignancies, however there are many complications that arise after this therapy; therefore, this treatment is only available to those who are in dire need of it. Here, we dive into possible solutions for these complications in hopes for better survival and a larger patient pool for HCT.

CHAPTER 2: ABSENCE OF CD11A EXPRESSION IDENTIFIES EMBRYONIC HEMATOPOIETIC STEM CELL PRECURSORS VIA COMPETITIVE NEONATAL TRANSPLANTATION ASSAY

Introduction

Author's Note: The following chapter is a completed manuscript that has been accepted for publication in Frontiers in Cell and Developmental Biology and is currently In Press. I share co-first authorship with Alborz Karimzadeh and we have contributed equally to this publication. I contributed to designing experiments and procedures, data analysis and interpretation, and writing. The co-authors include Vanessa M. Scarfone, Connie Chao, Karin Grathwohl, Pauline U. Nguyen, Yasamine Ghorbanian, Irving Weissman, Thomas Serwold, and last author Matthew A. Inlay.

Hematopoietic stem cells (HSCs) in adults are the multipotent and self-renewable source of the entire blood system and hold the regenerative capacity to engraft a myeloablated recipient upon transplantation.[93] While the identity, self-renewal ability, engraftment potential, and differentiation properties of adult HSCs has been extensively studied over the past 30 years, much less is known about the developmental origins of HSCs in the embryo. During early embryonic development and prior to the appearance of fully functional HSCs, distinct waves of blood-forming cells emerge, likely initiated from specialized endothelial cells called "hemogenic endothelium".[94,95] These waves overlap, with each wave functionally more mature than the last. In mice, the initial wave of hematopoiesis gives rise primarily to primitive nucleated erythrocytes

and arises in the yolk sac (YS) blood islands starting from embryonic day (e) 7.5.[8] After establishment of a heartbeat, definitive hematopoiesis begins at e8.5 in the YS and placenta (PL) with a transient wave of erythro-myeloid.[96-98] At e9.5, the first self-renewable and multipotent progenitors, that immediately precede HSCs, emerge in the YS, aorta-gonad-mesonephros (AGM), and PL, and are often called "pre-HSCs".[11,99-103] After e11.5, the pre-HSC wave transitions into an expanding BM-engraftable HSC pool in the fetal liver (FL).[104,105] The FL remains the major site of hematopoiesis until perinatal seeding of the BM.[106,107]

In adult mice, multi-parameter fluorescence-activated cell sorting (FACS) coupled with transplantation assays have enabled the isolation of a highly purified bone marrow (BM) HSC population for functional and molecular characterization.[108-111] Bone marrow HSCs can be sorted, then transplanted intravenously into lethally irradiated wild-type recipient mice, where they will home to the bone marrow, engraft, and reconstitute the hematopoietic system for the life of the recipient. Pioneering work on the embryonic origins of HSCs led to the present definition of pre-HSCs as cells that have the self-renewal and lineage potential of adult HSCs but lack the ability to engraft into the BM when transplanted intravenously into adult lethally-irradiated recipients.[112,113] However, two alternative assays have been developed to functionally identify pre-HSC activity in the embryo: *ex vivo* maturation and neonatal transplantation. In the former, candidate populations or tissues are harvested from the embryo and cultured *in vitro* with the addition of exogenous factors to induce *ex vivo* maturation of these cells into HSCs, which is then confirmed by adult transplantation.[100,114] However, these *ex vivo* maturation assays rely on the presence of cultured stromal lines as well as potent exogenous factors such as SCF, TPO, IL-3, and Flt3L. Accordingly, these assays can potentially drive HSC formation from cell-types that are more primitive than pre-HSCs, such as hemogenic endothelium.[115] An alternative approach to reveal pre-HSC activity is

via intravenous injection of embryonic cells directly into irradiated *neonatal* recipients.[10, 99,116] While less sensitive than *ex vivo* cultures, neonatal transplantation presents minimal risk of introducing artifacts by bypassing the non-physiological concentrations of cytokines and growth factors used *ex vivo*.[99,101,117]

Adult HSCs can be precisely identified by a combination of different markers expressed (or unexpressed) on their surface. While many different combinations can work, a commonly used definition for murine HSCs is Lineage- Kit+ Sca1+ CD150+ and CD34-. However, many adult HSC markers are not similarly expressed in the early embryo and can change depending on the tissue and timepoint examined.[118] Alternative assays have identified potential pre-HSC markers including hematopoietic markers CD41(Rybtsov et al., 2011), CD43 (Inlay et al., 2014), and CD45 (Taodi et al., 2008; Boisset et al., 2010), progenitor markers Kit (Boisset et al., 2010) and Sca1 (Inlay et al., 2014), and endothelial markers CD31 (Inlay et al., 2014), VE-Cadherin (CD144) (Taoudi et al., 2008), and EPCR (CD201) (Zhou et al., 2016). This has resulted in the identification of populations such as Type I (CD144+ CD41+ CD45-) and Type II (CD144+ CD45+) pre-HSCs (Rybtsov et al. 2011), or rarer CD201^{hi} subsets within these populations (Zhou et al., 2016).[114,11,100,117,103] However, a strictly-defined pre-HSC cell type has not been described to the same resolution as that in adult HSCs.

CD11a (integrin alpha L, or *Itgal*) forms the complex LFA-1 (leukocyte functional-associated antigen 1; $\alpha_L\beta_2$) upon dimerization with the β2-integrin CD18. LFA-1 interacts with ICAMs and has roles in lymphocyte activation, differentiation, and transendothelial migration.[119-121] CD11a is highly expressed on all circulating immune cells, including bone marrow progenitor populations.[122] However, our previous work found CD11a to be uniquely unexpressed in a subset of adult HSCs (defined as Lin- Kit+ Sca1+ CD150+ CD34-), and only the CD11a- fraction of adult

HSCs displayed long-term multilineage reconstitution upon transplantation.[122,123] In a related study, we examined the potential of CD11a as a marker of embryonic multipotent progenitors in e9.5-11.5 embryos. Using a single-cell *in vitro* multipotency assay, we determined that only a rare CD11a- population we termed "CD11a- KLS" cells (defined as Ter119- CD43+ Kit+ Sca1+ CD144+ CD11a-) contained all multipotent progenitor activity, regardless of what timepoint or tissue it was isolated from.[11] Neonatal transplantation demonstrated these cells produce a variety of lineages *in vivo,* though their long-term engraftment and ability to give rise to HSCs was never assessed. Thus, in both studies, the absence of CD11a expression was an important marker to identify adult HSCs by transplantation, and a candidate pre-HSC population in the embryo by *in vitro* multipotency.

In the present study, we use an *in vivo* neonatal NSG transplantation system to prospectively identify pre-HSCs in e10.5 and e11.5 tissues. In line with our previous work, the absence of CD11a expression on pre-HSCs (defined as Ter119- CD43+ Kit+ Sca1+ CD144+ CD11a-) was critical for distinguishing them from downstream progenitors which were all CD11a+. Moreover, our data suggest the neonatal liver serves as an essential temporary niche for the maturation of embryonic progenitors which lack the expression of the BM homing receptor CXCR4 prior to seeding the BM. These findings establish CD11a as a key marker to identify and isolate a highly purified pre-HSC population, beyond what has been achieved, therefore paving the way for more detailed characterization of these immature progenitors.

Results

Establishing the NSG neonatal transplant system for *in vivo* detection of pre-HSCs.

To functionally detect pre-HSC activity *in vivo*, we used immunodeficient NSG (NOD/SCID/IL2rγ$^{-/-}$) neonatal mice as transplantation recipients.[124-126] We first tested this system on unsorted embryonic cells harvested from e9.5 to e11.5 tissues, the stages when pre-HSCs are thought to emerge, expand, and mature. From e9.5 embryos we harvested the YS, PL, and caudal half (CH), which contains the AGM. From e10.5 and e11.5 embryos we harvested the YS, PL, AGM, and FL (Figure 2.1A). Cells from whole tissues of e9.5-11.5 donors along with adult helper BM were transplanted into irradiated NSG neonates followed by tissue analysis and secondary transplants (Figures 2.1B, S2.1). While donor chimerism from e9.5 donors was detected at extremely low rates, we consistently detected BM HSC engraftment from all tissues of e10.5 and e11.5 donors (Figures 2.1C, S2.1). To confirm that none of the transplanted cells were already HSCs, we separately transplanted e10.5 and e11.5 donor cells into adult recipients and did not find any long-term adult BM engraftment (Figure S2.2). It should be noted that while e11.5 tissues can contain adult-engraftable HSCs, this activity is rare, often less than 1 HSC per embryo, and we did not find any HSC-engraftment in our transplants.[101] Therefore, any engraftment in the neonatal recipients must have come from cells which lack adult engraftability and are thereby pre-HSCs.

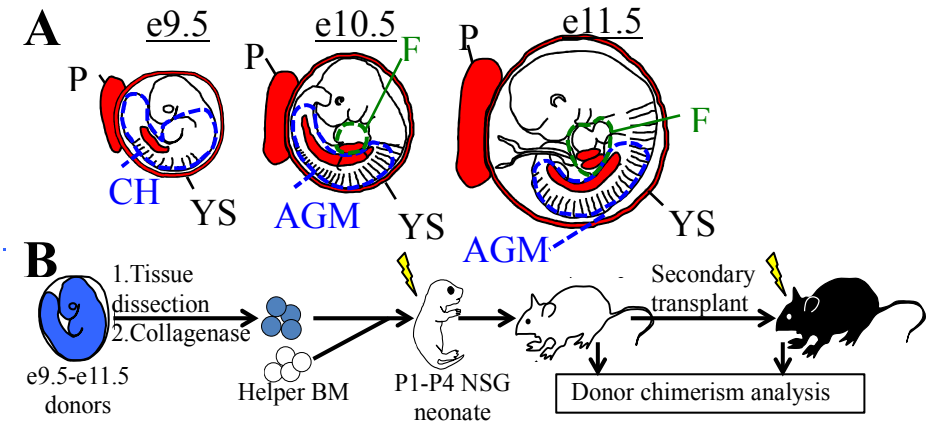

C

dpc	ee/ recipient	Helper BM	Donor tissue	LT-chimerism	Total blood chimerism	successful injections	LT-Engraftment efficiency
e8.5	4-8	none	WE	0	0	n.d.	NA
e9.5	4-8	0-500K	CH	2	6	16	0.12
			YS	0	8	16	NA
			PL	0	3	12	NA
e10.5	3	75-200K	AGM	4	10	16	0.25
			YS	9	16	20	0.45
			PL	2	6	12	0.17
			FL	1	2	10	0.10
e11.5	1	100-200K	AGM	6	7	7	0.86
			YS	6	11	12	0.50
			PL	5	8	8	0.63
			FL	6	12	12	0.50

Figure 2.1. Utilization of the NSG neonatal transplant system to reveal pre-HSCs in e9.5-11.5 embryos. A) Schematic representation of hematopoietic tissues (red) harvested from e9.5, e10.5, and e11.5 embryos. YS = yolk sac, PL = placenta, CH = caudal half, AGM = aorta-gonad-mesonephros, FL = fetal liver. Dissection sites of the CH/AGM and FL are shown in blue and green dashed lines, respectively. **B)** Schematic representation of the neonatal transplant system. Harvested tissues from e9.5-11.5 donor CFP+ embryos are dissected, dissociated, and combined with CFP- adult helper BM. Donor cells are administered intravenously (i.v.) into irradiated neonatal NSG recipients of 1-4 days of age (P1-P4). Recipients are bled for donor chimerism analysis at 4 week intervals and are then sacrificed for BM analysis and secondary transplants. **C)** Compilation of whole-tissue transplants from e8.5-11.5 embryos. Number of successful tissue-specific long-term engraftment ("LT-chimerism") is determined by the presence of ≥1% embryo donor granulocyte chimerism (at the last bleed) and HSPC (hematopoietic stem/progenitor cell) chimerism in the BM. "Total blood chimerism" refers to the number of recipients with ≥1% embryo chimerism in total CD45+ compartment of blood. "Successful injection" is defined as engraftment of either embryo or helper adult BM donors. "Engraftment efficiency" is determined by # of successful embryo engraftment / total successful injections. dpc=days post conception; ee=embryo equivalent; WE=whole embryo.

Establishment of an embryonic competitive transplant system.

We next used the NSG neonatal transplant system to assay sorted populations for pre-HSC activity. To allow us to directly compare sorted embryonic populations in a competitive setting, we bred mice to generate embryos that expressed either CFP or Tomato fluorescent reporters in the same litters. To accomplish this, males bearing two reporters, Tomato and CFP ($Rosa26^{Tomato/CFP}$), on different alleles of the *Rosa26* locus, were crossed to Wt females ($Rosa26^{wt/wt}$). Each offspring will receive only one reporter allele and be either Tomato+ ($Rosa26^{Tomato/wt}$) or CFP+ ($Rosa26^{CFP/wt}$). Therefore, age-matched littermates can be distinguished by color, sorted based on marker expression, and co-transplanted in a head-to-head competitive setting (Figure 1.2A-1.2B). Provided equal numbers of embryos of each color are used, we can directly compare two populations to determine which contains more pre-HSCs by measuring donor chimerism in the recipient animals. Unlabeled adult B6 BM was used as helper (CD45.2+),and could be distinguished from host NSG recipients (CD45.1+). As the injection into the facial vein of neonatal mice is technically challenging, the inclusion of helper BM (which also contains HSCs) also served as an internal control to determine injection success.

All pre-HSCs are within the CD11a- fraction of progenitors in e10.5 and e11.5 embryos.

Our previous study identified a population that contained all *in vitro* clonal multipotent activity in the early embryo.[11] These cells are within the CD144+ CD11a- fraction of "eKLS" cells (embryonic equivalent of the adult KLS population), which is defined as Ter119- CD43+ Kit+ Sca1+. To determine whether CD144+ CD11a- eKLS cells ("11a- eKLS"), contains pre-HSCs, we sorted and transplanted embryonic progenitors into neonatal recipients. Due to the low engraftment rate of e9.5 whole-tissue transplants (Figures 2.1C, S2.1A), we focused only on e10.5 and e11.5 tissues. We also sorted all other eKLS cells (not CD11a- CD144+ eKLS cells, or "Other eKLS"),

to ensure that other potential sources of pre-HSCs were also examined. We sorted "11a- eKLS" from one color of embryo (e.g. Tomato+), and mixed it with "Other eKLS" sorted from the other color embryo (e.g CFP+) and co-transplanted them along with helper BM into neonatal NSG recipients (Figures 2.2A-B, S2.3). We maintained the physiological ratios of the two populations, such that each recipient contained the equivalent of all eKLS cells from each embryo (Figure 2.2B). Thus, whichever fraction contained the most pre-HSCs would display greater donor chimerism in the recipients, regardless of how many non-pre-HSCs were contained in that fraction. On average, each recipient received 3-4 embryo equivalents (ee) of each population.

Blood analysis of recipients showed higher total CD45+ leukocyte chimerism (total blood chimerism) from the 11a- eKLS population compared to the "Other eKLS" source at both e10.5 and e11.5 timepoints and from all embryonic tissues examined (Figures 2.2Ci, S2.4). Within the short-lived granulocyte compartment, we found that only the 11a- eKLS cells gave rise to donor granulocytes in all recipients (Figures 2.2Cii, S2.4). BM analysis of recipients confirmed the presence of embryo-derived HSPCs (hematopoietic stem/progenitor cells, Ter119- CD27+ Kit+ Sca1+) only from the 11a- eKLS population with no contribution from the Other eKLS source (Figure 2.2Ciii). We then performed secondary transplants and confirmed long-term engraftability of 11a- eKLS-derived HSCs (Figure 2.2Civ). We also examined the distribution of donor lineages to determine whether 11a- eKLS cells exhibited any lineage biases depending on which tissue they were sorted from (Figure S2.4C-D). While some recipients displayed a minor increase in T cells over B cells, there did not appear to be a consistent bias for any specific tissue source or timepoint. Notably, 11a- eKLS cells from e11.5 FL had a significantly decreased myeloid output relative to lymphoid output, due to increase T cell production.

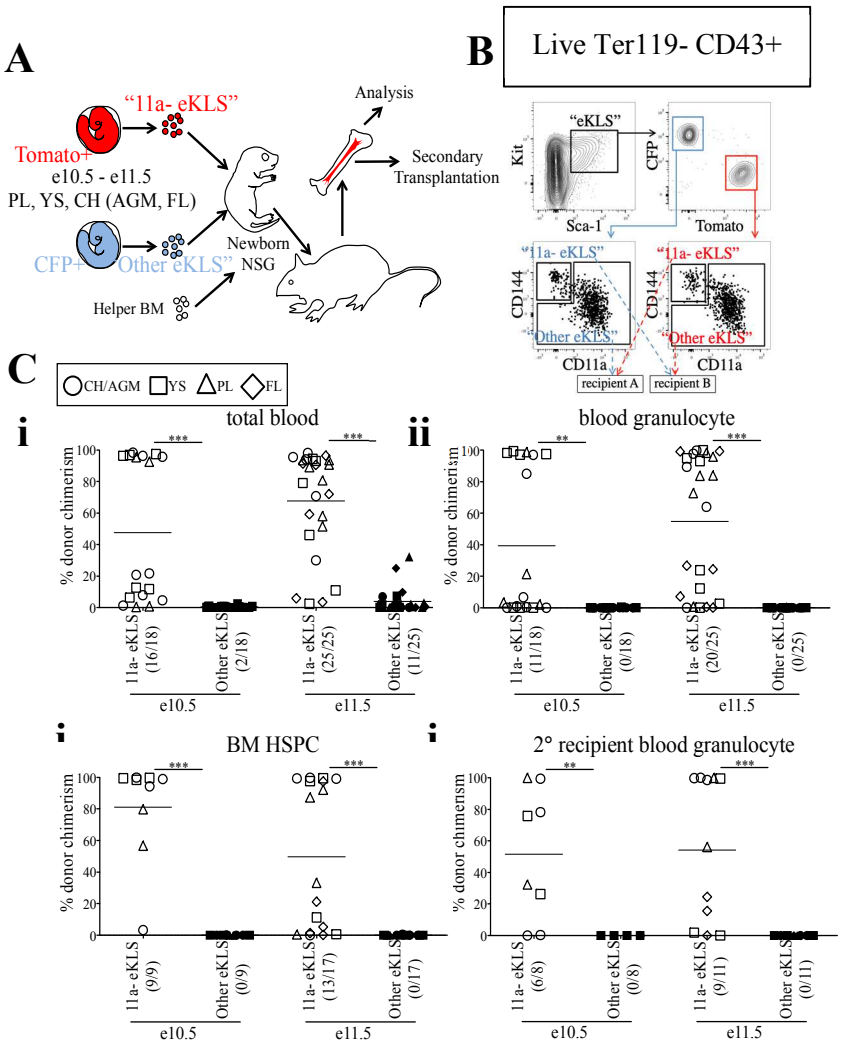

Figure 2.2. All functional pre-HSCs are contained within the CD11a- fraction of e10.5 and e11.5 embryonic progenitors. A) Schematic representation of the competitive transplant system. Sorted Tomato-expressing "11a-eKLS" and CFP-expressing "Other eKLS" cells (and vice versa) are combined and mixed with non-fluorescent CD45.2+ adult helper BM for transplantation into newborn NSG recipients. **B)** Representative sorting strategy for the competitive transplantation of 11a- eKLS and Other eKLS populations. Embryonic progenitors are defined as live, Ter119- CD43+ Kit+ Sca1+ cells. Tomato+ and CFP+ progenitors are then gated, and CD11a- CD144+ ("11a- eKLS") and everything else ("Other eKLS") are sorted. Opposing populations of different colors are mixed post-sort and transplanted into the same recipient. Representative plots and gates for each tissue and timepoint can be found in Figure S3. **C)** Donor chimerism from 11a- eKLS and Other eKLS populations in primary and secondary recipients. Percent donor chimerism of total blood **(i)**, blood granulocyte **(ii)**, BM HSPC **(iii)** in primary recipients and blood granulocyte chimerism in secondary recipients **(iv)** from 11a- eKLS (white symbols) and Other eKLS (black symbols). Numbers in parenthesis indicate successful chimerism / total recipients engrafted with embryonic cells of any source. Blood analysis was done after at least 12 weeks post primary transplant and after at least 6 weeks post-secondary transplant. 1% is set as a threshold to define successful chimerism. CH/AGM (circle), YS (squares), PL (triangles), and FL (diamond) are shown. For a tissue-specific analysis of both timepoints, refer to Figure S4.

While our data shows that up to e11.5, all pre-HSC activity is in the CD11a- fraction, at later timepoints, e13.5 and e14.5, we observed neonatal engraftment from both CD11a- and CD11a+ progenitors (Figure S2.5A). At e14.5, we also observed adult engraftment from both CD11a- and CD11a+ fractions (Figure S2.5B). This is consistent with our previous studies where we found multipotency within both CD11a- and CD11a+ fractions at e12.5 (Inlay et al., 2014), and found both CD11a- and CD11a+ fetal HSCs at e17.5.[11,122] This suggests that pre-HSCs/HSCs transiently upregulate CD11a during their maturation from pre-HSCs to HSCs.

All pre-HSCs are Sca1+ at e11.5 and efficiently identified by anti-Sca1 staining.

Some groups have reported low/undetectable Sca1 protein expression on early hematopoietic progenitors and require a Sca1-GFP transgenic reporter (Ly-6A-GFP) in order to identify Sca1+ cells in the embryo.[127] To rule out whether any pre-HSC activity was present in the Sca1- fraction, e11.5 CFP/Tomato embryos were separated into individual tissues (YS, FL, PL, AGM) and stained (Figure 2.3). CD43+ Ter119- Kit+ cells were separated into Sca1+ and Sca1- fractions (from different reporters) and co-transplanted into neonatal NSG recipients (Figure 2.3A). 12 weeks after transplantation, we found that only the Sca1+ fraction consistently produced donor chimerism (blood granulocytes and BM HSPCs) in the recipient mice, including in secondary recipients, indicating that few, if any, pre-HSCs are contained in the Sca1- population in e11.5 tissues (Figure 2.3B). It should be noted that in this set of experiments, not all tissues engrafted equally, and the PL and AGM eKLS populations had higher overall chimerism than that from the YS and FL.

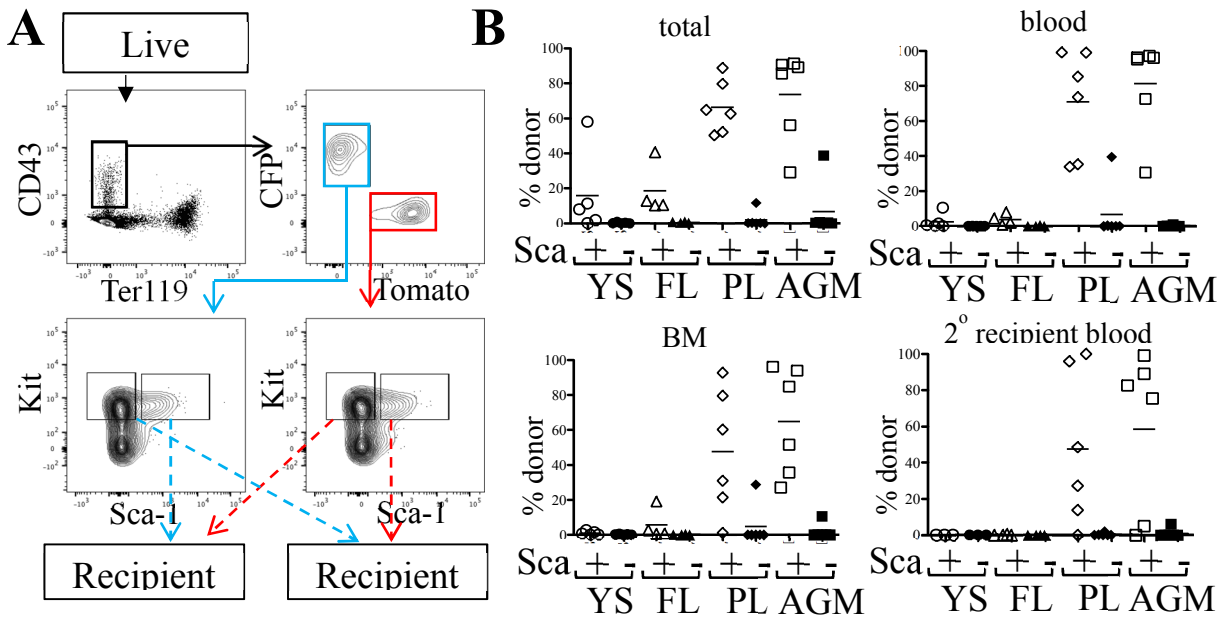

Figure 2.3. Sca1 "plus/minus" sort and neonatal transplant. **A)** Representative FACS plot of sorted populations for transplantation (AGM shown). Live cells from e11.5 embryonic tissues were first gated on CD43+ Ter119-, then separated into CFP+ and Tomato+ fractions. Kit+ cells within these gates were sorted into Sca1+ and Sca1- fractions. Prior to transplantation into neonatal NSG recipients, cells were mixed such that Sca1+ fraction of one color (e.g. CFP) was co-transplanted with the Sca1- fraction of the other color (e.g. Tomato). **B)** Total blood (CD45+ cells), blood granulocyte, and BM HSPC chimerism of the Sca1+ (white symbols) and Sca1- (black symbols) fractions of e11.5 embryos are shown at week 12. Week 12 bone marrow was harvested and transplanted into lethally irradiated B6 adult recipients and blood granulocyte chimerism was analyzed 6 weeks post-secondary transplant.

CD11a- embryonic progenitors are more quiescent compared to their CD11a+ counterparts.

Next, we examined the absolute numbers of CD11a- and CD11a+ eKLS progenitors at different embryonic stages and in different tissues. At e10.5, both populations were most abundant in the YS, followed by the PL and AGM, with the fewest found in the FL. However, by e11.5, both populations were most abundant in the FL, and reduced in the other tissues (Figure 2.4Ai-ii). These data support the previously described migration of hematopoietic progenitors from the AGM, YS, and PL to the FL over time and confirm the FL as the primary site of hematopoiesis in mid-gestation.[104] Furthermore, a much higher frequency of CD11a+ eKLS cells in e14.5 FL suggested the higher expansion rate of CD11a+ progenitors and/or less frequent division of the CD11a- progenitors.

We next examined the cell cycle status of early (e10.5) and late (e14.5) embryonic progenitor (eKLS) fractions (Figure 2.4B), using staining for the proliferation marker Ki-67 and the nuclear dye DAPI, which collectively can distinguish cells in G0, G1, and S/G2/M phases.[128] In e10.5 tissues, we observed a shift in the fraction of cells in G0/G1 phase versus S/G2/M phase between CD11a- and CD11a+ eKLS cells respectively, suggesting a higher rate of division among the CD11a+ fraction (Figure 2.4Ci). This difference was more pronounced in e14.5 FL tissues, as many CD11a- eKLS cells were in G0 phase while the CD11a+ fraction had increased S/G2/M phase cells (Figure 2.4Cii). These observations support the notion that the CD11a- and CD11a+ embryonic progenitors begin to resemble quiescent adult HSCs and downstream transit-amplifying cells, respectively.

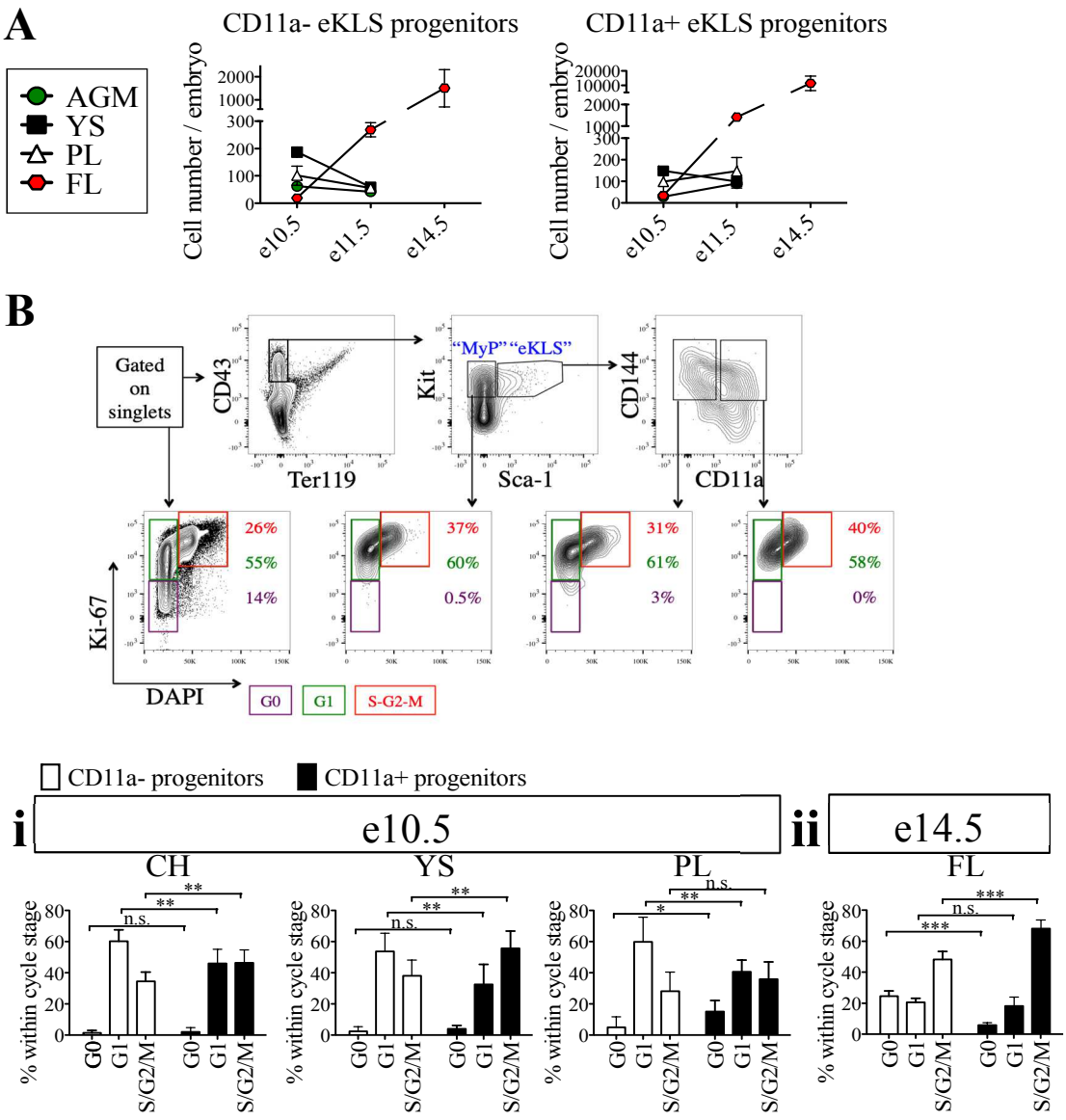

Figure 2.4. Cell cycle analysis of 11a- eKLS cells and CD11a+ progenitors. A) Numbers of CD11a- and CD11a+ progenitors in embryos over time. Estimated number of CD11a- progenitors **(i)** and CD11a+ progenitors **(ii)** per embryo is depicted in embryonic tissues at e10.5, e11.5, and e14.5. "eKLS progenitors" are defined as Ter119- CD43+ Sca1+ Kit+ CD144+ at e10.5 and e11.5, and as Ter119- CD43+ Sca1+ Kit+ EPCR+ at e14.5. *e10.5, n=4 (2 independent experiments); e11.5, n=5 (3 independent experiments; e14.5, n=10 (2 independent experiments).* **B)** Representative analysis of the cell cycle status in embryonic population. Bottom plots show DAPI (x-axis) and Ki-67 (y-axis) within total single cells, myeloid progenitors (MyP), 11a- eKLS, and 11a+ eKLS from left to right. The color of percentage values inside the gates correlates with the color of each gate/cell cycle phase. e10.5 CH is shown as a representation. **C)** Cell cycle analysis of CD11a- and CD11a+ progenitors at e10.5 and e14.5. Cell cycle status of each population is depicted for e10.5 tissues **(i)** and e14.5 FL **(ii)**. "Progenitors" are defined as Ter119- CD43+ Sca1+ Kit+ CD144+ at e10.5, and as Ter119- CD43+ Sca1+ Kit+ CD150+ at e14.5. *$p \leq 0.05$, **$p \leq 0.01$, ***$p \leq 0.001$ (Student's unpaired t test) e10.5, n=8 (2 independent experiments); e14.5=5 (2 independent experiments).*

The neonatal liver harbors transplanted embryonic progenitors shortly after transplant.

Why do pre-HSCs engraft in neonates, but not adult recipients? Previous studies have suggested a role for the neonatal liver in providing a niche for the maturation of pre-HSCs prior to BM seeding.[101] To determine whether embryonic progenitors seeded the FL directly, we transplanted e10.5 and e11.5 sorted hematopoietic progenitors (Ter119- CD43+ Kit+) along with adult BM into NSG neonates and analyzed recipient tissues 15 hours post-transplant for the presence of transplanted cells (Figures 2.5A, S2.6). Amongst the different tissues examined, the liver of the recipients contained by far the highest number of transplanted progenitors originating from both e10.5 and e11.5 embryonic sources as well as the adult donor source (Figure 5B). Similar results were found when we investigated the presence of embryo-derived donor leukocytes (Ter119- CD43+) and donor eKLS (Figure S2.6). These results suggest that pre-HSCs and other Kit+ progenitors may be unable to migrate directly to the BM upon transplantation, but instead first seed the FL.

To that end, we also investigated the expression of CXCR4, a receptor on HSCs known to be involved in homing to the BM on adult HSCs and embryonic pre-HSCs.[12] CXCR4 was expressed on a very low percentage of e10.5 11a- eKLS cells regardless of tissue, whereas it was expressed on nearly all adult HSCs (Figure 2.5Ci-ii). At e14.5, the FL contains adult-engraftable phenotypic HSCs (defined as CD150+ CD48- KLS). These HSCs also expressed CXCR4 on their surface to a similar degree as adult HSCs (Figure 2.5Ciii). This suggests that pre-HSCs are unable to directly home to the BM in part because they lack CXCR4 expression. Together, these results suggest that the neonatal liver may serve as the initial site of engraftment of transplanted embryonic cells until their eventual maturation and seeding of the BM.

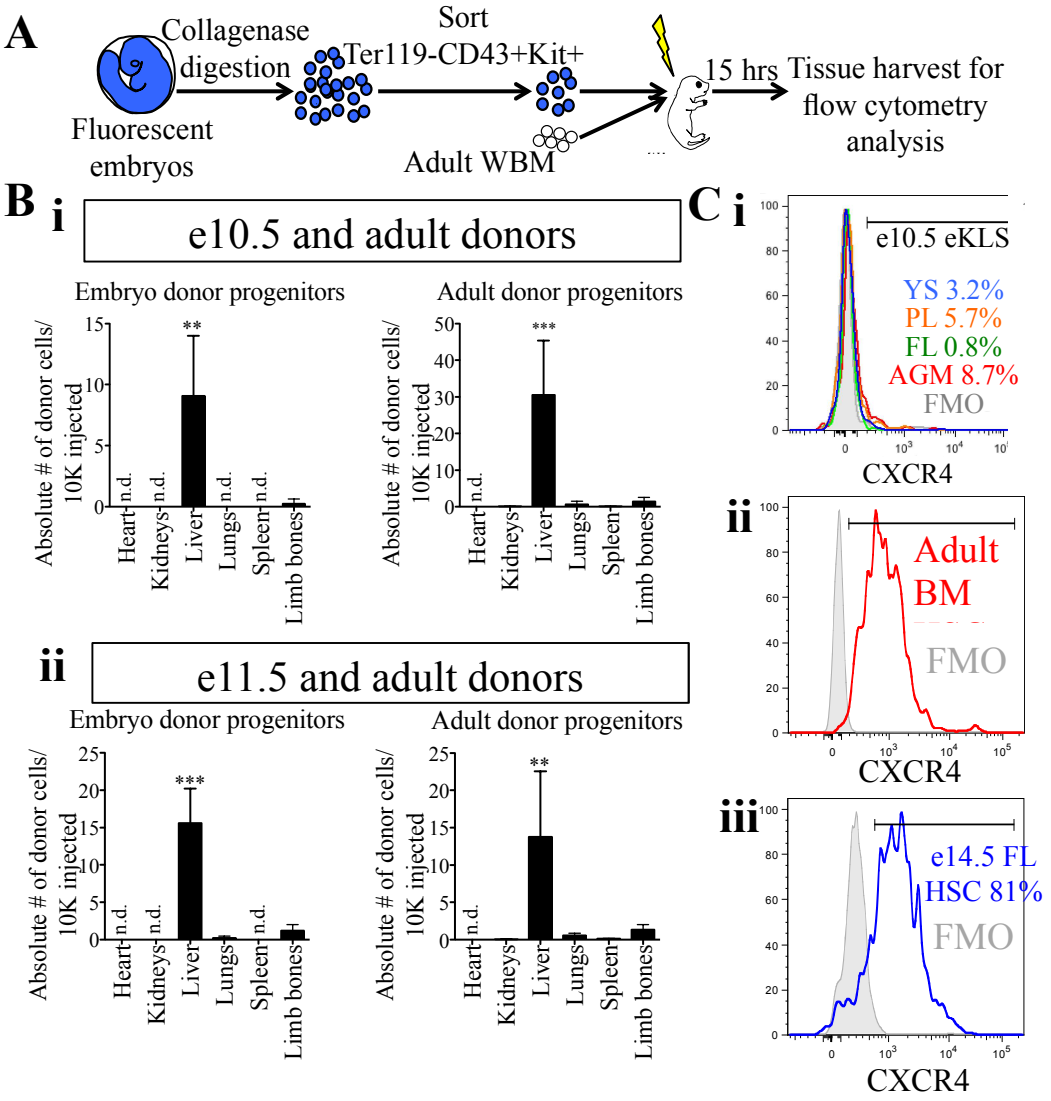

Figure 2.5. Neonatal liver harbors transplanted embryonic and adult donors in the short-term post-transplant. A) Schematic representation of short-term homing assay. Ter119- CD43+ Kit+ progenitors were sorted from whole embryos, mixed with 100,000 adult WBM and transplanted into irradiated P1-P4 neonatal recipients. 15 hours post-transplant, organs were harvested for FACS analysis. **B)** Detection of donor progenitors shortly after transplant. Absolute number of Ter119- CD43+ Kit+ progenitors originating from e10.5 **(i)** and e11.5 **(ii)** embryos and the accompanying adult source normalized to 10,000 injected cells are shown in the heart, kidneys, liver, spleen, and limb bones of the neonatal recipients. Tissues were harvested and processed in their entirety. "Limb bones" includes femurs and tibias from the hind limbs and humeri from the forelimbs. ***p ≤ 0.01, ***p ≤ 0.001 (Student's unpaired t test). e10.5, n=3 (2 independent experiments); e11.5, n=4.* **C)** Surface expression of CXCR4 in e10.5 pre-HSCs **(i)**, adult BM HSCs **(ii),** and e14.5 FL HSCs **(iii)**. Percentages of CXCR4+ cells are shown in histograms. FMOs were used to set the positive gate. Adult BM and e14.5 FL HSCs were stained and analyzed in the same experiment. e10.5 pre-HSCs were analyzed in a separate experiment alongside appropriate positive staining controls (adult BM HSCs, data not shown). *FMO, fluorescence minus one. n.d., not detected.*

Discussion

The precise surface marker identity of pre-HSCs in the embryo has remained elusive, hampering efforts to understand how HSCs arise during embryonic development. Our previous results identified a candidate pre-HSC population using an *in vitro* multipotency assay.[11] Here, using an *in vivo* neonatal transplantation assay, we demonstrate that this population, which we call "11a-eKLS" (Ter119- CD43+ Kit+ Sca1+ CD144+ CD11a-), contains all *in vivo* pre-HSC activity at gestational days e10.5 and e11.5 in the mouse embryo. As we compared 11a- eKLS cells to all other KLS cells in the embryo (Figure 2.2), as well as all Kit+ cells (Figure 2.3), we are confident 11a- eKLS cells are the *only* source of pre-HSCs at these timepoints. Additional markers may subdivide this population further, but 11a- eKLS cells also express CD41, CD105, and Tie2, and lack expression of Fcγr, CD11b, and Flk2.[11] Importantly, the lack of CD11a expression on these cells was critical for distinguishing them from downstream progenitors and could not be replaced with other pre-HSC markers such as VE-Cadherin (CD144), CD41, or CD45. Additionally, our analysis of the cell cycle status of these populations (Figure 2.4) supports the notion that CD11a-eKLS cells contain pre-HSCs that slowly transition to quiescent HSCs, while the CD11a+ fraction represents downstream transit-amplifying cells.

Many groups studying embryonic origins of HSCs have found success in identifying embryonic cells with HSC potential by first culturing them *ex vivo* in cytokine combinations that drive hematopoietic maturation.[129] We chose an *in vivo* approach to identify cells with neonatal engraftability as an alternative, independent method of identifying HSC precursors. While primitive hematopoiesis is known to begin at e7.0-e7.5, and definitive hematopoiesis at 8.5, we did not identify neonatal engraftable cells until e9.5. Furthermore, we only identified this from unsorted caudal half tissue, and could not consistently achieve neonatal engraftment from sorted

cells at e9.5. While we could identify 11a- eKLS cells at e9.5 (Inlay et al., 2014), we cannot claim this population is neonatal engraftable until e10.5.[11]

We found 11a- eKLS cells (and its pre-HSC activity) in all tissues we examined, and thus this study is agnostic as to which embryonic tissue(s) produce pre-HSCs. Due to the challenges and highly variable engraftment rates in the neonatal transplantation system, we did not attempt to compare engraftment levels of sorted pre-HSCs between each tissue to determine which tissue contained more pre-HSCs. Unfortunately, we were unable to consistently sort enough 11a- eKLS cells from the vitelline vessels to transplant them, though they are likely an important source of pre-HSCs.[130] It should be noted that at e9.5, only the unsorted cells from the caudal half (CH) engrafted long-term (Figure 2.1C). In the sorted experiments, we more often observed higher chimerism from AGM than from the YS (Figure 2.2C). Lastly, in the Sca1 plus/minus transplants (Figure 2.3B), we observed robust engraftment only from the Sca1+ (CD43+ Ter119- Kit+) cells sorted from the AGM and placenta, but not the YS or FL. Thus, while we observed engraftment from 11a- eKLS cells regardless of which timepoint or tissue we sorted them from, those sorted from the AGM tended to lead to higher engraftment. It is possible that 11a- eKLS cells are distinct from one another depending on which tissue they originated in. There appeared to be some differences in lineage distribution amongst the 11a- eKLS derived cells in the recipients (Figure S4), most notably an increase in T cells in several recipients. However, given that the recipients are immunodeficient and devoid of their own lymphocytes, the expansion of T cells in these recipients after transplantation may be due to variability in their reconstitution kinetics and not due to intrinsic lineage biases *per se*. We had hypothesized that extra-embryonic sources of pre-HSCs (YS, PL) may contain a myeloid bias compared to embryonic sources (AGM, FL), but our results do not support that.

Whether fully functional HSCs emerge *de novo* from hemogenic endothelium (HE) is unclear. Our results support the notion that a precursor emerges first from HE and then later matures into HSCs. This may require migration to a different site in order to complete development. As part of the LFA-1 complex, CD11a is involved in the extravasation of circulating immune cells. Thus, the differentiation of a pre-HSC (CD11a-) to a downstream transit amplifying progenitor (CD11a+) could be associated with a transition to a more migratory state. Interestingly, CD11a upregulation correlates with the downregulation of VE-Cadherin (CD144), a molecule necessary for forming junctions between endothelial cells. Downregulation of VE-Cadherin could allow pre-HSCs to detach from the endothelium and enter circulation while CD11a upregulation signals their extravasation to other tissues. In support of this concept, we have observed CD11a+ pre-HSC at e14.5 (Figure S2.5), and CD11a+ fetal HSCs at e17.5.[122] CD11a upregulation could be coupled to the migration of pre-HSCs into the fetal liver, and HSCs into the newly formed BM cavity.

Why can pre-HSCs engraft in neonatal recipients, but not adult? The liver persists as an active site of hematopoiesis until shortly after birth (up to 3 weeks).[131] As such, the neonatal liver might provide a temporary and readily accessible niche for transplanted pre-HSCs. Indeed, we found that almost all transplanted embryonic progenitors homed to the liver of neonatal recipients shortly after transplantation (Figure 2.5). We also observed that adult HSCs also preferentially seeded the neonatal liver over the bone marrow, suggesting a more passive mechanism for liver seeding rather than direct homing (Figure 2.5B). Regardless, this suggests that the developing liver microenvironment provides pre-HSCs with maturation signals required for eventual BM homing/engraftment, such as the upregulation of the BM homing receptor CXCR4. Indeed, the upregulation of CXCR4 in the FL from e10.5 to e14.5 suggests the ability to respond to BM

homing signals (CXCL12) correlates with the maturation of pre-HSCs into BM-engraftable HSCs. In this regard, many previous studies have highlighted the supportive effects of the FL niche stroma on HSC maintenance/expansion.[132-135]

In summary, we report a highly enriched population "11a- eKLS" that contains *all* pre-HSC activity in the embryo. Upon transplantation into neonatal recipients, these cells appear to seed the liver first, and therein mature into BM-engraftable HSCs. As such, our data implicate this population as the immediate precursor population to HSCs. CD11a negativity was critical for identifying these cells up to e11.5 and can allow for improved isolation and characterization of developing pre-HSCs. This in turn can lay the groundwork to determine the molecular cues required for maturation into HSCs. Efforts aimed to generate HSCs from pluripotent sources, although promising and improving, have failed to display robust BM engraftment of the differentiated HSCs.[136-138] Given the similarities between pluripotent source-derived HSCs and pre-HSCs (e.g. HSC-like phenotype without BM homing/engraftment potential), identification of environmental stimuli involved in pre-HSC maturation could reveal how to generate engraftable HSCs from pluripotent stem cells.

Materials & Methods

Antibodies

A detailed list of all antibodies used in this study is shown in Table S2.1.

Mice

In our experiments, we used embryos from a *Rosa26*$^{Tomato/CFP}$ male crossed to a *Rosa26*$^{wt/wt}$ (C57Bl/6; Jackson Laboratory; stock no. 00664) female. *Rosa26*$^{Tomato/CFP}$ males were generated from a cross between *Rosa26*$^{Tomato/Tomato}$ (mT/mG; Jackson Laboratory; stock no. 007576) and *Rosa26*$^{CFP/CFP}$ (TM5; generous donation by Dr. Irving Weissman). NSG (NOD-*scid* IL-2Rγ^{null}; Jackson Laboratory; Stock no. 005557) mice were used as neonatal recipients. All strains were maintained at the Gross Hall and Med Sci A vivarium facilities at UCI and fed with standard chow and water. All animal procedures were approved by the International Animal Care and Use Committee (IACUC) and University Laboratory Animal Resources (ULAR) of University of California, Irvine.

Embryo harvest and tissue processing

Mating cages were established, and vaginal plugs were checked every morning to determine the time of pregnancy. The morning of plug detection was assigned as day 0.5. Pregnant mice were dissected, and embryos harvested in PBS + 2% fetal bovine serum (FACS buffer) and kept on ice during tissue dissection. Somite pairs were counted and averaged for each experiment to determine dpc. Dpc designation is as follows: 15-29 somite pairs: e9.5; 30-39 somite pairs: e10.5; 40-50 somite pairs: e11.5. For tissue analyses and non-sorted transplants, CH, YS, and PL were harvested from e9.5 embryos. For e10.5 and e11.5 embryos, AGM and FL were harvested separately instead of together (e.g. CH). For sorted transplants, CH, YS, and PL were harvested from e10.5 donors

and AGM, YS, PL, and FL from e11.5 donors. For non-sorted transplants, YS was harvested with the vitelline vessels, and PL was harvested with umbilical vessels. For sorted transplants, YS was separated without the vitelline vessels, and PL was harvested with umbilical vessels. Separated tissues were digested with 1 mg/mL Collagenase Type IV (ThermoFisher Scientific; cat. no. 17104019) for 30-45 minutes at 37°C. Tissues were pipetted up and down at 15-minute intervals to aid with the digestion. Single cell suspension was filtered using a 40 μ mesh. We recommend using 40 μ (instead of 70 μ) mesh for donor cells to minimize clogging of blood vessels upon injection into neonatal recipients. Cells were washed twice and resuspended in FACS buffer for staining/transplantation.

Cell sorting

Single cell suspensions of cells were typically stained for 20-30 minutes on ice. We recommend using ACK lysis buffer *after* completion of cell staining as pre-staining use can affect the VE-Cadherin signal. For sorting, a BD FACS-Aria II (Becton Dickinson) with FACSDiva software was used. For sorted transplants, the "purity" mode was used for cell sorting. Since opposing populations from differentially labeled embryo cells were pooled together, only embryo batches with close to 50-50% color distribution were used for the competitive sorted transplant. Therefore, physiological ratios of opposing populations were reflected in the final tube to be transplanted. For short-term homing sorts, the "yield" mode was used for cell sorting to maximize cell recovery.

In vivo transplantation and analysis

For non-sorted transplants, the embryo equivalent used for each timepoint is as follows: ≥4 ee for e9.5, ≤3 ee for e10.5, and ≤1 ee for e11.5. For all transplants, single cell suspensions were resuspended in 50-70 μL FACS buffer for injection with defined numbers of adult helper BM

added. For neonatal transplants, cells were injected into the facial vein of sublethally irradiated (180-200 Rads; XRAD 320, Precision X-ray) P1-P4 NSG recipients. Nursing NSG mothers were fed an antibiotic chow of Trimethoprim Sulfa (Uniprim, Envigo) for 4 weeks post-transplant to prevent bacterial infections. For secondary transplantation into adult recipients, recipient C57BL/6 mice were conditioned with 800 Rads, anesthetized by isoflurane, and retro-orbitally injected with 1-2 million whole BM harvested from primary recipients. For peripheral blood analysis, blood was obtained from the tail vein of transplanted mice at various timepoints, and red blood cells were depleted using ACK lysis buffer. For BM analysis, BM was harvested from tibias and femurs by flushing with ice-cold FACS buffer followed by ACK lysis and filtration. Cells were stained with lineage antibodies and analyzed on the BD FACS-Aria II. FlowJo software (Tree Star) was used for data analysis.

Cell cycle analysis

FoxP3 / Transcription Factor Staining Buffer Kit (Tonbo Biosciences; cat. no. TNB-0607) is a paraformaldehyde/saponin based fixation/permeabilization buffer set for intracellular staining and was adapted here for cell cycle analysis. Briefly, cells stained with extracellular antibodies were fixed with 1X Tonbo Foxp3/Transcription Factor Fix/Perm buffer for 45 min at 4°C, permeabilized/stained with PE anti-ki-67 antibody (Biolegend; cat. no. 652403) diluted in 1X Tonbo Flow Cytometry Perm Buffer for 45 min in the dark at room temperature. Cells were then washed and stained with 1 μM DAPI (Biolegend; cat. no. 422801) for 10 min prior to flow cytometric analysis. Ki-67 is a nuclear protein associated with cellular proliferation and is expressed on cells that have entered the cell cycle, but not on quiescent G0 cells.[128] DAPI is a nuclear dye that can distinguish cells that have undergone DNA replication. We recommend

avoiding separation of e10.5 tissues into fewer than 4 ee as the fix/perm process results in loss of cells.

Short-term homing analysis

Neonatal recipients were sacrificed 15 hours post-transplant for tissue dissection. Care was taken to harvest tissues in their entirety. All tissues except bones were harvested by crushing in between slides followed by separation using a 28-gauge needle. Limb bones were crushed using a pestle and mortar. Crushed bone particles were passed through a 28-gauge needle for further separation. All tissues were filtered through a 40 μ mesh and ACK lysed prior to staining.

Statistical analysis

Statistical analysis was performed with GraphPad Prism 5 software (La Jolla, CA).

Supporting Information

Supplemental Figures

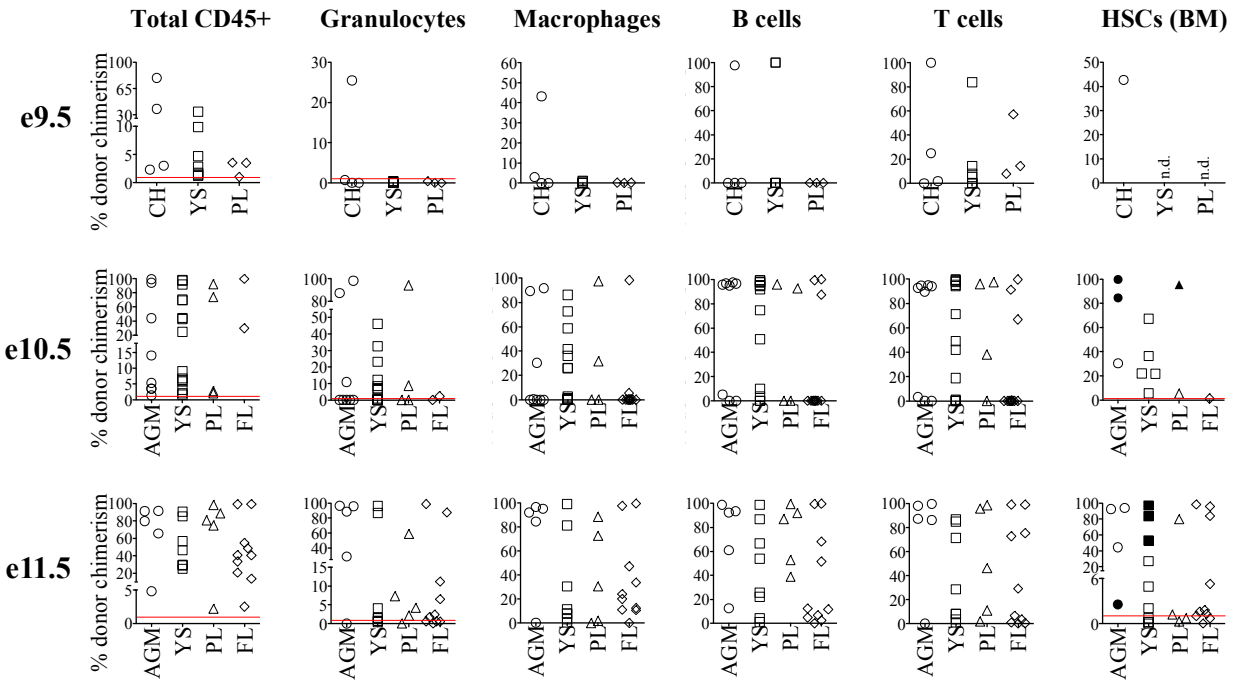

Supplementary Figure S2.1. Donor lineage and HSC chimerism in recipients transplanted with unsorted embryonic tissues. Donor output (% donor chimerism) in the blood of recipients transplanted with unsorted embryonic e9.5 (top row), e10.5 (middle row), and e11.5 (bottom row) tissues at the time of the last bleed (at least 12 weeks post-transplant). Percentages are relative to total output in each lineage, which includes both helper- and host-derived cells. CH = caudal half, AGM = aorta-gonad mesonephros, YS = yolk sac, PL = placenta, FL = fetal liver. Any donor chimerism (CFP+, CD45.2+) above 1% (red line) was scored as positive for that lineage. Recipients with positive donor granulocyte chimerism were further analyzed for donor-derived HSCs in the bone marrow (rightmost column). Recipients selected for secondary transplantation are indicated by closed symbols (black). See Figure 1C for a table summarizing these results. These data indicate efficient engraftment and multilineage output of e10.5 and e11.5 embryonic cells whereas e9.5 counterparts exhibited very low engraftment efficiency. *n.d. = not detected*.

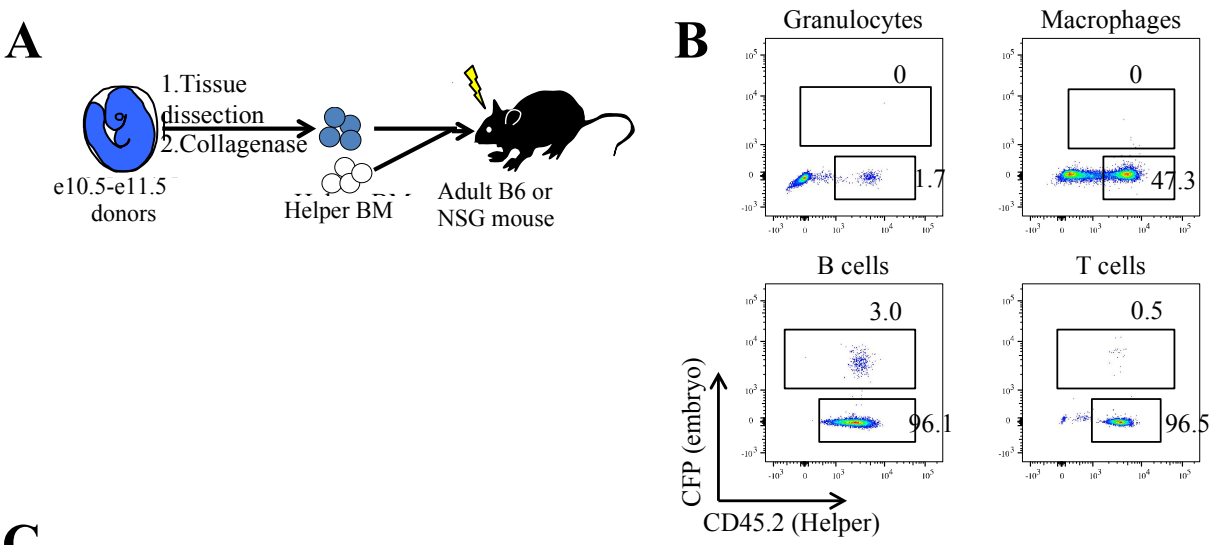

C

dpc	ee/ recipient	Adult recipient genotype	LT-chimerism	Total blood chimerism	Macrophage chimerism	B cell chimerism	T cell chimerism	Total successful transplants
e10.5	3-4	NSG	0	2	n.d.	n.d.	n.d.	3
		B6	0	0	0	0	0	5
e11.5	1-2	NSG	0	3	1	2	3	4
		B6	0	1	0	1	0	6

Supplementary Figure S2.2. Lack of engraftment of e10.5 and e11.5 tissues into adult recipients. **A**) Experimental strategy. Whole embryos (CFP+) were dissociated in collagenase and transplanted along with helper bone marrow (50,000 helper cells for e10.5, 100,000 helper cells for e11.5) into lethally irradiated adult B6 and NSG recipients. **B**) Representative blood analysis at 12 weeks post-transplant. Embryo donor-derived cells are CFP+ and CD45.2+, helper-derived cells are CFP- and CD45.2+, and host cells are CFP- and CD45.2-. **C**) Table summarizing results. *n.d. = not detected*. LT-chimerism is defined as recipients with donor-derived HSCs in the BM at 12 weeks. Successful transplants are those with donor chimerism in any lineage (either embryo-derived or helper-derived) and is used to indicate mice that were "successfully" injected. While limited donor chimerism of specific mature cell types was detected, embryonic tissue-derived HSCs were not detected in the BM of any recipient, suggesting that BM-engraftable HSCs had not yet matured at these embryonic stages. This supports the notion that the neonatal engraftment observed from e10.5 and e11.5 tissues came from pre-HSCs, and not HSCs.

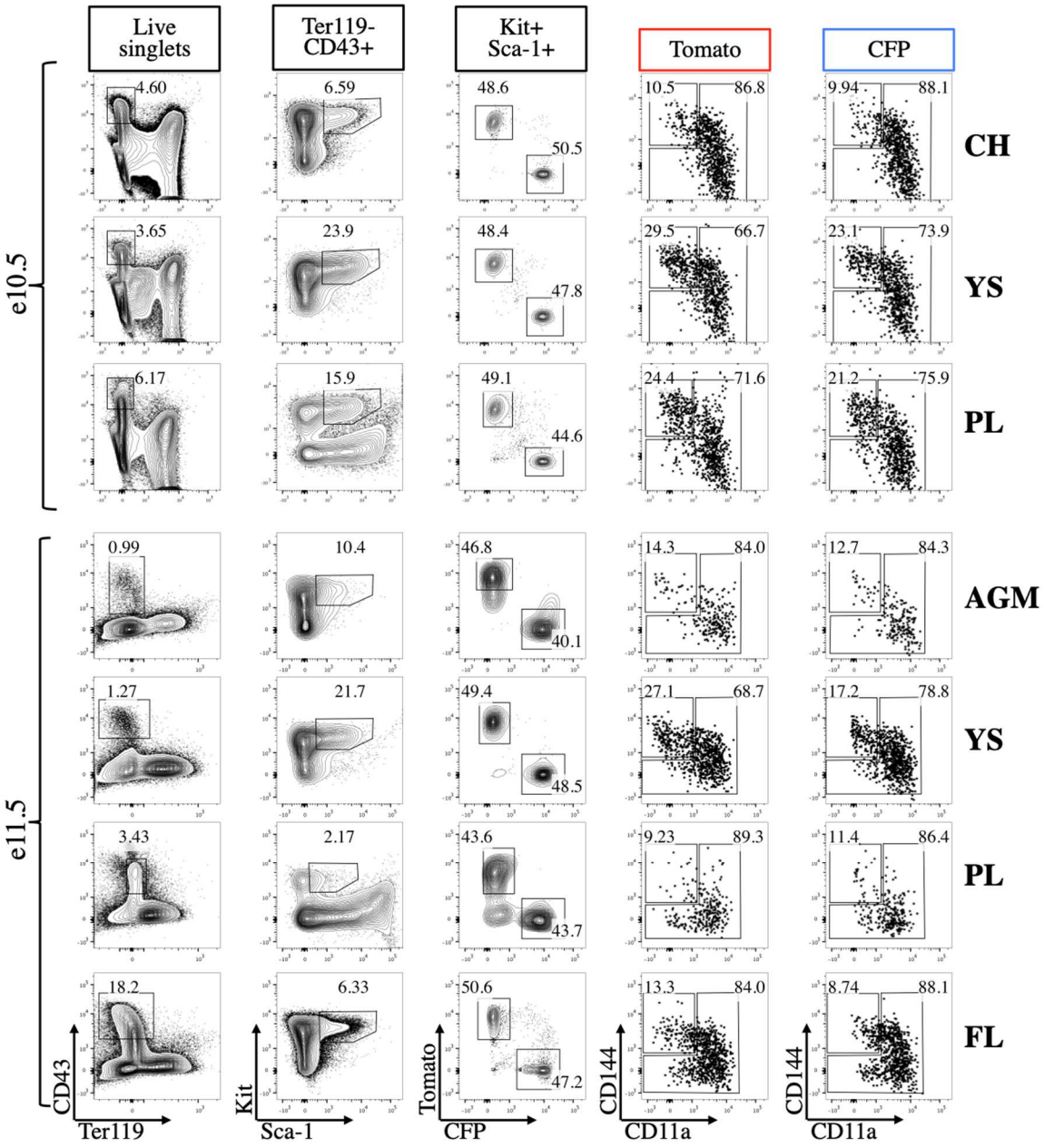

Supplementary Figure S2.3. Representative gating for competitive sort. A) Representative sorting strategy for the competitive transplantation of 11a- eKLS and Other eKLS populations. Each column represents the boxed population at the top of the column, and gated populations are shown to the right side of parent gates. Tissues of origin are indicated on the right side. Live Ter119- CD43+ Kit+ Sca-1+ cells are gated on based on Tomato or CFP fluorescence. Within each color of the progenitor population, CD11a- CD144+ ("11a- eKLS") and everything else ("Other eKLS") are sorted. Opposing populations of different color (i.e. CFP+ 11a- eKLS and Tomato+ Other eKLS) are mixed post-sort and transplanted into the same recipient along with helper adult BM.

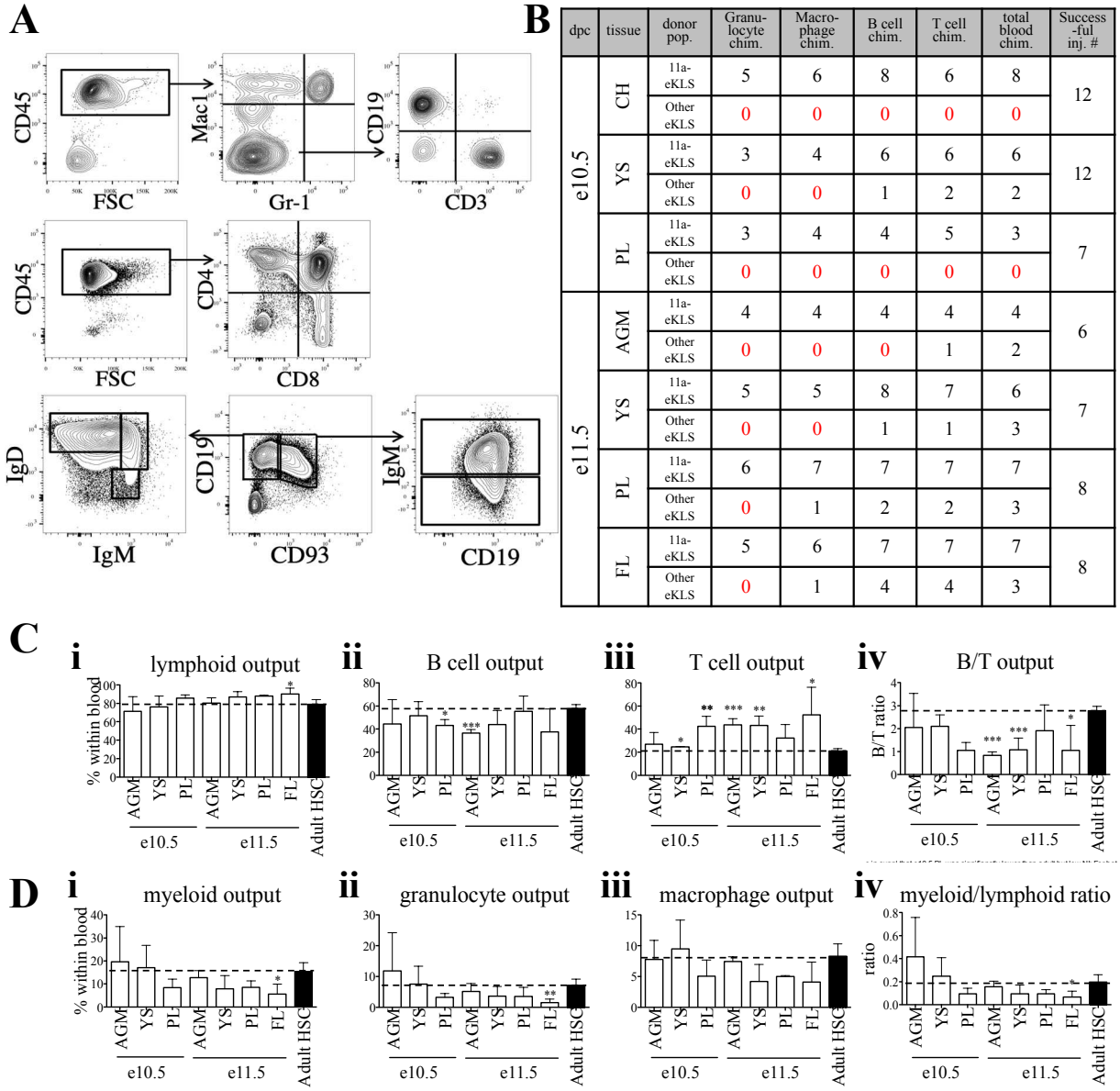

dpc	tissue	donor pop.	Granu-locyte chim.	Macro-phage chim.	B cell chim.	T cell chim.	total blood chim.	Success-ful inj. #
e10.5	CH	11a- eKLS	5	6	8	6	8	12
		Other eKLS	0	0	0	0	0	
	YS	11a- eKLS	3	4	6	6	6	12
		Other eKLS	0	0	1	2	2	
	PL	11a- eKLS	3	4	4	5	3	7
		Other eKLS	0	0	0	0	0	
e11.5	AGM	11a- eKLS	4	4	4	4	4	6
		Other eKLS	0	0	0	1	2	
	YS	11a- eKLS	5	5	8	7	6	7
		Other eKLS	0	0	1	1	3	
	PL	11a- eKLS	6	7	7	7	7	8
		Other eKLS	0	1	2	2	3	
	FL	11a- eKLS	5	6	7	7	7	8
		Other eKLS	0	1	4	4	3	

Supplementary Figure S2.4. Lineage output dynamics of 11a- eKLS embryonic donors in neonatal recipients. A) Representative FACS plots of donor lineage output in neonatal recipients at the final timepoint in blood (top row), thymus (middle row), and spleen (bottom row). All gates are pregated on donor embryo-derived cells. For the blood, macrophages (CD11b+ Gr1-), granulocytes (CD11b+, Gr1+), B cells (CD19+) and T cells (CD3+) represent the gates used for the blood analyses throughout the study. Analysis of T cell populations in the thymus, and B cell subpopulations in the spleen demonstrate that donor hematopoiesis appears normal in these tissues. **B**) Table summarizing results in Figure 2C. The number of recipients with donor lineage chimerism (chim.) and total donor CD45+ chimerism (total blood chim) are indicated. The number of mice that displayed either donor embryo or helper chimerism greater than 1% are considered successfully injected is indicated in the rightmost column (successful inj. #). While many conditions (population/timepoint/tissue) supported lymphocyte reconstitution, myeloid reconstitution was only observed with 11a- eKLS donor cells, and never with "other eKLS" cells. This demonstrates that pre-HSCs are only found in the 11a- eKLS population. **C)** Lymphoid lineage analysis at 12 weeks post-transplant of CD11a- eKLS cells from e10.5 and e11.5 tissues. **i**) donor lymphoid output (B cells and T

cells) as a percentage of total donor CD45+ cells, from different 11a- eKLS sources. Only the e11.5 FL showed a statistically significant difference, albeit mild, in lymphoid output compared to recipients transplanted with adult HSCs. This suggests there does not appear to be a bias towards or against lymphocyte production or homeostasis with embryonic donors. Output specifically in B cells (**ii**) and T cells (**iii**) is shown as well as the ratio of B:T cells (**iv**). The dashed horizontal bar represents the output from adult recipients transplanted with adult HSCs (black bar), which was used for comparison to represent normal hematopoietic constitution. All statistical analyses are relative to those recipients. There appears to be a statistically significant increase in T cell output relative to B cells with several of the embryonic tissues but is inconsistent and could be due to the variability in lymphopoiesis that occurs in NSG recipients, which lack lymphocytes and therefore undergo a rapid expansion of lymphocytes. **D**) Donor myeloid output in recipient mice. Total myeloid output (**i**), as well as specific granulocyte (**ii**) and macrophage (**iii**) are shown. The ratio of myeloid to lymphoid cells is shown. Only the e11.5 FL displayed a statistically significant decrease in myeloid cells relative to lymphoid compared to the adult HSC transplanted controls. This could be due to a burst of lymphopoiesis in NSG recipients, which lack lymphocytes of their own. This data shows that there does not appear to be a lineage bias of 11a- eKLS cells depending on which tissue they are obtained from.

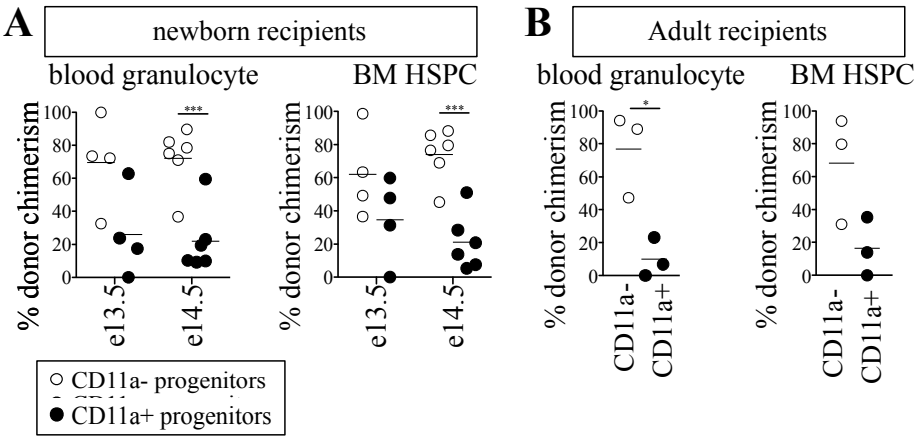

Supplementary Figure S2.5. At later timepoints (e13.5 and e14.5), both CD11a- and CD11a+ cells are capable of neonatal and adult engraftment. Long-term engraftment of CD11a- and CD11a+ progenitors from e13.5-e14.5 FL in neonatal recipients **(A)** and from e14.5 FL in adult recipients **(B)**. "Progenitors" are defined as Ter119- CD43+ Sca1+ Kit+ EPCR+. Blood granulocyte chimerism and BM HSPC chimerism are shown for each set of recipients. These results demonstrate that at later embryonic timepoints, neonatal engraftable pre-HSCs and bone marrow engraftable HSCs begin to upregulate CD11a. *$*p \leq 0.05$, ***$p \leq 0.001$ (Student's unpaired t test). Each condition (e13.5 or e14.5 transplanted into neonatal or adult recipient) performed in 2 independent experiments.*

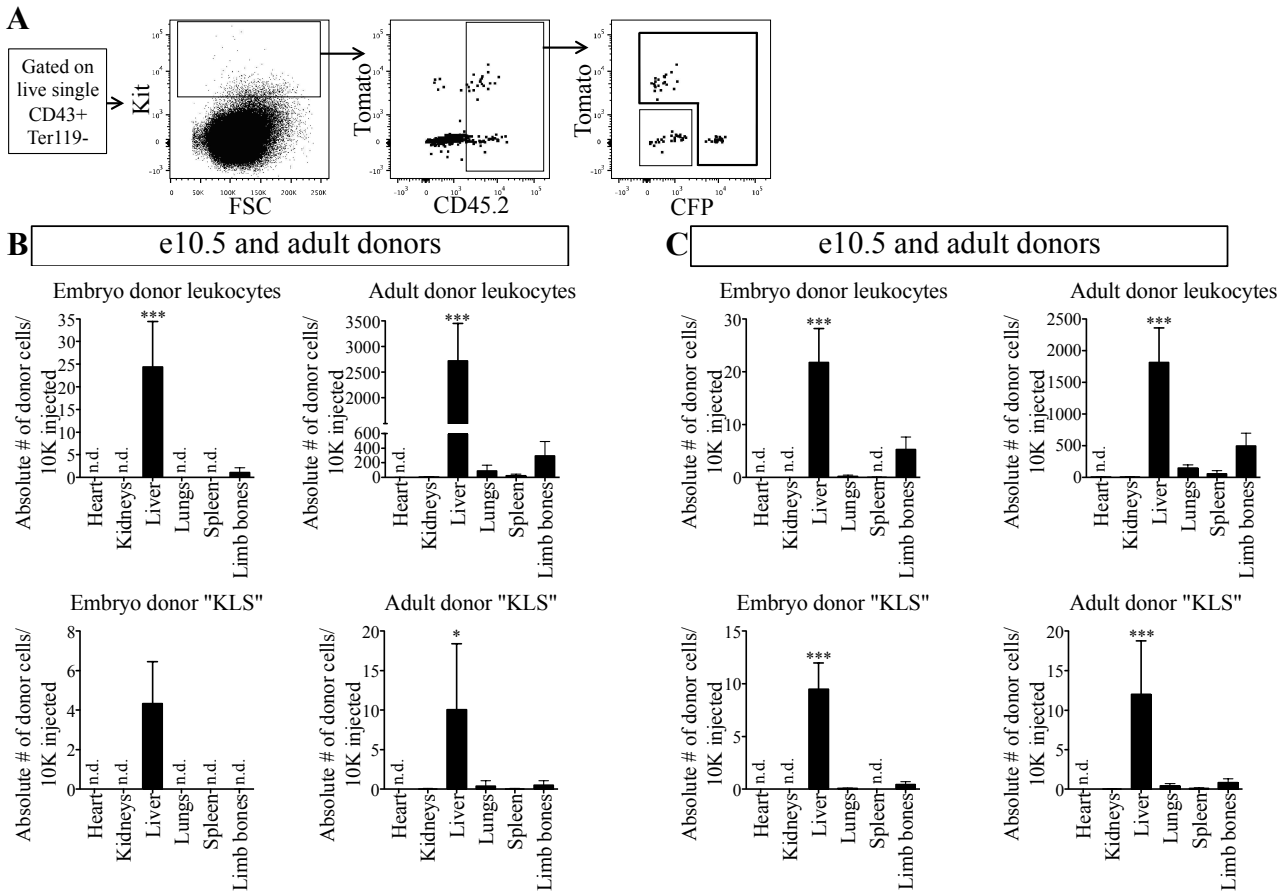

Supplementary Figure S2.6. Detection of embryo donor- and adult donor-derived populations in neonatal recipients shortly after transplantation. A) Representative analysis of recipient tissues in short-term homing assays. Embryo donors are identified as CFP+ or Tomato+ cells expressing CD45.2+ within the population of interest (in this case, Ter119- CD43+ Kit+). Adult WBM is distinguished by the expression of CD45.2 (recipient NSGs exclusively express CD45.1) along with lack of fluorescence (fluorescent proteins are specific to embryos). Although rare, donor cells were readily identifiable in distinct populations. **B-C)** Detection of e10.5 **(B)** and e11.5 **(C)** donor cells shortly after transplant. "Donor leukocytes" is defined as Ter119- CD43+ and "donor KLS" is defined by Ter119- CD43+ Kit+ Sca-1+. ***p ≤ 0.01, ***p ≤ 0.001 (Student's unpaired t test). e10.5, n=3 (2 independent experiments); e11.5, n=4. n.d., not detected.*

Supplementary Tables

Table S2.1. Antibodies Table				
Antigen	**Clone**	**Conjugate**	**Source**	**Catalogue #**
TER119	TER119	PE/Cy5	Biolegend	116210
	TER119	BV421	Biolegend	116233
SCA1 (Ly-6A/E)	E13-161.7	PE/Cy7	eBioscience	122514
	E13-161.7	PE	Biolegend	122507
KIT (CD117)	ACK2	APC	Biolegend	135107
	2B8	APC-eFluor 780	eBioscience	47-1171-82
	2B8	BV421	Biolegend	105828
CD27	LG.7F9	eFluor 780	eBioscience	47-0271-82
	LG.7F9	APC	eBioscience	17-0271-82
CD11A	M17/4	PE/Cy7	eBioscience	25-0111-30
	M17/4	Biotin	Biolegend	101103
	M17/4	APC	Biolegend	101119
	M17/4	PE	Biolegend	101107
	M17/4	FITC	Biolegend	101106
	M17/4	Alexa Fluor 488	Biolegend	101111
EPCR (CD201)	eBio1560	PerCP-eFluor 710	eBioscience	46-2012-82
	eBio1560	APC	eBioscience	17-2012-82
GR1 (Ly-6G/Ly-6C)	RB6-8C5	Alexa Fluor 700	eBioscience	108422
MAC1 (CD11b)	M1/70	APC	Biolegend	101212
	M1/70	FITC	Biolegend	101205
CD19	6D5	APC	Biolegend	115512
	eBio1D3	PerCP-Cy5.5	eBioscience	45-0193-82
	6D5	BV421	Biolegend	115537
CD45	30-F11	APC/Cy7	Biolegend	103116
	30-F11	Alexa Fluor 700	Biolegend	103128
CD45.2	104	FITC	Biolegend	109806
CD45.1	A20	PE/Cy7	Biolegend	110729
CD3ε	17A2	PerCP-eFluor 710	eBioscience	46-0032-82
	17A2	PE/Cy7	Biolegend	100220
CD150 (SlamF1)	TC15-12F12.2	Brilliant Violet 650	Biolegend	115931
CD4	RM4-5	PE/Cy7	Biolegend	100527
CD8a	53-6.7	APC/Cy7	Biolegend	100714
CD93 (AA4.1)	AA4.1	APC	eBioscience	17-5893-81
IgD	11-26c.2a	Alexa Fluor 700	Biolegend	405729
IgM	RMM-1	APC/Cy7	Biolegend	406515
B220	RA3-6B2	BV605	Biolegend	103243
Cxcr4	2B11	PE	BD Biosciences	561734
Ki-67	16A8	PE	Biolegend	652403
CD43	S7	APC	BD Biosciences	560663
CD144	BV13	Biotin	Biolegend	138008
Secondary antibodies				

		Qdot 655-Streptavidin	Life Technologies	Q10121MP
		Qdot 605-Streptavidin	Life Technologies	Q10103MP
		eFluor710-Streptavidin	eBioscience	49-4317-80

CHAPTER 3: FLUTICASONE PROPIONATE (FLONASE) ENHANCES HEMATOPOIETIC STEM CELL TRANSPLANTATION IN MICE

Introduction

Author's Note: I spearheaded this project and contributed most of the work for this chapter. I created this thesis project with input from my PhD advisor Dr. Matthew Inlay and my committee members. I designed all the experiments for this chapter. Dr. Craig Walsh suggested the method for our experiment that produced data for Figure 3.4. I conducted most of the experimental work and had help from a first-year graduate student Angel Ayala who conducted experiments for Figure 3.4A under my guidance. I collected, interpreted and made figures for all the data in this chapter. I also wrote this chapter with edits from my committee members.

Hematopoietic cell transplantation (HCT), also known as blood and marrow transplantation, is a potentially curative treatment for many hematologic malignancies.[139] HCT is the process of ablating a diseased blood system and replacing it with a healthy one from donor Hematopoietic stem cells (HSCs). HSCs are the key component to HCT due to their ability to self-renew, differentiate into lineage blood cells, and engraft the bone marrow from the blood. Unfortunately, not all injected donor HSCs seed and engraft the bone marrow, limiting blood cell reconstitution.[140-143] A low number of transplanted HSCs can result in disease relapse and opportunistic infections after HCT, therefore increasing engraftment efficiency and number of engrafted HSCs would be beneficial to a successful HCT.[144,145]

C-X-C chemotactic receptor type 4 (CXCR4) is important for HSC engraftment and chemotaxis to the bone marrow through a blood chemotactic gradient of stromal derived factor 1 (SDF-1) secreted by bone marrow stromal cells.[146,147] Transgenic expression of CXCR4 on

human HSCs has been shown to increase bone marrow engraftment in immunocompromised mice.[19] Furthermore, Guo et. al. found that treating human cord blood HSCs with the glucocorticoid, fluticasone propionate (Flonase), increases bone marrow engraftment in immunodeficient mice by increasing surface CXCR4 expression.[20] CXCR4 is also important for HSC retention in the bone marrow niche demonstrated by HSC mobilization into the blood after AMD3100, CXCR4 antagonist, treatment.[148] Inducing CXCR4 expression on HSCs with Flonase holds promise to improving HSC engraftment efficiency and is worth further investigation in mouse models.

Besides relapse, a major complication that causes high morbidity and mortality after allogeneic HCT (allo-HCT) is acute or chronic GVHD. Up to 40-60% of patients develop acute GVHD after allo-HCT due to a human leukocyte antigen (HLA) mismatch between donor and recipient.[149] Subsequently, donor T cells systemically infiltrate and damage healthy recipient tissues. Advances in disease treatment have significantly reduced incidence of GVHD related mortality.[150,151] The standard of care for acute GVHD (aGVHD) is methotrexate in combination with calcineurin inhibitors to suppress allogeneic immune responses.[152-154] Due to drug toxicity, other prophylactic strategies have targeted allogeneic T cells to suppress graft-host inflammation. T cell depletion prior to transplantation is used to prevent GVHD, yet results in increased relapse due to graft failure and a lack of a graft vs leukemia (GVL) effect.[155] Treatment with high dose cyclophosphamide (PTCy) after haplo-identical transplantation in mice has shown to create graft-host immunogenic tolerance while maintaining GVL.[156] Additionally, clinical studies of this method resulted in a low incidence of severe GVHD.[157] However, long-term studies have recently reported PTCy toxicity and no significant differences in GVHD onset when compared to

established methods.[158,159] While there are many effective prophylactic treatments for GVHD, there is still a need for new strategies to eliminate GVHD.

Glucocorticoids are used to prevent GVHD after onset of symptoms by suppressing allogeneic induced inflammation. However, there are harmful side effects when administered globally and in prolonged courses.[160] In this study, our goal was to suppress the allogeneic immune response and create immunogenic tolerance by directly treating donor splenocytes *in vitro* with a single dose of Flonase prior to allo-HCT in mice. We demonstrate that in addition to increasing murine HSC engraftment efficiency in a syngeneic setting, Flonase can also decrease aGVHD severity despite a robust donor T cell engraftment. Both outcomes are a proof of principle for improving HCT.

Results

Flonase increases surface CXCR4 on murine HSCs via glucocorticoid receptor

In the study by Guo et al., the authors found improvements in human cord blood HSC CXCR4 expression, migration and engraftment upon pre-treatment with Flonase, but were unable to identify similar effects on murine HSCs.[20] To determine whether glucocorticoids had similar effects on murine HSCs as Guo et al. reported for human, we first cultured c-kit enriched murine BM with different concentrations of Flonase or Dexamethasone (Dex) for 16 hours, then examined CXCR4 expression and viability on phenotypic HSCs (Ter119- CD27+ ckit+ Sca1+ CD150+ CD34-) (Fig S3.1A, S3.1B). We found that 3nM Flonase was the best concentration and glucocorticoid that led to a significant upregulation of CXCR4 expression on HSCs and the overall KLS population with no observable impact on HSC viability (Fig 3.1A, S3.1C, S3.1D). Flonase-induced CXCR4 expression increase was also not specific to cell culture media (Fig S3.1E).

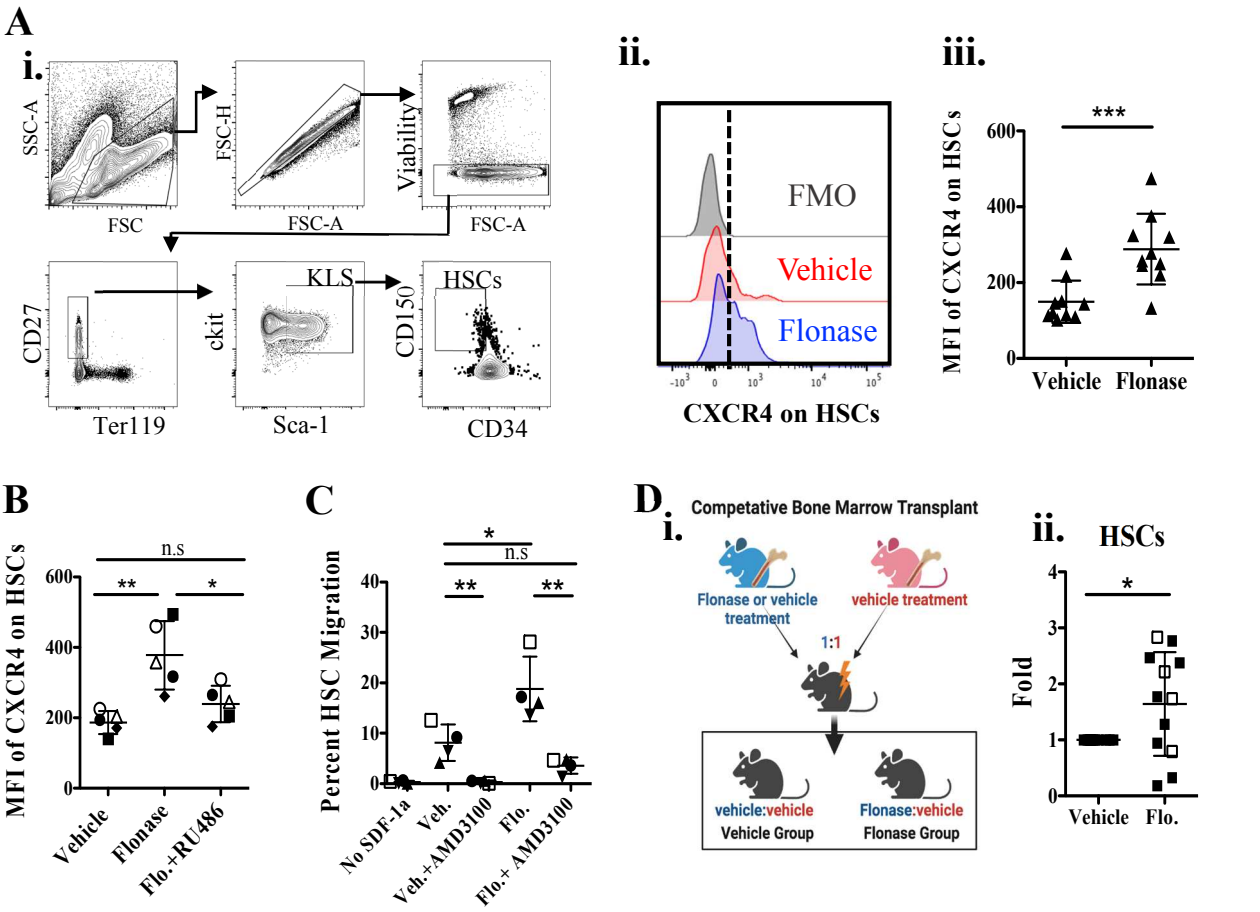

Figure 3.1. CXCR4 surface expression and function of murine HSC after Flonase treatment. (A) (i) Representative gating strategy for KLS population (CD27+ Ter119- ckit+ Sca1+) and HSCs (CD27+ Ter119- ckit+ Sca1+ SlamF1+ CD34-). (ii) Representative histograms of surface CXCR4 expression on HSCs after 16hr of culture in Vehicle (DMSO, red histogram) or 3nM Flonase (blue histogram). The dashed line indicates cutoff for positive CXCR4 expression based on the fluorescence minus one (FMO, grey histogram) control. Histogram is normalized to mode. (iii) Flow cytometry quantification of median fluorescent intensity (MFI) of surface CXCR4 expression on HSCs (n=10, representative of 7 independent experiments using). Flonase concentration is 3nM in this study unless otherwise labeled. **(B)** MFI of surface CXCR4 on HSCs after Vehicle, Flonase or Flonase+ RU486 (GR antagonist) treatment (n=5, representative of 3 independent experiments). **(C)** Transwell migration of HSCs toward SDF-1α (50ng/mL) after 16hr pre-treatment in Vehicle or Flonase then a 30-minute incubation with or without CXCR4 antagonist (AMD3100) (n=4, representative of 4 independent experiments). **(D)** (i) Scheme of competitive syngeneic transplant of FACs sorted bone marrow KLS cells from fluorescently labeled CFP+ (blue) or tdTomato+ (red) mice co-transplanted in equal amounts into lethally irradiated (850cGy) C57BL/6J recipients. (ii) Flow cytometry analysis of CFP+% to tdTomato+% donor HSC chimerism in the bone marrow 12 weeks post-transplant in both recipient groups. "Flonase Group" was normalized to the "Vehicle Group", and "Vehicle Group" was set to 1 (n=12, representative of 9 independent experiments). Open symbols are females, closed are males. *, $p \leq .05$; **, $p \leq .01$; ***, $p \leq .001$ (One sample t-test). $M \pm$ SD shown. Abbreviations: BM, bone marrow, HSC, Hematopoietic stem cell, KLS, kit+ lineage- sca-1+ cell population, GR, glucocorticoid receptor, Flo., Flonase, Veh., Vehicle, FMO, fluorescence minus one.

The suggested mechanism responsible for Flonase-induced CXCR4 expression on human CB HSCs is through Flonase-glucocorticoid receptor (GR) binding resulting in histone acetylation on the CXCR4 locus.[20] To evaluate if this was also true in mice, we cultured c-kit enriched bone marrow cells in Flonase in the presence or absence of the GR antagonist RU486. CXCR4 was upregulated on Flonase-treated HSCs compared to vehicle-treated cells, but this upregulation was blocked when RU486 was included (Fig 3.1B). This suggests that CXCR4 is upregulated through the GR pathway in murine HSCs after Flonase treatment. In addition, we saw a significant increase of percent CXCR4+ HSCs, but not MFI on existing CXCR4+ HSCs after Flonase culture suggesting an induction of CXCR4 expression on non-expressing HSCs (Fig S3.1F, S3.1G).

Flonase increases hematopoietic stem cell (HSC) bone marrow migration and engraftment.

We next tested whether increasing CXCR4 surface expression with Flonase also increases HSC migration toward the CXCR4 binding chemokine stromal derived factor 1α (SDF-1α) also known as CXCL12. A trans-well migration assay using Flonase pre-treated c-kit-enriched BM showed a significant increase in the percentage of HSC migration towards SDF-1α relative to vehicle-treated HSCs (Fig 3.1C, S3.1H). In addition, when the CXCR4 antagonist molecule AMD3100 was added to the Flonase culture, improvement in migration was blocked, further supporting the notion that Flonase improved HSC migration through the CXCR4 pathway.

To determine whether Flonase treatment led to improvements in HSC engraftment in vivo, we performed syngeneic competitive transplantations with HSCs pre-treated with Flonase or Vehicle. In these experiments, sorted KLS cells were obtained from vehicle pre-treated Rosa26$^{tdTomato/tdTomato}$ (tdTomato+) and vehicle or Flonase pre-treated Rosa26$^{CFP/CFP}$ (CFP+) mice then transplanted them 1:1 into lethally irradiated B6 recipients (Fig 3.1Di, S3.1I). Flonase group recipients were normalized to the vehicle control group to calculate fold change. Although mild,

there was a significant fold increase in bone marrow engraftment from Flonase pre-treated HSCs 3 months after transplantation (Fig 3.1Dii, S3.1J). However, there was no difference in blood (Fig S3.1K) CD45 engrafted lineage cells from the Flonase treated group possibly due to injecting KLS cells containing other progenitors causing noisiness of engrafted donor cell populations. Overall, we have shown that Flonase increases CXCR4 expression on murine HSCs and improves murine HSC bone marrow engraftment after bone marrow transplantation.

Pre-treating donor cells with Flonase decreases aGvHD in mice

A frequent complication in HCT is GvHD, a disease that causes an inflammatory response from donor cells to recipient tissue due to an MHC mismatch (HLA for humans, H-2 for mice). GvHD leads to tissue damage especially in the liver, gut and skin, and in severe cases it can end in death. We took an additional approach to improving HCT by utilizing Flonase to reduce lethality and tissue damage in a lethal acute GvHD (aGvHD) mouse model. We pre-treated fresh whole bone marrow cells (2-3 x 10^6 cells) and splenocytes (6 x 10^6 cells) with 3nM Flonase from CFP+ mice (which have an H-2^b MHC background) and transplanted them into lethally irradiated (850cGy) Balb/cJ mice (H-2^d background) (Fig 3.2A). Recipient mice were scored for GvHD severity based of off Naserian et. al. assigning 1 point for each GvHD symptom including hunched back, skin lesions, dull fur, diarrhea, and 10% loss of initial weight.[161] There were two groups of Flonase pre-treated recipient mice used with a single vehicle-treated control group: one Flonase group was used to create a survival curve, and the other Flonase group was used for flow cytometry analysis where recipients were paired with vehicle recipients and euthanized when one of the two developed GvHD.

After unblinding the study, we observed a phenotypic difference between recipients that received Flonase- or Vehicle-treated donor cells (Fig 3.2B, S3.2A, S3.2B). “Vehicle” mice

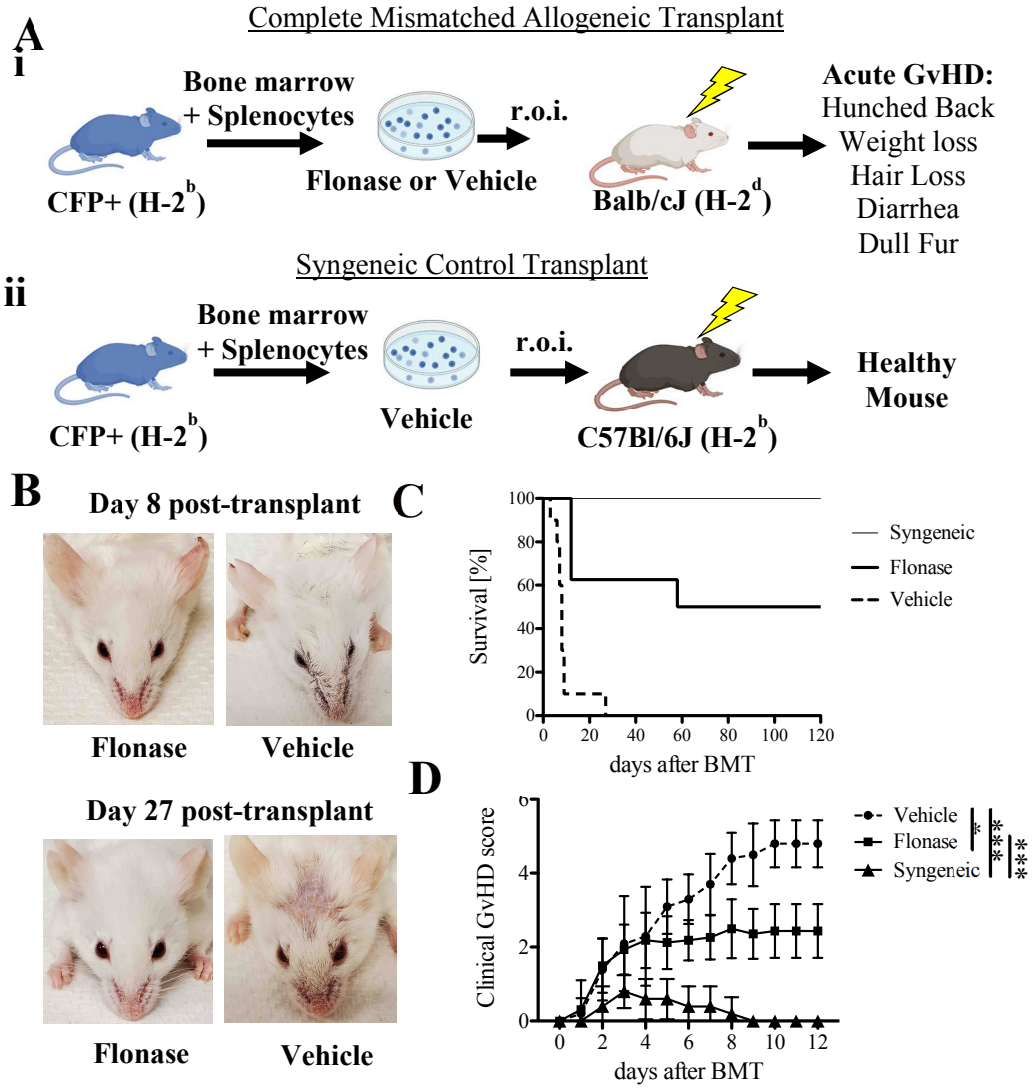

Figure 3.2. GvHD analysis after allogeneic transplantation of Flonase pre-treated splenocytes and bone marrow cells in mice. (A) (i) Scheme of allogeneic transplant of $6x10^6$ whole splenocytes plus $3x10^6$ whole bone marrow cells from CFP+ (H-2^b) mice after Flonase or vehicle culture into lethally irradiated (lightning symbol) Balb/cJ recipients. (ii) Scheme of Syngeneic transplant of $6x10^6$ whole splenocytes plus $3x10^6$ whole bone marrow cells from CFP+ (H-2^b) mice after vehicle culture into lethally irradiated C57Bl/6J (H-2^b) recipients. **(B)** Representative images of allogeneic Balb/cJ (H-2^d) recipients euthanized due to GvHD at 8 days (top females) and 27 days (bottom males) post transplantation of Flonase (left) or vehicle (right) treated cells. **(C)** GvHD survival study of **"**Flonase" or "Vehicle" allogeneic recipients or "Syngeneic" recipients throughout 120 days post transplantation (n=10 for "Vehicle" group, n=8 for "Flonase" group, n=4 for "Syngeneic" until day 27 then n=2 thereafter not due to GvHD, but data collection for Figure 3; with half females and half males for all groups; representative of 3 independent experiments); mice were euthanized at ≥30% loss of initial weight or after receiving a clinical score of 5. **(D)** Quantification of clinical scoring system of visual observation of GvHD in recipients. One point was assigned for each symptom of GvHD: hunched back, dull fur, skin lesion, diarrhea, and 10% loss of initial weight. An automatic full score of 5 was assigned to recipients that experienced ≥30% loss of initial weight (n=10 for Vehicle group and n=16 for Flonase group with half females and half males for both groups; representative of 3 independent experiments). *, $p \leq .05$; **, $p \leq .01$; ***, $p \leq .001$ (Student's unpaired t-test). $M \pm$ SD shown. Abbreviations: GvHD, graft-vs-host disease, r.o.i, retro-orbital injection, CFP, cyan fluorescent protein.

displayed discharge around their eyes with dull fur around the nose around 1-week post-transplant (p.t.) and were euthanized within 9 days p.t. due to a weight loss of ≥30%. One mouse was euthanized at day 27 p.t. for obtaining a full clinical score of 5 (Fig 3.2B, 3.2C). On the other hand, only half of the "Flonase" recipients were euthanized due to weight loss, with the other half surviving with only minimal GvHD symptoms (clinical score < 2, Fig. 3.2C, S3.2C). Flonase recipients also had a significantly lower overall clinical score compared to the vehicle group (Fig 3.2D), with no gender difference observed (Fig. S3.2D). In summary, this showed that Flonase recipients had diminished acute GvHD severity compared to the vehicle group.

Flonase-pretreated donor CD3 T cells engrafted and expanded in allogeneic recipients

Our next goal was to characterize the donor immune cells after allotransplantation in recipient mice receiving Flonase- or vehicle-treated cells. Glucocorticoids like Flonase are known to cause apoptosis in lymphocytes, therefore, we assessed the percent of cell death of both treated groups prior to transplantation. We found that after 16 hours in culture, there was a significant reduction of T and B lymphocyte viability in the Flonase-treated group compared to the vehicle control (Fig 3.3A, S3.3A). Interestingly, there was no reduction in macrophage nor granulocyte viability (Fig S3.3A). This suggested that the reduction in GvHD symptoms in the "Flonase" mice could be due to a decrease in alloreactive T lymphocytes. However, after approximately 1-week post-transplantation, we surprisingly saw a robust engraftment of donor T cells in the Flonase recipients' blood, spleen, and liver (Fig 3.3B, 3.3C). While the percent engraftment of donor CD3+ T cells (as a percentage of total CD45+ cells) was reduced in the blood, there were comparable levels between Flonase and Vehicle treated group recipients. Importantly, in both groups the majority of CD45+ cells in the blood and liver were T cells indicating a major expansion of T cells after transplantation (Fig. 3.3B, 3.3C). In addition, we also performed a syngeneic transplant

(vehicle-treated CFP+ donor cells into B6 recipients), and there was a significant decrease in engrafted donor CD3+ T cells in this group compared to either allogeneic setting, indicating an expansion of T cells in the allogenic recipients. This magnitude of donor cell engraftment and expansion in Flonase group recipients was unexpected knowing the unequal number of T cells transplanted into recipients from each treated group. Therefore, this demonstrates that GvHD resistance in the Flonase group was not due to a lack of donor T cell engraftment.

Flonase pre-treatment reduces expression of CD69 and CD44 activation markers on donor CD4 T cells after allogeneic transplantation

Glucocorticoids are immunosuppressive and decrease many immune cell functions such as cytokine production, signal transduction and TCR signaling. To assess possible activation reduction in the Flonase group donor T cells, we analyzed leukocyte early activation markers CD69 and CD44 (Fig. 3.3E-3.3G). Both markers are known to be elevated on infiltrating T cells in allogeneic transplantation in mice.[162,163] In the vehicle group spleens, we observed a significant increase in the percentage of CD69+ CD4 T cells (~21.7%) compared to the syngeneic recipient (7.03%), indicating activation of CD4 T cells. However, in the Flonase group, there was a significant decrease in the percentage of CD69+ CD4 T cells (~10.7%) compared to vehicle, indicating a suppression of activation of Flonase-treated T cells. Similar differences were observed in the blood and liver (Fig. 3.3F). All donor T cells expressed CD44, but we observed a significant decrease in CD44 MFI on CD4 T cells pre-treated with Flonase in recipient blood, liver and spleen compared to the Vehicle group (Fig 3.3E-G).

CD8 T cells appeared less activated in both Vehicle and Flonase groups, with little difference in CD69 positivity or CD44 expression. This is in concurrence with Beilhack et. al. where they showed donor CD8 T cells lose CD69 expression after day 6 post allogeneic

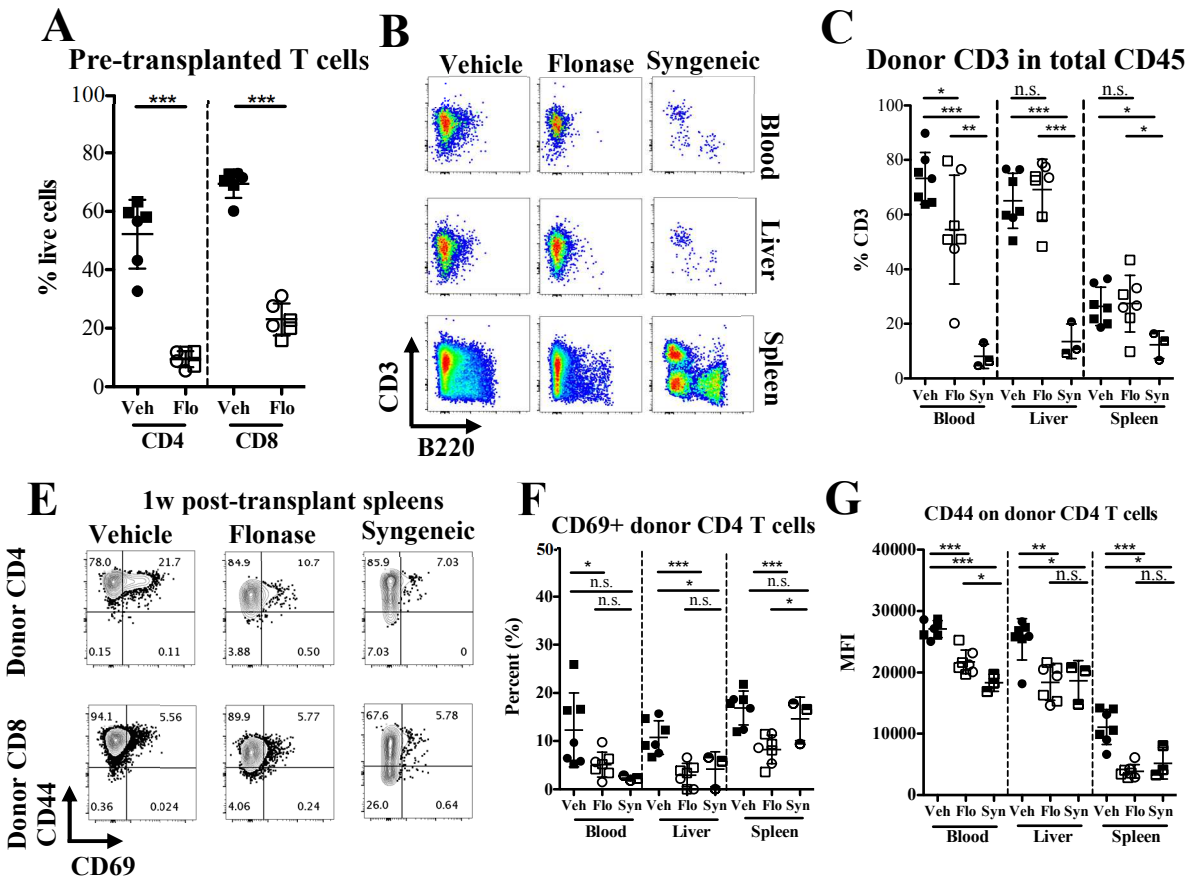

Figure 3.3. Characterization of donor T cells in allogeneic transplanted recipients receiving either Flonase or vehicle-treated whole splenocytes and bone marrow cells. (A-F) Data from allogeneic transplant of whole splenocytes plus whole bone marrow cells from CFP+ (H-2^b) mice after Flonase or vehicle (DMSO) culture into lethally irradiated Balb/c (H-2^d) or C57BL/6J (H-2^b) recipients. **(A)** Percent live (Annexin V-, PI-) CD4+ T cells (CD11b-, Gr1-, CD19-, CD45+, CFP+, CD8-, CD4+) and CD8 T cells (CD11b-, Gr1-, CD19-, CD45+, CFP+, CD4-, CD8+) from spleen after 16h culture and before transplantation with Flonase or vehicle (n=6, representative of 3 independent experiments). Circles represent males and squares represent females. **(B)** Representative plots of donor CD3 and B220, populations in blood, liver and spleen of recipient Balb/c mice transplanted with donor CFP+ C57BL/6J cells treated with Vehicle (left column), and Flonase (middle column). Syngeneic (Syn) transplant control (C57BL/6J recipient) (right column) received Vehicle treated CFP+ cells. Gated on live, CD45+, CFP+, CD11b-, Gr1- single cells. **(C)** Quantification of percent donor CD3 in total CD45+ population in blood, liver and spleen of donor mice. Gated on live, CD45+, CFP+, CD11b-, Gr1-, B220- single cells. **(E)** Representative plots showing activation markers CD44 and CD69 expression on donor CD4 (top row) and CD8 (bottom row) T cells from Vehicle, Flonase and Syngeneic recipient groups. Gated on live, CD45+, CFP+, CD11b-, Gr1-, B220-, CD3+, single cells. **(F-G)** Quantification of percent CD69+ cells (F) and MFI of CD44 (G) in donor CD4 population. Gated on live, CD45+, CFP+, CD11b-, Gr1-, B220-, CD3+, CD8-, CD4+ single cells. (C, F, G) (n=7 for Flonase and Vehicle groups days 6-9 p.t., representative of 3 independent experiments) (n=3 for Syngeneic Vehicle (Syn) CFP+ C57BL/6J into C57BL/6J group day 9 (1 mouse) and day 27 (2 mice) p.t., representative of 2 independent experiments). Circles represent males and squares represent females. *, $p \leq .05$; **, $p \leq .01$; ***, $p \leq .001$ (Student's unpaired t-test). $M \pm$ SD shown. Abbreviations: p.t., post-transplant, Veh, Vehicle, Flo, Flonase, syn, syngeneic.

transplantation (Fig S3.3C).[162] Together, these data provide some insight on a possible explanation for Flonase-mediated reduction in aGvHD in mice which might involve a decrease in activity in CD4 T cells.

T cells treated with Flonase activate and expand after CD3 and CD28 co-stimulation, however not when cultured with allogeneic splenocytes

We next wanted to elucidate whether Flonase inhibits T cells from activation through TCR stimulation. To address this, we conducted an *in vitro* T cell activation assay using anti-CD3/CD28 antibody cultures with splenocytes pre-treated for 16 hours in vehicle or Flonase. Cultured cells increased in size (via forward scatter, FSC-A) in both the Flonase and Vehicle pre-treated groups when stimulated with CD3/CD28 compared to the unstimulated Vehicle group, indicative of activation (Fig 3.4Ai.). Unstimulated Flonase cells did not survive in culture possibly due to a lack of stimulation and Flonase toxicity. Stimulated CD4 and CD8 cells appeared activated indicated by a dilution of CFSE, and significant increases and high expression of the activation markers CD25 and PD-1 compared to unstimulated Vehicle group which had low expression of these markers (Fig 3.4Aii, 3.4Aiii, S3.4A).

We next performed a mixed lymphocyte reaction to see if Flonase pre-treated T cells can be activated in an allogeneic manner *in vitro*. CFP+ splenocytes (H-2^b) were cultured in Flonase or vehicle for 16 hours then mixed with syngeneic (B6) or allogenic (Balb/cJ, H-2^d) irradiated splenocytes (Fig. 3.4B, S3.4B, S3.4C). Flonase pre-treated splenocytes did not survive, proliferate nor activate when cultured with allogeneic irradiated splenocytes (Fig 3.4Bi). In contrast, we observed cell activation and proliferation in the allogeneic stimulated Vehicle group, demonstrated by CFSE-dilution, and CD25 and PD1 upregulation (Fig 3.4Bii, S3.4B, S3.4C). In the syngeneic setting, neither Flonase nor vehicle-treated splenocytes were activated.

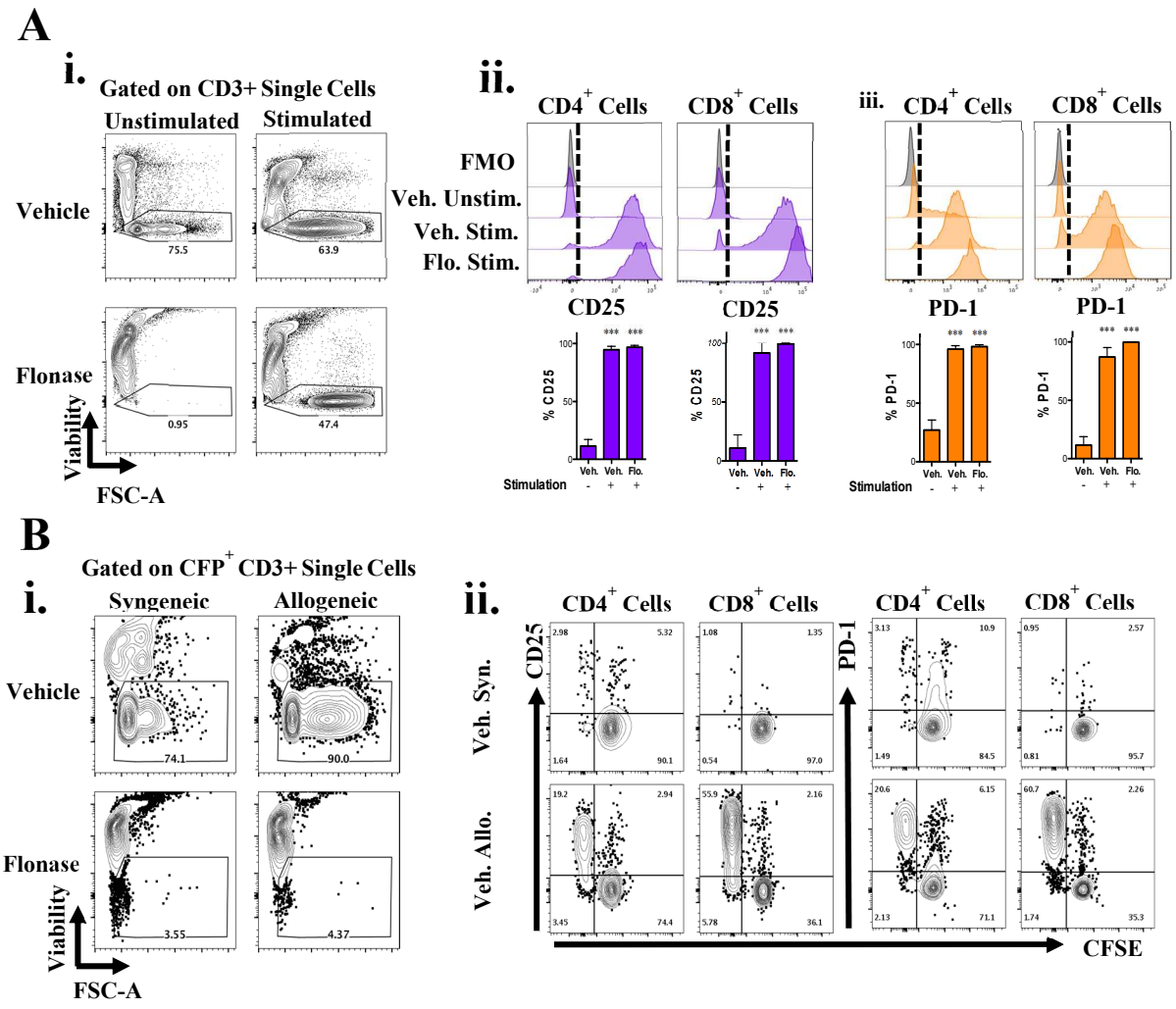

Figure 3.4. Murine splenic T cells pre-treated with Flonase retain their ability to activate when stimulated with CD3/CD28, but do not in an allogeneic mixed lymphocyte reaction (MLR) *in vitro*. **(A)** Analysis of anti-CD3/CD28 T cell activation assay with Flonase or Vehicle pre-treated splenocytes from CFP+ mice. $6x10^5$ splenocytes were stimulated for 4 days (n=3; M ± SD; 2 male and 1 female, representative of 2 independent experiments). (i) Representative plots of viability vs FSC-A gated on single cells. (ii-iii) Histograms and quantification of activation marker CD25 (ii) and PD-1 (iii) expression on CD4+ and CD8+ cells. Gated on live, single cells. **(B)** MLR analysis after 4 days in culture using a 1:1 ratio of $3x10^5$ irradiated (2500 cGy) stimulator cells, to $3x10^5$ responder cells (n=3; M ± SD; 2 male and 1 female) (i) Representative viability vs FSC-A plots of the following co-culture combinations of stimulator with responder splenocytes: Syngeneic Flonase (CFP+, H-2^b with Flonase-treated CFP+, H-2^b), Allogeneic Flonase (Balb/cJ, H-2^d with Flonase-treated CFP+, H-2^b), Syngeneic Vehicle (CFP+, H-2^b with Vehicle-treated CFP+ B6, H-2^b), and Allogeneic Vehicle (Balb/cJ, H-2^d with Vehicle-treated CFP+ B6, H-2^b cells). (ii) Representative plots of cell proliferation (CFSE staining) vs activation marker expression (CD25 and PD-1) on CD4+ and CD8+ cells after stated culture conditions. *, $p \leq .05$; **, $p \leq .01$; ***, $p \leq .001$ (Student's unpaired t-test). Abbreviations: Syn., Syngeneic, Allo., Allogeneic, Veh., Vehicle, Flo, Flonase, FMO, fluorescence minus one.

Thus, Flonase-treated T cells appear unable to activate in an allogeneic setting. Together, these data suggest that Flonase treated T cells can be activated in some contexts (anti-CD3/anti-CD28) but not others (MLR). A possible cause for the reduction of aGvHD in mice could be that Flonase decreases T cell activity in an allogeneic setting leading to less severe tissue damage and death.

Overall, Flonase improves hematopoietic stem cell transplantation in mice by increasing bone marrow HSC homing and engraftment likely from increasing CXCR4 expression. We also have shown that treating splenocytes and whole bone marrow with Flonase prior to allogeneic transplantation increases survival in transplanted recipients and reduces GvHD phenotype.

Donor T cells pre-treated with Flonase were not alloreactive when transplanted into secondary allogeneic recipients

We next explored whether Flonase pre-treated T cells retain long term tolerance towards an allogeneic host by performing secondary transplants into Balb/cJ mice. Splenocytes were harvested from mice receiving either CFP+ (H-2^b) Flonase or Vehicle treated splenocytes and bone marrow 7 days post transplantation. These splenocytes along with $2x10^6$ helper BM from tdTomato+ (H-2^b) were then transplanted into Balb/cJ (H-2^d) recipients (Fig 3.5A). Secondary syngeneic controls received vehicle treated primary recipient splenocytes. Based on a survival curve all but one Flonase secondary transplanted recipient survived to 60 days post-transplant compared to the vehicle group with less than half survival (Fig 3.5B). The non-surviving recipient in the Flonase group was euthanized for an inflamed/enlarged head, a symptom not related to GvHD in mice. There was also a significant reduction in the clinical grade for recipients that received Flonase pre-treated cells transplanted into primary recipients (Fig 3.5C).

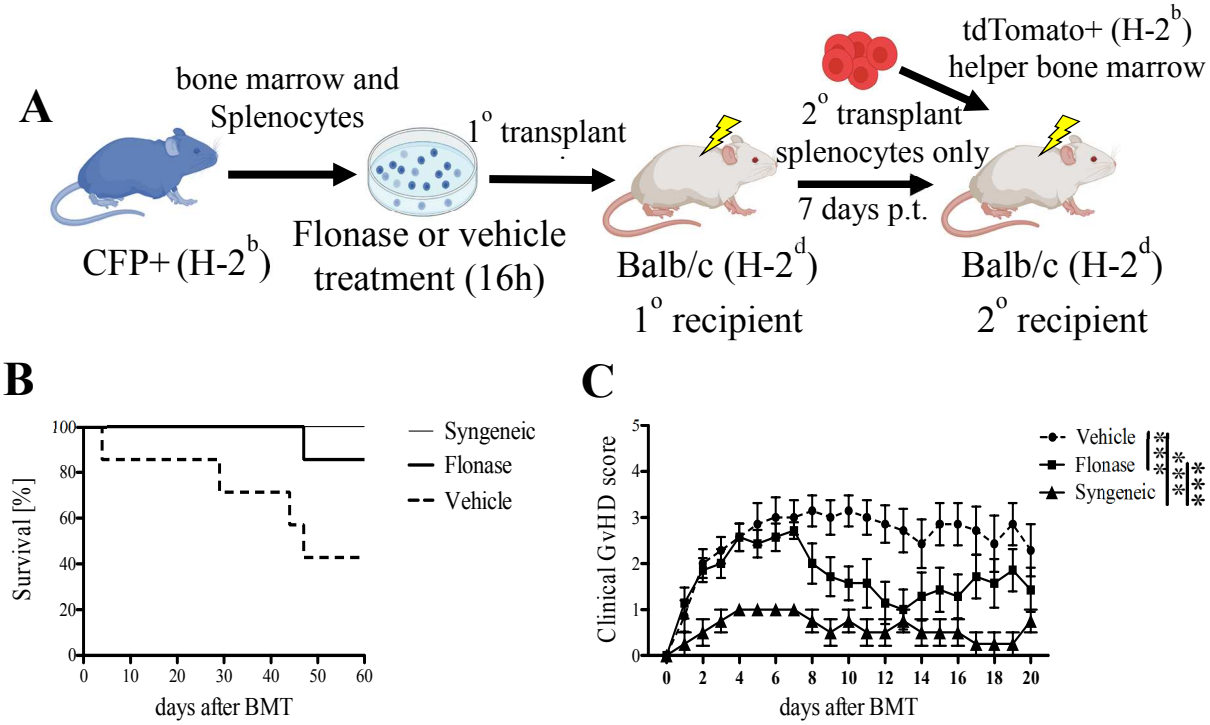

Figure 3.5. Flonase treated T cells retained long term tolerance in secondary transplanted allogeneic recipients. (A) Scheme of primary transplant of CFP+ $3x10^6$ whole bone marrow (wBM) plus $6x10^6$ splenocytes (s.c.) pre-treated with Flonase or Vehicle and secondary transplant using $1x10^6$ s.c. from lethally irradiated primary recipient and $2x10^6$ tdTomato+ H-2^b helper wBM into lethally irradiated Balb/c H-2^d mice. **(B)** Survival study over a 60-day period post transplantation of secondary recipients receiving allogeneic Flonase or Vehicle pre-treated primary recipient splenocytes ("Flonase" n=7, "Vehicle" n=7, 3 male and 4 female; "Syngeneic", 2 male and 2 female; representative of 2 independent experiments). "Syngeneic" secondary mice received cells from vehicle treated primary transplant group. **(C)** GvHD clinical grades of mice used in (B) over a period of 20 days (Error bars are SEM). Circles represent males and squares represent females. *, $p \leq .05$; **, $p \leq .01$; ***, $p \leq .001$ (Student's unpaired t-test). Abbreviations: Syn., Syngeneic, Allo., Allogeneic, Veh., Vehicle, Flo, Flonase, FMO, fluorescence minus one.

Overall, the elevated survival in the Flonase secondary group suggests that there were no alloreactive T cells transferred from the primary recipient. T cell engraftment in primary recipient blood and spleens were confirmed (data not shown). Blood was taken at a later time point (29 days post-transplant) from secondary recipients as to not skew early survival data and clinical grade scores. There was approximately 100% donor chimerism in both groups (Fig S3.5A). However, at this later time point, there was less primary recipient spleen-derived T cell engraftment compared to BM-derived T cells that are likely derived from transplanted HSCs and progenitors that often undergo thymic development after 4 weeks post-transplant (Fig S3.5B). Although not statistically significant, three vehicle group recipients later euthanized for GvHD (shown with crossed symbols) have a higher T cell engraftment from primary donor splenocytes in secondary recipient blood compared to those from recipients not euthanized in the vehicle group and Flonase group (Fig S3.5C). Taken together, Flonase pre-treated cells retained tolerance towards secondary recipient allogeneic tissues, suggesting that Flonase had lasting suppressive effects on treated cells.

Regulatory T cells are resistant to Flonase-induced apoptosis and had a higher engraftment in allogeneic recipient spleens after Flonase treatment.

Regulatory T cells (Tregs) are known to reduce GvHD in mice when added to an allogeneic transplant, therefore we investigated any differences in Tregs in our Flonase-treated allogeneic transplantation system.[164] Compared to conventional CD4+ cells (CD4 Tconv), Tregs are more resistant to dexamethasone-induced apoptosis when treated in vitro.[165] To test if Flonase had a similar effect on Tregs, we measured cell viability after Flonase or vehicle treatment of cultured splenocytes from mice that have green fluorescent protein (EGFP) labeled forkhead box protein P3 B6-Foxp3^{EGFP} (H-2^{b}). There was a slight significant reduction of about 1.1-fold in Treg (Foxp3+ cells) viability when comparing Flonase to vehicle treatment, however, CD4 Tconv, CD8

T cell and B cell viability significantly decreased about 6-fold after Flonase treatment compared to vehicle control (Fig 3.6A, S3.6A-C). Almost no Tregs were positive for propidium iodide (PI) after Flonase treatment while the other lymphocytes were mostly dead or apoptotic after treatment suggesting that Tregs were less sensitive to Flonase mediated apoptosis. This large reduction of CD4 Tconv, but not Treg viability after Flonase treatment increases the number of Tregs per CD4 Tconv or Treg:Tconv ratio transplanted into allogeneic recipients (Fig 3.6B, S3.6D).

We next assessed the level of Treg engraftment in blood, liver and spleen from recipient Balb/cJ (H-2^d) mice 9 days after allogeneic transplantation of Flonase or vehicle treated splenocytes and bone marrow cells from B6-Foxp3^{EGFP} (H-2^b) mice (Fig 3.6Ci). There was a significantly higher percentage of engrafted donor Tregs than Tconv in CD4+ cells in Flonase pre-treated cell recipient spleens compared to spleens from the vehicle control group, however, there was no difference in the blood or liver (Fig 3.6Cii-iii, S3.6E). This might have been a result of transplanting fewer Tconv cells and not necessarily an increase in Treg expansion compared to Tconv cells in the Flonase group. Reduced CD4 Tconv viability, but not Tregs skews the Tcon:Treg ratio in favor of Tregs with a possibility of increasing alloreactive immune suppression. These results were not due to a difference in donor engraftment, among different tissues or among Vehicle and Flonase treated groups, indicated by a high CD45 donor chimerism (Fig S3.6F). Although this data hints of a possible mechanism of action, we still cannot claim that the increased transplanted Treg:Tconv ratio is what causes the reduction in GvHD in mice after transplanting allogeneic Flonase treated splenocytes and bone marrow cells.

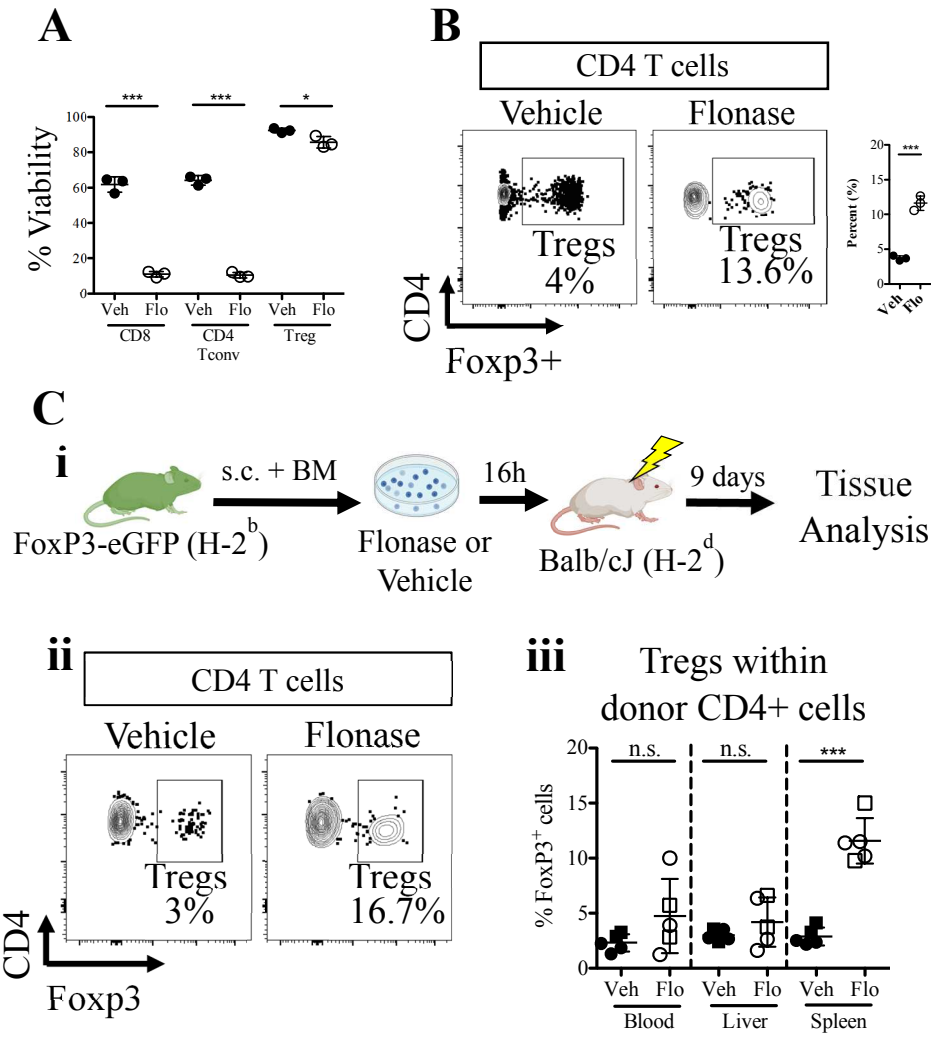

Figure 3.6. Characterizing of Flonase-treated regulatory T cells *in vitro* and in allogeneic recipient mice. (A) Flow cytometry analysis of live (Propidium Iodide (PI)-, Annexin V-) Tregs (CD3+, CD4+, FoxP3+, single cells), CD4 conventional T cells (Tconv) (CD3+, CD4+, Foxp3-, single cells), and CD8 T cells (CD3+, CD4+, Foxp3-, single cells) from spleen after 16h Flonase (3nM) and vehicle (DMSO) treatment (n=3). **(B)** Representative FACS plots (left) and quantitative data (right) showing percentage of Tregs (CD4+, Foxp3+) within live, CD3+, CD4+ T cell single cell population after 16h Flonase (3nM) or vehicle (DMSO) treatment (n=3). **(C)** (i) Scheme of allogeneic transplant of $6x10^6$ whole splenocytes plus $3x10^6$ whole bone marrow cells from Foxp3-GFP (H-2^b) mice after culture with Flonase or vehicle transplanted into lethally irradiated (850cGy, lightning symbol) Balb/cJ (H-2^d) recipients. Tissues (blood, spleen and liver) were harvested 9 days after transplant. (ii) Representative gating scheme of donor Tregs (shown in gate as H-2Db+, CD45+, CD3+, CD4+, CD25+, Foxp3+ (GFP+), live, single cells) in recipient mouse spleens 9 days after transplant from Flonase or vehicle pre-treated cells. (iii) Quantitative date from flow cytometry of percent engrafted donor Tregs (H-2Db+, CD45+, CD3+, CD4+, CD25+, Foxp3+ (GFP+), live, single cells) in recipient blood, liver and spleen (Flonase or "Flo" and Vehicle or "Veh" n=5). M ± SD shown. Circles represent males and squares represent females. Abbreviations: s.c., splenocytes, BM, bone marrow, Syn., Syngeneic, Veh., Vehicle, Flo, Flonase, r.o.i., retro-orbital injection PI, Propidium iodide. *, $p \leq .05$; **, $p \leq .01$; ***, $p \leq .001$ (Student's unpaired t-test).

Discussion

A low percentage, about 10%, of injected donor HSCs seed and engraft the bone marrow after HCT in mouse studies.[141-143] In humans, the number of donated HSCs is critical to HCT success, thus increasing engraftment efficiency would be beneficial.[166-168] Guo et. al. sought to improve human cord blood HSC transplantation by increasing engraftment efficiency.[20] They found that fluticasone propionate (Flonase) can increase human cord blood $CD34^+$ cell engraftment in immunodeficient mice by increasing surface CXCR4. Transgenic expression of CXCR4 on human $CD34^+$ also increases engraftment in immunocompromised mice.[19] Our reason for exploring Flonase treatment in mice instead of human CB is that mouse models are widely used for HCT and easier to acquire than CB $CD34^+$ cells. Our data show that Flonase increases surface CXCR4 on murine HSCs and HSC migration towards the CXCR4 chemokine ligand SDF-1α.

Flonase increased HSC bone marrow engraftment in a competitive transplantation mouse model. This transplantation included an injection control to account for any discrepancies in injection and an experimental control to set baseline engraftment of injected cells. We also observed a lack of increase and variability in total CD45 cells, granulocyte, macrophage, B cell or T cell engraftment from Flonase treated group compared to the vehicle group, possibly due to transplanting KLS cells containing lineage progenitors. We used 3nM of Flonase throughout the study based on the data from the HSC migration assay where 10nM was too high of a dose to induce a significant migration towards SDF-1α possibly due to toxicity. This dose was kept consistent when culturing splenocytes with bone marrow for our GvHD studies.

GvHD is a common life-threatening complication after allo-HSCT. Therefore, we set out to explore ways to decrease GvHD severity using an established acute GvHD allogeneic

transplantation model B6→Balb/c.[54] We saw a reduction in aGvHD severity in this system when transplanting Flonase pre-treated donor done marrow and splenocytes. This was not due to hematopoietic failure based on donor blood chimerism data from recipients.

We have not tested this method in a chronic GvHD (cGvHD) mouse model, however previous work has indicated that having early onset aGvHD is a risk factor for developing cGvHD, therefore reducing aGvHD can possibly lower the chance of acquiring cGvHD.[169] We also observed a lower GvHD clinical grade in the Flonase group. Human GvHD has a similar clinical grade system where the higher the clinical grade score the higher the chance of developing transplant-related mortality is.[170] Thus, lowering the overall clinical grade can make a difference in survival.

Initially, our goal was to deplete allogeneic T cells from donor transplanted cells using Flonase which induces T cell apoptosis. Depleting T cells in the clinic is shown to alleviate GvHD in patients after allo-HSCT.[171,172] However, to our surprise there was a large engraftment of donor T cells in the Flonase recipient group along with the Vehicle group. Both groups had similar percentages of engrafted donor CD3 cells in the liver and spleen, however not in the blood. This could be due to resilient host cells outcompeting Flonase cells in the blood or possible T cell trafficking differences yet to be explored. One can argue that the reduction of aGvHD severity in the Flonase group is due to injecting a smaller number of T cells into these recipients. While number difference could be partially responsible, there was still a high percent of engrafted donor T cells in the Flonase recipient group.

Engrafted donor T cells from the Flonase group had a lower overall expression of early activation markers CD69 and CD44 compared to Vehicle group T cells. This might suggest that Flonase causes a lower allogeneic T cell inflammatory response in the Flonase group. Both

Vehicle and Flonase treated donor T cells were positive for CD44, but Vehicle cells were CD44+++ which is associated to higher cellular activity.[163] It is also possible that CD69 and CD44 expression difference is unrelated to the cause of aGvHD reduction in the Flonase group. However, our *in vitro* T cell activation studies add to the credibility that Flonase inhibits T cells from becoming activated to allogeneic stimuli. It remains in question as to how donor T cells from the Flonase group were able to proliferate *in vivo* without eliciting a severe allogeneic reaction in half of the recipients. Irradiation conditioning could have induced a cytokine storm that expanded these T cells *in vivo* or they could have undergone homeostatic expansion. The novelty of these findings is that Flonase could potentially select against alloreactive T cell while maintaining some functionality, which would be beneficial for preserving a graft vs tumor effect while simultaneously eliminating GvHD. Future experiments will have to be conducted if these cells retain a graft vs tumor response. It is worth noting that CD3/CD28 stimulation provides a broader activation signal than allogeneic activation in an MLR which only induces up to 10% of T cells.[25,26,173] Interestingly, Sca-1 expression was overexpressed when analyzing the hematopoietic stem and progenitor population (KLS) in both allogeneic transplantation groups. Sca-1 is usually overexpressed on KLS in a pro-inflammatory environment due to type 1 interferons.[174]

Glucocorticoids have been used in many clinical treatments for decades. Fluticasone propionate (Flonase) is commonly used in over-the-counter allergy nasal sprays. Dexamethasone is widely used in the clinic and has already been FDA approved for use in inflammatory diseases such as allergic reactions, arthritis, and multiple sclerosis.[175] Corticosteroid therapy is also the first-line therapy to treat aGvHD after allo-HCT, however this is a long-term treatment with many harmful side effects. Reducing GvHD in allogeneic transplantation by specifically

targeting pre-transplanted donor cells with Flonase could potentially be safer than systemically treating the patient with corticosteroids long-term. However, studies using human cells are necessary to test for reproducibility, safety and efficacy of this method. Tackling GvHD is challenging and there is a need for new and effective ways to treat this disease and make allo-HCT safe enough to increase the pool of patients able to receive this curative treatment for hematologic malignancies.

Materials & Methods

Antibodies

A detailed list of all antibodies used in this study is shown in Table S3.1.

Mice

C57Bl/6J (H-2^b)(stock no. 00664) , tdTomato+ (*mT/mG*)(stock no. 007576), B6-Foxp3^{EGFP} (H-2^b)(stock no. 006772) and Balb/cJ (H-2^d)(stock no. 000651) mouse strains from Jackson Laboratory 8-12 wk of age (Bar Harbor, ME) along with CFP+ (H-2^b) (Rosa□ECFP aka TM5) mice 8-12 wk of age, generously donated by Dr. Irving Weissman , were used as donors and recipients for competitive transplantation. All strains were maintained at the Gross Hall and Med Sci A vivarium facilities at UCI and fed with standard chow and water. All animal procedures were approved by the International Animal Care and Use Committee (IACUC) and University Laboratory Animal Resources (ULAR) of University of California, Irvine.

HSC Cell Culture for CXCR4 analysis

BM was harvested from C57Bl/6 mice by crushing tibias and femurs using a mortar and pestle. Cells were processed in ice□cold fluorescence activated cell sorting (FACS) buffer (phosphate buffered saline (PBS) + 2% fetal bovine serum). Red blood cells were lysed by ACK lysis buffer then cells were filtered through a 70μ mesh. Cells were then resuspended in 100μL FACS buffer and incubated with 5μL of mouse anti-Kit (anti-CD117) Microbeads (Miltenyi Biotec, #130-091-224) for 15 minutes then magnetic separation was performed using the Milyenyi AutoMACs Pro cell separator (Miltenyi Biotec, Somerville, MA). About 500k CD117 positive cell fraction was cultured per well in a 24-well culture plate in 500μL of X-VIVO 15 cell culture media (Fisher Scientific, #BW04-418Q) with 50ng/mL murine stem cell factor (SCF) (PeproTech, #250-03) and 20 ng/mL murine thrombopoietin (TPO) (PeproTech, #315-14). Fluticasone propionate (Flonase) (Sigma-Aldrich, F9428) was cultured at a concentration of 3nM unless otherwise specified. Flonase and dexamethasone (abcam, ab120743) were reconstituted in DMSO. To block glucocorticoid receptor (GR), 1μM Mifepristone (RU486) (Sigma-Aldrich, #M8046) was simultaneously cultured with cells and Flonase. Poly vinyl alcohol (PVA) (Sigma-Aldrich, #P8136) culture media was taken from Wilkinson et. al. (2019).[176] All cells were cultured for 16h in 37ºC and 5% CO_2. After incubation, cells were analyzed using flow cytometry with antibodies listed in Supporting Information Table S1 (“Antibodies Table”) in FACS buffer.

Chemotaxis Assay

Transwell migration assays were performed in 24 well-6.5mm diameter and 5.0μm pore size insert tissue culture treated transwell plates (Corning, 3421). After HSC cell culture with Flonase or Vehicle culture, cells from each condition were washed and resuspended in 100μL X-VIVO 15 plus SCF and TPO culture media lacking Flonase. Cells were transferred into transwell porous inserts resting in a bottom well containing 650μL prewarmed X-VIVO 15/SCF/TPO media and

50ng/mL mouse recombinant SDF-1 alpha (CXCL12) (Stem Cell, 78121). Transwells were cultured for 5h in 37ºC and 5% CO_2.To block CXCR4, cells were pre-treated with 10µg/mL AMD3100 (Sigma-Aldrich, 239820) for 30 minutes in 500uL of X-VIVO 15/SCF/TPO media lacking Flonase. After chemotactic assay incubation, cells were analyzed using Flow cytometry using antibodies listed in Supporting Information Table S1 ("Antibodies Table") in FACS buffer. Cells from the top insert and bottom well were stained separately and counted using Countbright beads (Thermofisher, #C36950) to determine the number of migrated HSCs.

Cell Sorting

BM was harvested from donor mice by crushing leg bones in ice□cold FACS buffer followed by red blood cell lysis by ACK lysis buffer and filtration through a 70 µ mesh to remove debris. BM was Kit enriched using the Milyenyi AutoMACs Pro (Miltenyi Biotec, Somerville, MA). Cells were stained with antibodies listed in Supporting Information Table S1 ("Antibodies Table") in FACS buffer. Cells were then fluorescence-activated cell sorted using a BD FACS□Aria II (Becton Dickinson, Franklin Lakes, NJ) into a 96-well U bottom plate containing 100 µL of X-VIVO 15/SCF/TPO culture media with or without Flonase. Donor Tm5 and mtmg mouse-derived cells were sorted into separate wells and Tm5 was further split into Flonase or vehicle containing wells. Mtmg cells were all sorted into media only containing vehicle. Each well contained $1x10^4$ KLS gated cells.

Competitive Hematopoietic Stem Cell Transplantation, and Blood and Bone Marrow Analysis

Sorted cells were cultured for 16h in 37ºC and 5% CO_2. A well of either Flonase-treated or Vehicle-treated Tm5 cells were combined 1:1 with a well containing vehicle-treated mtmg cells for a total of $2x10^4$ KLS donor sorted cells per recipient. These cells were transplanted via retro□

orbital injection into lethally irradiated isoflurane□anesthetized gender matched C57Bl/6 recipients. Lethal dose of x□ray irradiation was 850 cGy single dose (XRAD 320, Precision X□ ray, North Branford, CT). Transplanted recipients were fed an antibiotic chow of Trimethoprim Sulfa (Uniprim, Envigo, East Millstone, NJ) to prevent potential bacterial infections. For peripheral blood analysis, blood was obtained from the tail vein of transplanted mice at various time points, and red blood cells were depleted using ACK lysis buffer. For BM analysis, BM was harvested from tibias and femurs by flushing with ice□cold FACS buffer followed by ACK lysis and filtration. BM HSC population is defined as single cell, PI-, Ter119-, CD27+, c-kit+, sca-1+, CD150+, cells with donor cells expressing CFP. Cells were analyzed on the BD LSRFortessa. For more antibody information refer to Table S1 in supporting information. FlowJo software (Tree Star) was used for data analysis.

GvHD Cell Culture and Transplantation

A fully MHC mismatched allogeneic transplantation between mice with different haplotypes, H-2^b and H-2^d, was utilized as a mouse model for acute GvHD (aGvHD). Fresh bone marrow cells and splenocytes were harvested from H-2^b mice (either C57Bl/6J or B6-Foxp3^{EGFP}) by flushing tibias and femurs using insulin syringes and utilizing a cell homogenizer respectively. Red blood cells were lysed by ACK lysis buffer then cells were filtered through a 70μ mesh. Donor H-2^b cells were cultured with either 3nM Flonase or vehicle (DMSO) at a concentration of 6x10^6 splenocytes plus 3x10^6 whole bone marrow cells per well in a 24-well culture plate in 500μL of previously mentioned serum free X-VIVO 15 media. Cells were cultured for 16h in 37ºC and 5% CO_2.

For lineage cell viability analysis, unlike transplanted sample wells, splenocytes were cultured without bone marrow then collected and washed after incubation and stained for flow

cytometry analysis. Different lineage cell markers were used depending on experiment (see Supplemental Table 1 for antibody information). Viability (percent live cells) was measured using the dead cell stain propidium iodide (PI) and the apoptotic cell marker Annexin V (Biolegend; cat. no. 640905 and 640911). After adding Annexin V, Annexin V binding buffer was used to suspend cells (Biolegend; cat. no. 422201). Biolegend Annexin V staining protocol was used.

For transplantation, each well containing splenocytes and bone marrow cells was washed and resuspended in 100 µL of FACS buffer and injected retro-orbitally into lethally irradiated (850cGy) isoflurane anesthetized gender matched Balb/cJ (H-2^d) recipient mice or C57Bl/6J (H-2^b) syngeneic control mice. Transplanted recipients were fed an antibiotic chow of Trimethoprim Sulfa (Uniprim, Envigo, East Millstone, NJ) to prevent potential bacterial infections. This transplantation was a blinded study where treatment condition for recipient mice was unknown until after analysis/ data collection.

For secondary transplants, $1x10^6$ whole splenocytes were taken 7 days post transplantation from primary recipients, from the previously mentioned GvHD/ allogeneic transplantation protocol, along with fresh $2x10^6$ helper tdTomato+ (H-2^b) whole bone marrow and immediately transplanted into lethally irradiated (850cGy) secondary Balb/cJ (H-2^d) allogeneic or C57Bl/6J (H-2^b) syngeneic control.

GvHD Transplant Tissue Analysis

For splenocyte and liver analysis, first, tissues were harvested and homogenized with ice cold FACS buffer in a glass tissue homogenizer, second, red blood cells were ACK lysed and lastly, cells were filtered through a 70µ mesh. Blood from the heart was collected in 10mM EDTA solution immediately after euthanizing recipient then ACK lysed and filtered. The following cell

populations were analyzed in recipient blood, spleen and liver using flow cytometry: donor CD3 T cells (single cell, PI-, CD45+, CFP+, Gr-1-, CD11b-, B220-, CD3+), CD4 T cells (single cell, PI-, CD45+, CFP+, Gr-1-, CD11b-, B220-, CD3+, CD8-, CD4+), CD8 T cells (single cell, PI-, CD45+, CFP+, Gr-1-, CD11b-, B220-, CD3+, CD4-, CD8+), macrophages (single cell, PI-, CD45+, CFP+, Gr-1-, CD11b+), granulocytes (single cell, PI-, CD45+, CFP+, CD11b-, Gr-1+) and B cells (single cell, PI-, CD45+, CFP+, Gr-1-, CD11b-, CD3-, B220+). For BM analysis, BM was harvested from tibias and femurs by flushing with FACS buffer using an insulin syringe followed by ACK lysis and filtration. BM KLS population is defined as single cell, PI-, Ter119-, CD27+, c-kit+, sca-1+ cells with donor cells expressing CFP. Cells were analyzed on the BD LSRFortessa. For more antibody information refer to Table S1 in supporting information. FlowJo software (Tree Star) was used for data analysis.

GVHD Grading

Mice were observed daily for GVHD and scored according to a previously described scoring system.[161]

T cell Activation Assay

A culture-treated flat bottom 96-well plate (Costar) was incubated with 30 μg/ml anti-hamster IgG (Vector Laboratories) for 1 hour at 37°C. Non-stimulated condition wells were incubated with only PBS. Wells were then washed with PBS and then incubated with 5 μg/ml anti-mouse CD3e (eBiosciences) for 2 hours at 37°C. Non-stimulated condition wells were incubated with only PBS. Freshly harvested splenocytes (1.2×10^6) from CFP+ C57BL/6J (Tm5) mice, pre-treated in triplicate with 3nM Flonase or DMSO Vehicle, were stained with 5 μM CFSE (Biolegend) at a concentration of 10×10^6 cells/mL for 20 minutes at room temperature in the dark. Splenocytes

were washed then split into 2 samples of 0.6 x 10^6 cells in 200µL complete RPMI-1640 (C-RPMI) stimulated and unstimulated condition with and without 2 µg/ml anti-mouse CD28 (eBiosciences) respectively and plated in respective stimulated, with eCD3, or non-stimulated, without eCD3, prepared plate and incubated for 4 days at 37°C and 5%CO_2. Complete RPMI (C-RPMI) media was composed of RPMI 1640 +L-Glutamine, 25mM HEPES, 0.11mM 2-Mercaptoethanol, 1x MEM Non-Essential Amino Acids, 1mM sodium pyruvate, and 10% heat inactivated (HI) FBS all from Gibco and 1X Penicillin/Streptomycin from Corning. After incubation, cells were analyzed using flow cytometry with antibodies listed in Supporting Information Table S1 ("Antibodies Table") in HI FACS buffer.

Mixed Lymphocyte Reaction

Freshly harvested splenocytes ($3x10^5$) from CFP+ (H-2^b) mice were pre-treated in triplicate with 3nM Flonase or DMSO Vehicle then used for responder cells. Responder cells were co-cultured (1:1) with ($3x10^5$) irradiated (2500cGy) allogeneic Balb/cJ or syngeneic C57BL/6J stimulator splenocytes for 4 days in 96-well round bottom plate with 200uL of C-RPMI. C-RPMI was used throughout this experiment. After incubation, cells were analyzed using flow cytometry with antibodies listed in Supporting Information Table S1 ("Antibodies Table") in HI FACS buffer.

Statistical Analysis

Statistical analysis was performed with GraphPad Prism 5 software (La Jolla, CA).

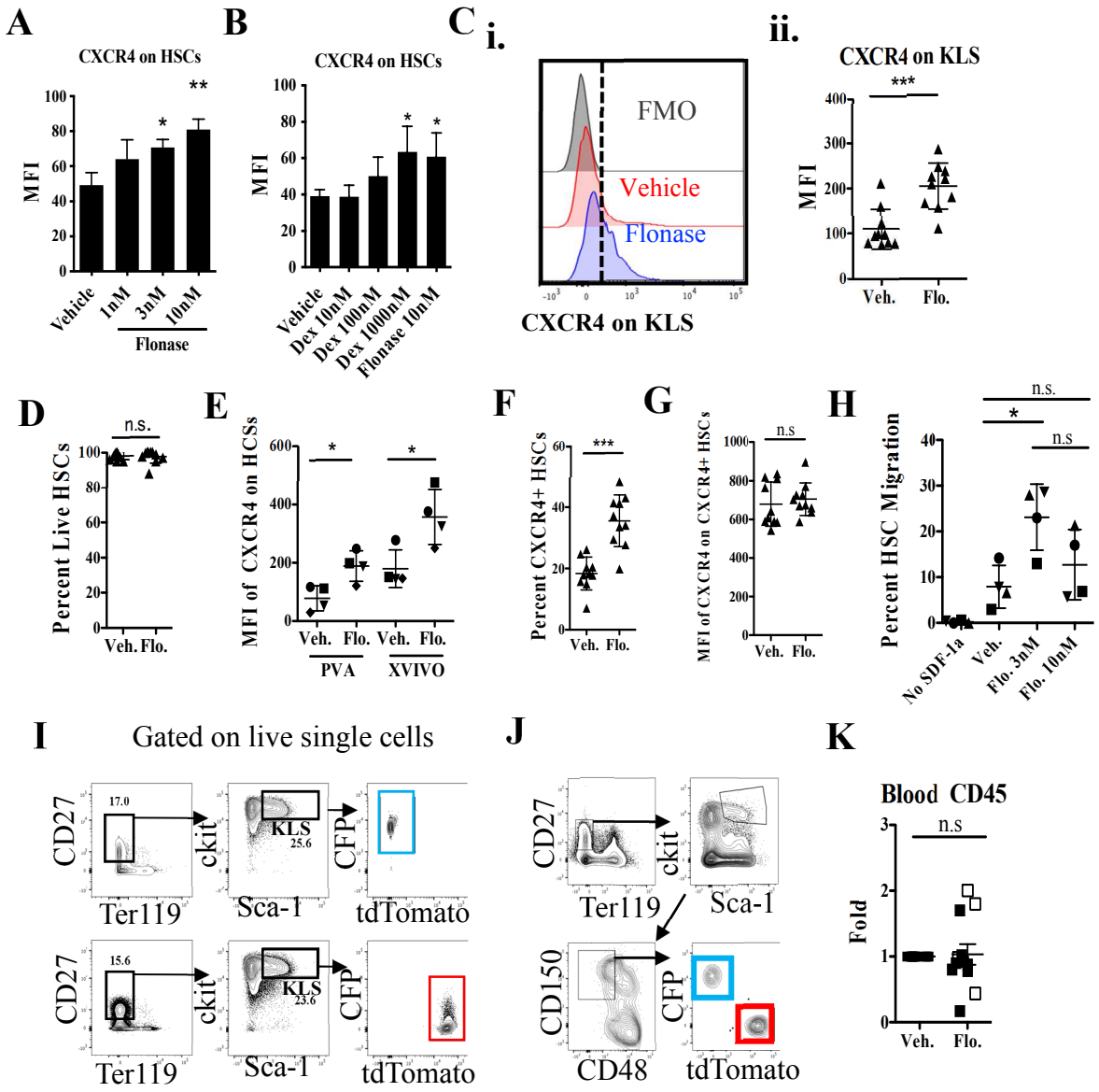

Supporting Information Figure S3.1. Characterizing murine cells after Flonase treatment. (A) (i) Representative histogram normalized to mode shows CXCR4 expression on KLS after Flonase (blue) and Vehicle (DMSO, red) culture conditions. The dashed line indicates cutoff for positive CXCR4 expression based on the fluorescence minus one (FMO, grey histogram) control. (ii) MFI of cell surface CXCR4 on KLS population after culture conditions (n=10, representative of 7 independent experiments). Data indicates an approximately 2-fold increase of CXCR4 expression on KLS cells after Flonase treatment relative to vehicle control similar to that observed in HSCs in Figure 1A. **(B-C)** Comparison of MFI of CXCR4 on HSCs treated with Vehicle and three different doses of (B) Flonase and (C) Dexamethasone (Dex), n=3. Both 3nM and 10nM had significant increases in CXCR4 compared to vehicle, but not relative to each other. Only 1000nM Dex led to a significant increase in CXCR4 expression relative to vehicle, and similar to 10nM Flonase. **(D)** Percent CXCR4 positive HSCs. **(E)** MFI of CXCR4 on CXCR4+ HSC population. These data indicate that CXCR4 expression is not increasing on CXCR4+ HSCs, but rather that CXCR4- HSCs begin to turn on CXCR4. **(F)** Total live HSCs after culture conditions. (D-F) n=10, representative of 7 independent experiments. **(G)** MFI of CXCR4 on HSCs treated with Flonase or Vehicle

cultured in two different mediums, either serum free XVIVO medium or polyvinyl alcohol (PVA) supplemented medium (n=4, representative of 4 independent experiments). **(H)** HSC migration toward SDF-1α (50ng/mL) after treatment of Vehicle or two different concentrations of Flonase quantified by flow cytometry (n=4, representative of 4 independent experiments). **(I)** Representative sorting scheme of c-kit+, CD27+, Sca-1+ (KLS) live single cells from either CFP+ (top) or tdTomato+ (bottom) c-kit enriched bone marrow. **(J)** Representative analysis of donor HSCs, c-kit+, CD27+, Sca-1+, CD150+, CD48- from competitive sort transplanted recipient bone marrow after 12w post-transplant. Recipient from "Vehicle" control group is shown. **(K)** Fold change in blood CD45 chimerism 12w post transplantation normalized to Vehicle group (n=12, representative of 9 independent experiments). Open symbols are females. *, $p \leq .05$; **, $p \leq .01$; ***, $p \leq .001$ (Student's unpaired t-test). $M \pm$ SD shown. Abreviations: HSC, Hematopoietic stem cell, KLS, c-kit+ lineage- sca-1+ cell population, Dex, Dexamethasone, Flo., Flonase, Veh., Vehicle, FMO, fluorescence minus one.

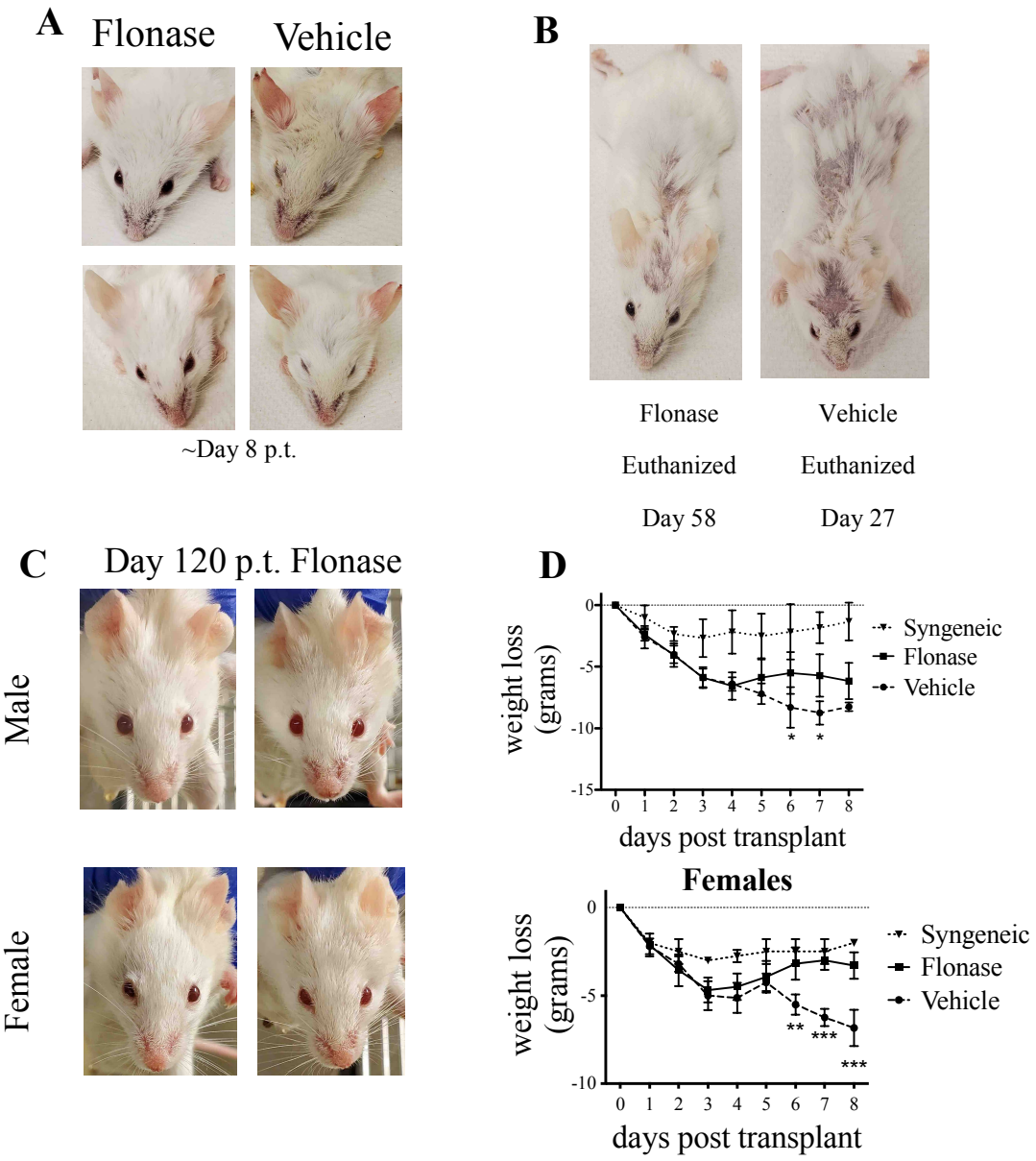

Supporting Information Figure S3.2. Mice that received Flonase treated cells show less symptoms of GvHD compared to mice that received Vehicle treated cells. (A) Additional representative photographs of Flonase and Vehicle treated cell recipients after approximately 7 days. Mice that were photographed were randomly chosen. Photos are taken of males with the exception of the bottom left photograph is a female. **(B)** Images of euthanized mice in each group at a later stage with skin lesions. Both are males. **(C)** Images from remaining live healthy mice from the Flonase-treated transplantation group approximately 120 days post transplantation. **(D)** Weight loss analysis of allogeneic transplants "Flonase" and "Vehicle", and "Syngeneic" vehicle (C57BL/6J into C57BL/6J) transplanted mice separating males (top; n=7 for "Vehicle", n=8 for "Flonase", n=3 for "Syngeneic" groups) from females (bottom; n=4 for "Vehicle", n=8 for "Flonase", n=2 for "Syngeneic" groups). Significance is Vehicle group comparison to Flonase group. Males at day 8 only had an n of 2. *, $p \leq .05$; **, $p \leq .01$; ***, $p \leq .001$ (Student's unpaired t-test). $M \pm$ SD shown. Abbreviations: p.t., post-transplant.

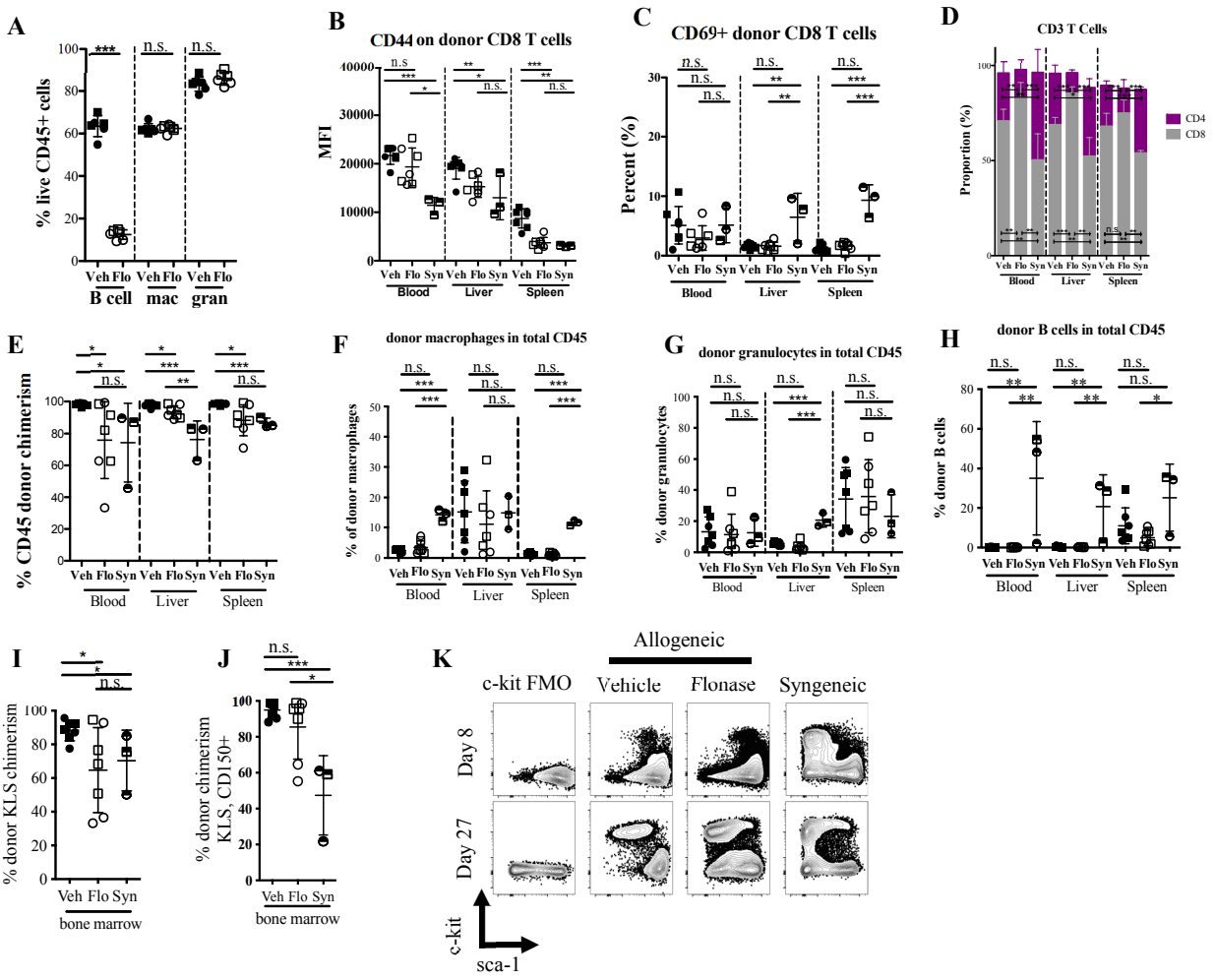

Supporting Information Figure S3.3. Characterization of donor cells in allogeneic transplanted recipients receiving either Flonase or Vehicle-treated whole splenocytes and bone marrow cells. (A) Quantification of live B cells (CD45+, CD11b-, Gr1-, CD3-, B220+), macrophages (mac) (CD45+, Gr1-, CD11b+), and granulocytes (gran) (CD45+, CD11b-, Gr-1+) after 16h culture with Flonase or Vehicle (n=6, representative of 3 independent experiments). **(B-C)** Quantification of MFI of CD44+ (B) and percent CD69+ cells (C) in donor CD8 population. Gated on live, CD45+, CFP+, CD11b-, Gr1-, B220-,

CD3+, CD4-, CD8+ single cells. **(D)** Proportion (%) of CD4 and CD8 T cells within CD3 T cell population. **(E)** Total donor CD45 chimerism in blood, liver and spleen of transplanted recipients. **(F-H)** Quantification of percent donor macrophages (F) granulocytes (G) and B cells (H) in total CD45 cells. **(I-J)** Donor KLS (I) and KLS, CD150+ (J) chimerism in recipient bone marrow after transplant. (B-J) n=7 for Flonase and Vehicle groups days 6-9 p.t., representative of 3 independent experiments, n=3 for Syngeneic Vehicle (Syn) CFP+ C57BL/6J into C57BL/6J group day 9 (1 mouse) and day 27 (2 mice) p.t., representative of 2 independent experiments. **(K)** Representative plot of donor KLS population in bone marrow from transplanted recipients of Vehicle-treated, Flonase-treated, and Vehicle-treated-syngeneic donor cells from mice euthanized on day 8 p.t. (top) and on day 27 p.t (bottom). Circles represent males and squares represent females. *, $p \leq .05$; **, $p \leq .01$; ***, $p \leq .001$ (Student's unpaired t-test). Error bars is SD. Abbreviations: p.t., post-transplant, KLS, kit+ lineage- sca-1+ cell population, FMO, fluorescence minus one, syn, syngeneic.

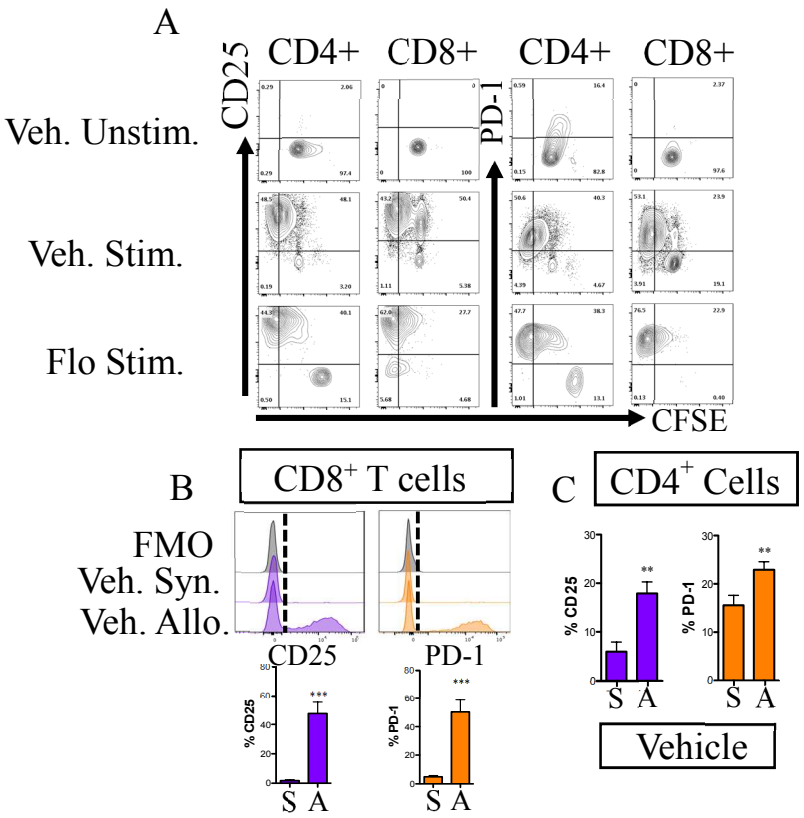

Supporting Information Figure S3.4. Activation analysis of Flonase-treated splenocytes after CD3/CD28 stimulation and MLR. (A) Representative plots of proliferation (CFSE staining) vs activation markers CD25 and PD-1 expression on either Flonase or Vehicle pretreated CD4+ and CD8+ cells after in vitro T cell activation assay via CD3/CD28. Cells were cultured for 4 days in respective conditions (n=3, 2 male and 1 female, representative of 2 independent experiments). **(B)** Representative histograms and quantification from MLR of CD25 and PD-1 expression on CD8+ cells. **(C)** Quantification of CD25 and PD-1 expression on responder CD4 T cells after MLR. Cells were cultured for 4 days in respective conditions (n=3; M ± SD; 2 male and 1 female). *, $p \leq .05$; **, $p \leq .01$; ***, $p \leq .001$ (Student's unpaired t-test). Abbreviations: Syn., Syngeneic, Allo., Allogeneic, Veh., Vehicle, Flo, Flonase, FMO, fluorescence minus one.

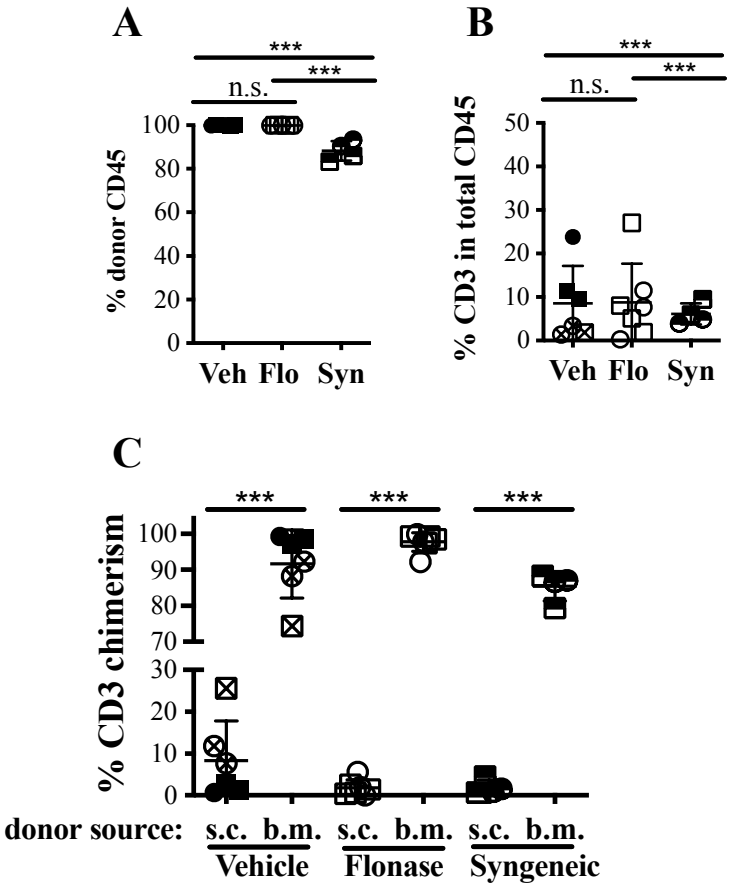

Supporting Information Figure S3.5. Characterizing engrafted donor cells from secondary recipient blood 29 days post-transplant. (A-C) Quantification of donor cells in secondary recipient blood by flow cytometry analysis. **(A)** Percent of donor CD45 chimerism including both primary recipient splenocytes and bone marrow derived cells in secondary recipients. **(B)** Percent total CD3+ donor cells (splenocytes plus bone marrow-derived) within total live, CD45 single cell population. **(C)** Chimerism of donor primary splenocyte-derived (s.c.) or donor tomato+ bone marrow-derived (b.m.) CD3+ cells. (Flonase n=7; 3 male and 4 female; Vehicle n=6; 3 male and 3 female; Syngeneic vehicle (Syn or Syngeneic) n=4; 2 male and 2 female; M $\pm$ SD). Circles represent males and squares represent females. Crossed symbols represent mice later euthanized due to GvHD. *, $p \leq .05$; **, $p \leq .01$; ***, $p \leq .001$ (Student's unpaired t-test).

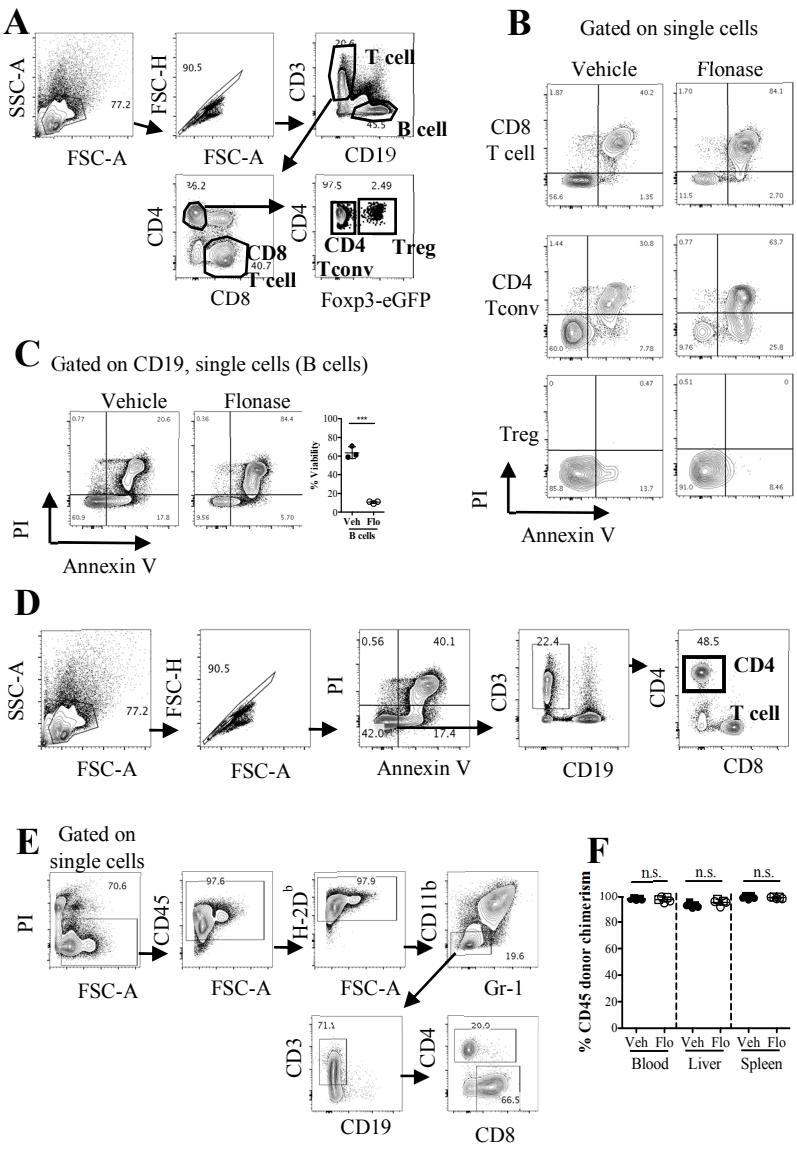

Supporting Information Figure S3.6. Characterizing Tregs and lineage cells after Flonase treatment *in vitro* and after allogeneic transplantation. (A) Representative FACS gating scheme of splenocytes after 16h of treatment with Flonase (3nM) or vehicle (DMSO) before gating on viability using Propidium Iodide (PI) and apoptotic marker Annexin V (Vehicle treated cells shown). **(B)** Representative FACS plots showing live (PI-, Annexin V-) apoptotic (PI-, Annexin V+), and dead (PI+, Annexin V+) CD8 T cells, CD4 Tconv, and Tregs after 16h Flonase or vehicle culture. **(C)** Representative FACS plots (left) and quantitative data (right) showing B cell viability (n=3). **(D)** Representative FACS gating scheme of splenocytes after 16h treatment with Flonase or vehicle after gating on live (PI-, Annexin V-) cells (Vehicle treated cells shown). **(E)** Representative FACS gating scheme of lineage cells from allogeneic recipient Balb/cJ (H-2^d) mice (spleen shown) 9 days after transplantation with donor Foxp3-eGFP (H-2^b) mouse splenocytes and bone marrow. **(F)** Percent CD45 donor Foxp3-eGFP (H-2^b) chimerism in recipient Balb/cJ (H-2^d) blood, liver and spleen 9 days post transplantation (n=5). Open symbols are females, closed are males. *, $p \leq .05$; **, $p \leq .01$; ***, $p \leq .001$ (One sample t-test). $M \pm$ SD shown.

Supplementary Table S3.1. List of Antibodies Table				
Antigen	**Clone**	**Conjugate**	**Source**	**Catalogue #**
TER119	TER119	PE/Cy5	Biolegend	116210
SCA1 (Ly-6A/E)	E13-161.7	PE/Cy7	Biolegend	122514
	D2	Alexa Fluor 700	Biolegend	108142
c-kit (CD117)	2B8	APC/Cy7	Invitrogen	47-1171-80
	2B8	BV421	Biolegend	105828
CD27	3A10	FITC	Biolegend	124208
	3A10	APC/Cy7	Biolegend	124226
	LG.3A10	PE/Cy7	Biolegend	123215
CD150(SlamF1)	TC15-12F12.2	PE	Biolegend	115904
	TC15-12F12.2	BV421	Biolegend	115925
CD34	RAM34	eFluor660	Invitrogen	
CD48	HM48-1	FITC	eBioscence	11-0481-82
	HM48-1	BV421	Biolegend	103427
CXCR4	L276F12	APC	Biolegend	146507
	L276F12	PE	Biolegend	146507
GR1 (Ly-6G/Ly-6C)	RB6-8C5	Alexa Fluor 700	Biolegend	108422
MAC1 (CD11b)	M1/70	APC	Biolegend	101212
	M1/70	APC/Cy7	Biolegend	101226
CD19	6D5	BV421	Biolegend	115537
CD45	30-F11	APC/Cy7	Biolegend	103116
	30-F11	Alexa Fluor 700	Biolegend	103128
	30-F11	BV 510	Biolegend	103137
	30-F11	BV421	Biolegend	103133
B220	RA3-6B2	PE/Cy5	Biolegend	103209

CD69	H1.2F3	FITC	Biolegend	104505
CD44	IM7	APC	Biolegend	103012
PD-1	29F.1A12	BV421	Biolegend	135217
CD25	PC61.5	PE	eBioscienc	12-0251-83
	PC61	APC	Biolegend	102011
	3C7	FITC	Biolegend	101907
CD3ε	17A2	PE/Cy5	eBioscience	46-0032-82
	17A2	PE/Cy7	Biolegend	100220
CD4	RM4-5	PE/Cy7	Biolegend	100528
	RM4-5	BV605	Biolegend	100547
CD8a	53-6.7	APC/Cy7	Biolegend	100714
	53-6.7	PE	Tonbo	50-0081
H-2D^{b}	KH95	PE	Biolegend	111507
Annexin V Stain		FITC	Biolegend	640906
		Alexa Fluor 647	Biolegend	640911
Propidium Iodide Solution			Biolegend	421301
CFSE Stain			Biolegend	423801

CHAPTER 4: DEVELOPING A MOUSE MODEL FOR THE AUTOIMMUNE DISEASE IDIOPATHIC THROMBOCYTOPENIC PURPURA

Introduction

Author's Note: I spearheaded this project where I partially contributed to designing our LMOH mouse construct. The UCI mouse transgenic facility designed and created our LMOH mice using CRISPR technology and in vitro fertilization. I genotyped the founder mice we received from the mouse transgenic facility for quality control. I provided ideas for the different strategies to induce ITP phenotype in these mice. I conducted all the experiments, data collection, and data interpretation for this chapter.

Idiopathic thrombocytopenic Purpura (ITP), also known as immune thrombocytopenic purpura, is a rare platelet autoimmune disease, with an estimated prevalence of 9.5 out of 100,000 people acquiring this disease (Segal et. al).[177] The acute version of this disease mostly affects children and usually resolves upon entering adulthood; however, the acute version can switch to the chronic form which mostly occurs in adults. ITP arises spontaneously and has no known cause, however in some cases onset occurs shortly after viral infection and some patients are genetically predisposed to ITP if they have relatives who had ITP or systemic lupus erythematosus.[178,179] This disease often results in autoantibody secretion by B cells that are specific to platelet antigens and causes platelet destruction by antibody dependent phagocytosis by splenic macrophages. Besides autoantibody secretion, CD8+ and CD4+ T cells can also cause platelet destruction through T cell receptor recognition.[180] This immune response results in a decreased platelet, platelet progenitor, and megakaryocyte concentration decreasing blood

coagulation and increasing risk of hemorrhaging and uncontrollable bleeding. Patients with this disease also show a 1.5-fold higher mortality rate compared to the general population.[181] Currently, the best treatment for ITP is a splenectomy which cures approximately 70 percent of patients with ITP, however this invasive strategy comes with many possible complications, for example having a weaker immune system. There are also long-term treatments for ITP such as thrombopoietin receptor agonists (TPO-RA), intravenous immunoglobulin therapy (IVIG), Rituximab and corticosteroids, however these are temporary and regimented treatments with harsh side effects.[182]

Current mouse models of ITP have significantly contributed to what we know about this disease. Currently, the most widely used mouse model of ITP is made from a series of adoptive transfers of immune cells from a platelet integrin (CD61) knock out (KO) mouse into a wild-type mouse expressing CD61 to generate an immune response against platelets.[183] First, a CD61 KO mouse is repeatedly immunized with wild-type platelets to produce lymphocytes specific for CD61. Then, the CD61 KO mouse is euthanized and splenocytes are harvested then adoptively transferred into a wild-type mouse. Recently, there has been an adjustment made to this mouse model to resolve internal bleeding issues with the CD61 KO mice. In Li et. al., instead of immunizing CD61 KO mice they immunize CD41 KO mice.[184] This eliminates internal bleeding and birth complications for immunized mice, however the process of obtaining the mouse model is the same. The current ITP mouse model is moribund after 15 days which complicates long-term studies. We aimed to develop a new mouse model to study ITP past 15 days post disease onset, and to have a more efficient ITP mouse model for testing possible new therapies to eliminate this disease.

Results

Our mouse model strategy aims to elicit an immune response against platelets by expressing the foreign proteins chicken ovalbumin (OVA) and hen egg lysozyme (HEL) on the surface of platelets and megakaryocytes using CRISPR technology. A CRISPR construct containing the membrane bound fusion protein OVA-HEL was designed and inserted into the promoter region of the platelet specific glycoprotein V (GPV) gene in C57BL/6J mice (Fig 4.1). The OVA region contains $OVA_{323-339}$ specific for OT-II/CD4 T cells and $OVA_{257-264\ specific}$ for OT-I/CD8 T cells. The HEL sequence was chosen to stimulate B cells and antibody production. The OVA-HEL fusion protein was designed to be membrane bound by using the human Fas ligand transmembrane domain (hFasL-TM) to create membrane bound OVA-HEL (mOVA-HEL). Initially, the fusion protein was designed to be tamoxifen/Cre-ER inducible to prevent any immune tolerance that may be established from protein expression since development, therefore we added a lox-STOP-lox (LSL) sequence which inhibits fusion protein transcription in absence of Cre recombinase. Mice baring this construct with an intact LSL are referred to as LMOH mice. The self-cleaving peptide or P2A portion of the construct was included to separate mOVA-HEL from GPV proteins after being translated together.

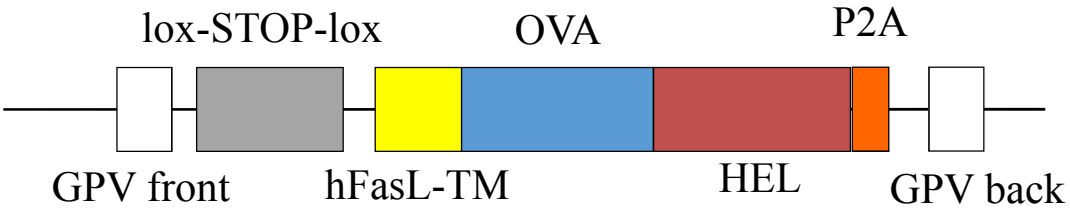

Figure 4.1. Inducible ITP CRISPR construct of membrane bound OVA-HEL fusion protein. GPV front and back represent GPV gene homology arms for insertion into the correct GPV locus in mice. Lox-STOP-lox (LSL) (grey) is for Cre recombinase excision and to prevent transcription of OVA-HEL fusion protein without Cre. LSL is used to prevent immunogenic tolerance towards the fusion protein. Abbreviations: hFasL-TM (yellow), human Fas ligand transmembrane domain; OVA (blue), ovalbumin; HEL (red), hen egg lysozyme; P2A (orange), 2A self-cleaving peptide.

Mice baring the CRISPR construct were bred, genotyped and sequenced to confirm presence of the LMOH construct in the GPV locus. Mice heterozygous for LMOH were crossed to heterozygous UBC-Cre-ERT2 mice in hopes to induce reduced blood platelet concentration after tamoxifen treatment (Fig 4.2Ai, Aii). Tamoxifen treatment activates the Cre-ER through estrogen receptor (ER) binding to excise the LSL to allow mOVA-HEL transcription. F1 mice from LMOHxUBC-Cre-ERT2 breeder are immunized once before and once after tamoxifen injection with soluble OVA and HEL to prime the immune system against platelet mOVA-HEL protein expression. Blood was taken after tamoxifen treatment to measure platelet concentration. There were reduced platelet concentrations below average platelet concentration after the second OVA and HEL immunization post-tamoxifen treatment in all F1 mouse groups including the negative control groups including heterozygous LMOH, heterozygous UBC-Cre-ERT2, and B6 mice (Fig 4.2Aiii). This made it difficult to move forward with this model strategy because tamoxifen plus OVA/HEL immunization creates an off-target effect that reduces platelets in mice that do not express membrane bound OVA/HEL.

We later discovered that some mice expressing both LMOH construct and the UBC-Cre-ERT2 gene (LMOH-UBC mice) had missing LSL prior to tamoxifen injection, suggesting a leaky Cre recombinase (Fig 4.2B). This is problematic for preventing possible immune tolerance toward OVA-HEL fusion protein. We decided to proceed with immunizations with the leaky LMOH-UBC mice to test any blood platelet reduction after immunization. There was indeed a reduction in platelet concentration below normal levels in an almost completely leaky (LSL excised before tamoxifen) LMOH-UBC mouse compared to the control mice and a partial leaky LMOH-UBC mouse after the second immunization (Fig 4.2C). This suggests that the LSL may not be needed to make our ITP mouse model. Immune tolerance is not completely evaded

however, since platelet counts go back to normal 4 weeks after the second immunization in the complete leaky mouse.

Alternative ITP mouse model induction strategy: Crossing LMOH and Vav-iCre mice

We next decided to cross our LMOH construct mice with Vav-iCre mice expressing Cre under the pan hematopoietic cell-specific guanine nucleotide exchange factor (Vav) promoter. F1 mice heterozygous for both Vav-iCre and LMOH genes express mOVA-HEL on platelets since birth. F1s were immunized and bled for platelet counts every week throughout immunizations (Fig 4.3A). After the second immunization, there was a decrease in blood platelet concentration in LMOH-Vav-iCre mice compared to the litter mate control mice that were heterozygous for Vav-iCre, heterozygous for LMOH and B6 mice. It is important to note that there was no significant difference between the LMOH-Vav-iCre mice and heterozygous Vav-iCre and LMOH control mice, however there was comparing LMOH-Vav-iCre to B6 mice (Fig 4.3B). This might suggest that the immune system in LMOH-Vav-iCre mice is inducing platelet destruction. There is variation among mice within the same experimental group therefore other strategies to reduce blood platelet levels should be explored.

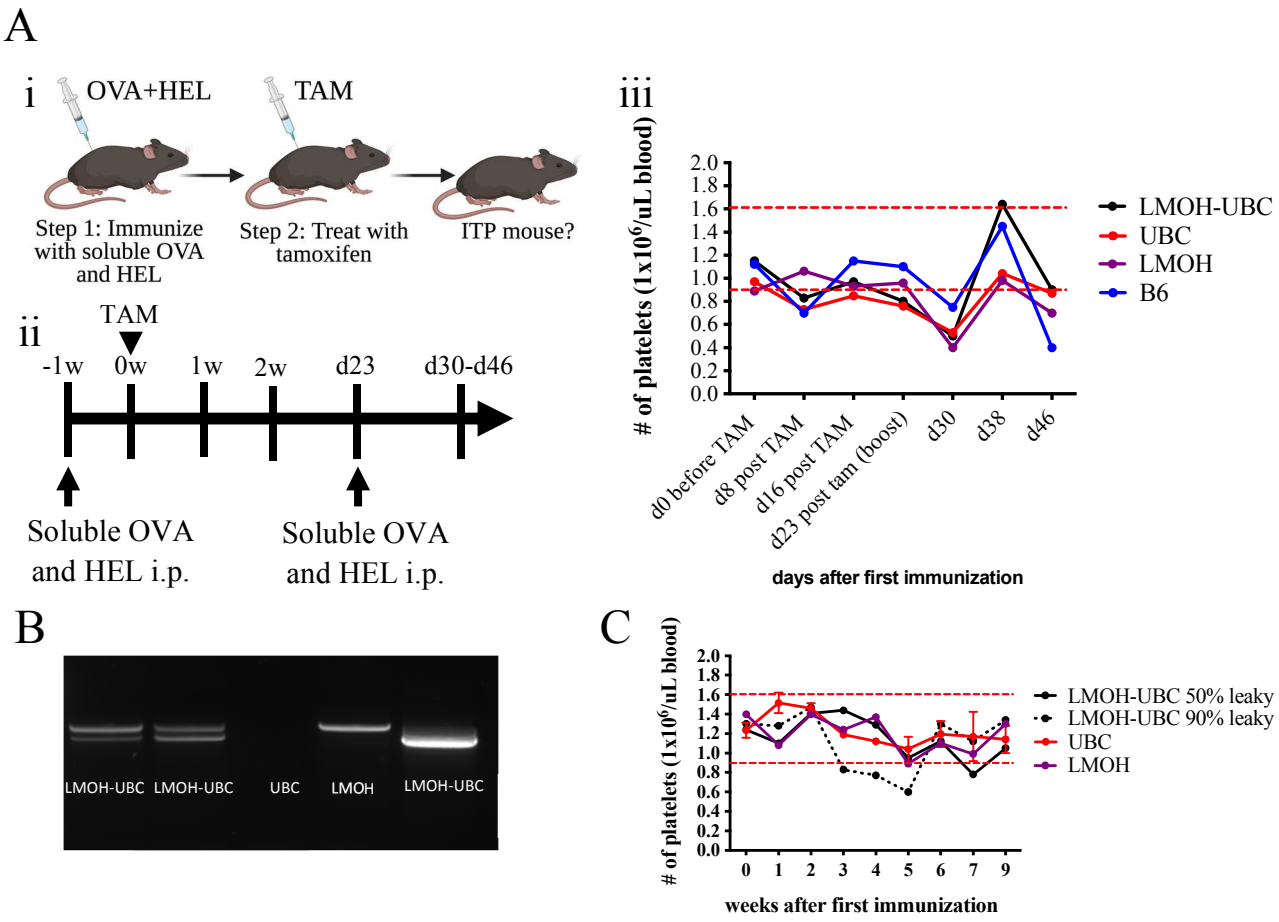

Figure 4.2. ITP mouse model development using tamoxifen inducible mOVA-HEL LMOH-UBC mice. (A) (i) Scheme and (ii) timeline of ITP mouse model strategy immunizing LMOH-UBC-CreERT2 (LMOH-UBC) mice or littermate controls with soluble ovalbumin (OVA) and hen egg lysozyme (HEL) delivered by intraperitoneal injection (i.p.) then later i.p. injecting tamoxifen (TAM) to induce membrane bound OVA-HEL protein expression on platelets. (iii) Platelet concentrations in blood from LMOH-UBC mice and littermate controls heterozygous for UBC-CreERT2 and LMOH. Boost is second OVA/HEL immunization. Female platelet count shown. Red dashed lines are average mouse platelet count range $0.9x10^6$- $1.6\ x10^6$.[185] **(B)** PCR electrophoresis gel showing mice with LMOH-UBC before tamoxifen administration with varying LSL leakiness. LMOH construct was PCR amplified with forward primer located before the homology arm and the reverse primer specific to the HEL region. Upper band is the LMOH construct with LSL (~1605bp) and the lower band is the construct without the LSL (~1,333bp). LMOH and UBC are heterozygous litter mate controls. Females are shown. **(C)** Blood platelet concentration from approximately 50% and 90% leaky (excised LSL) LMOH-UBC mice and UBC and LMOH heterozygous littermate controls. Soluble OVA and HEL immunizations were administered on week 0 and 2 (n=1 for LMOH-UBC, and LMOH; n=2 for UBC). Female mice are shown. Red dashed lines are average mouse platelet count range $0.9x10^6$- $1.6\ x10^6$.[185] $M \pm$ SEM shown.

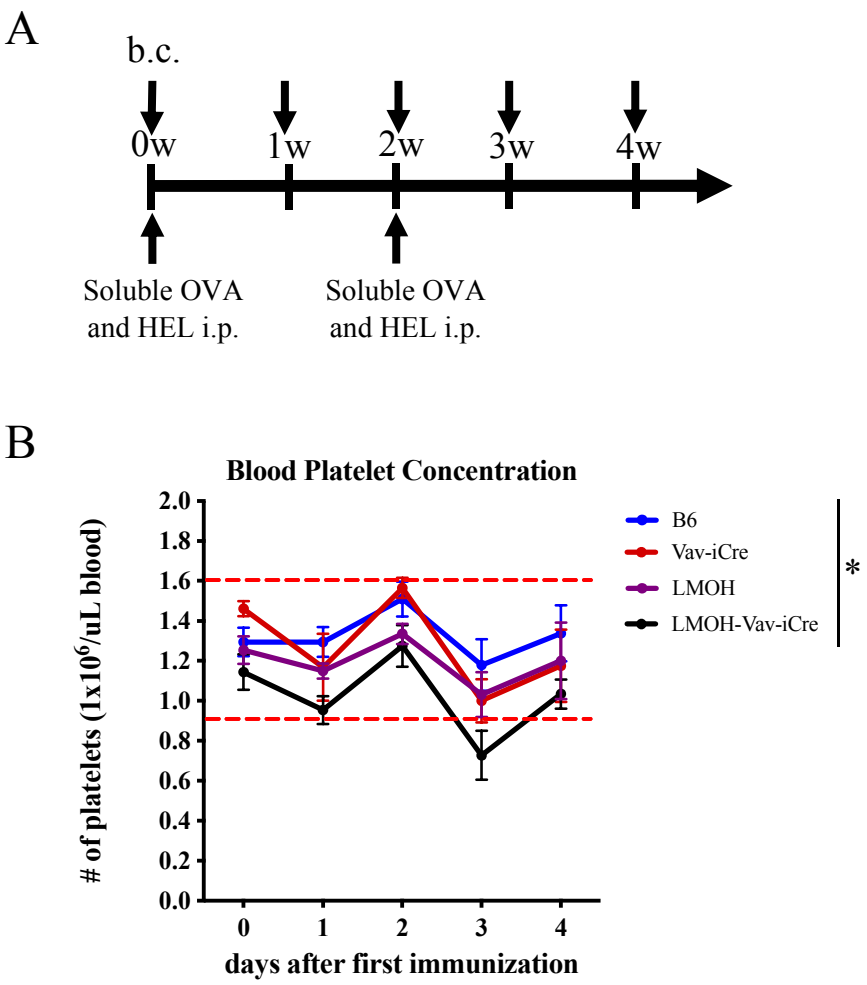

Figure 4.3. ITP mouse model development using immunized LMOH-Vav-iCre mice. (A) Soluble OVA and HEL intra-peritoneal (i.p.) immunizations and blood collection (b.c.) indicated by top arrows timeline in weeks (w) of F1 mice from heterozygous LMOH and heterozygous Vav-iCre cross. **(B)** Blood platelet concentration from F1 mice collected over 4 weeks with immunizations on week 0 and 2 (B6 and Vav-iCre, n=4; LMOH, n=6; LMOH-Vav-iCre, n=7; representative of 3 different experiments). Red dashed lines are average mouse platelet count range $0.9x10^6$- $1.6\ x10^6$.[185] Female mice are shown. F1 mice shown are heterozygous for transgenes. $M \pm$ SEM shown. *, $p \leq .05$; **, $p \leq .01$; ***, $p \leq .001$ (Student's unpaired t-test).

Discussion

Further studies need to be conducted in order to establish an ITP mouse model using our LMOH mice. Our data shows promise for platelet reduction in LMOH mice using different strategies, however additional methods must be explored to show consistent results. One future direction could be performing adoptive transfers of splenocytes from OT-II mice, that have CD4 T cells with TCRs specific to the OVA peptide sequence $OVA_{323-339}$, into MOH mice (LMOH mice without LSL). We predict that OT-II cells will recognize platelets and elicit an immune response against platelets to reduce platelet concentration in the blood.

When we establish a new ITP mouse model using LMOH mice, we will treat these mice with new therapies to challenge the current standard of care for ITP. There are existing treatment options to temporarily alleviate the effects of this disease, however the only "cure" is removing the patient's entire spleen rendering a patient immunocompromised for a lifetime. One unexplored possible therapy for ITP is bone marrow transplantation (BMT), also known as hematopoietic stem cell transplantation (HSCT), which is a procedure that replaces a patient's diseased immune system with one from a healthy donor using their hematopoietic stem cells (HSCs). HSCs can engraft the bone marrow where they self-renew and give rise to all the mature cell types of the blood system. In theory, replacing a patient's entire blood system would eliminate autoreactive immune cells, including autoantibody producing B cells, and would be a beneficial outcome for ITP. However, BMT remains a dangerous procedure that can result in severe complications. Improvements in the safety and efficacy of BMT could allow it to be an effective treatment option for ITP.

Materials & Methods

Antibodies

A detailed list of all antibodies used in this study is shown in Table S4.1.

LMOH Construct Sequence

Refer to Table S4.2 for full construct sequence

Mice

LMOH (LSL-mOVA-HEL) mice were designed by the Inlay Lab and made by the University of California Irvine transgenic mouse facility using CRISPR technology using mice on the C57Bl/6J (stock no. 00664) background. Vav-iCre mice were generously donated from the Fleischman lab at UCI. All mice were used at age 8-12w. Mice were maintained at the Gross Hall and Gross Hall vivarium facilities at UCI and fed with standard chow and water. All animal procedures were approved by the International Animal Care and Use Committee (IACUC) and University Laboratory Animal Resources (ULAR) of University of California, Irvine.

Polymerase Chain Reaction and DNA Sequencing

Mouse ear clips were collected using an ear punch for genotyping and sequencing. Each ear clip was submerged in 20μL of extraction buffer from Extracta^{TM} DNA prep for PCR kit (VWR; cat. no. 97065-350) and put on a 95^{o}C heat block for 30 minutes. Reaction was cooled to room temp and quenched with stabilization buffer from same kit as extraction buffer. Ears were diluted 1:20 using nuclease free H_2O. Polymerase chain reaction (PCR) was used to amplify the LMOH construct sequence region that includes the front homology arm up to the beginning HEL portion using forward primer: TGCTGACTGTTGGGGATAAA and reverse primer:

TTCATTGCTGCTGCAAGTTC. PCR was conducted using a final concentration of 1X Accustart™ II PCR Supermix (VWR; cat. no. 76047-140, 76047-072), 0.4μM of forward primer, 0.4μM of reverse primer and 1:4 dilution of 1:20 pre-diluted ear (~100ng DNA). Clear Accustart without Geltrack was used when sequencing DNA. Each PCR reaction used was 25μL then put in a thermocycler to amplify DNA with a melting temperature of 94ºC for 3 minutes, then 35 cycles of a denaturation temperature of 94ºC for 30s, an annealing temperature of 65ºC for 30s, and an extension temperature of 72ºC for 2 minutes. After PCR amplification, samples were run through a 1% agarose gel for electrophoresis. For sequencing, DNA was purified by incubating 2μL of the exonuclease ExoSAP-IT (Thermofisher Scientific; cat. no. 78205.10.ML) and 5μL of PCR product in a thermocycler at 37ºC for 15min and 80ºC for 15min. ExoSAP-IT purified DNA (2μL) was combined with 1μL of 20μM of either forward or reverse primer (custom made order from Sigma-Aldrich) along with 9μL of nuclease free water. Samples were sent to Retrogen Inc (San Diego, CA, US) for sequencing.

Platelet Collection and Counting from Mouse Blood

Blood was collected from mice by nicking the tail vein and carefully collecting 5uL using a pipette and dispensing the blood into an anticoagulation buffer made of 0.5% BSA, 10mM EDTA, and phosphate buffer saline (PBS). After blood collection, blood was mixed by gently pipetting it up and down. No vortex or centrifugation steps were included when handling blood. 25μL of collected diluted blood was mixed with 25μL of 2X master mix containing flow cytometry antibodies CD45, CD41, CD61, CD42d, and Ter119 from Table S4.1. Samples were incubated in room temp in the dark for 15min. After antibody incubation, samples were directly added without washing to 250μL of anticoagulation buffer containing 4000 CountBright™ counting beads (Thermofisher Scientific; cat. no. C36950). Samples were analyzed on a BD LSRFortessa.

OVA and HEL Immunizations

Soluble chicken ovalbumin (OVA) and hen egg lysozyme (HEL) (Sigma-Aldrich, 50μg of OVA and 50μg of HEL were mixed with aluminum adjuvant Imject^{TM} Alum (Thermofisher; cat. no. 77161) at a 1:1 ratio for 30 min on a rocker then i.p. injected into a mouse using an insulin syringe at a volume of 200μL.

Tamoxifen Preparation and Injections

Tamoxifen (TAM) (Sigma-Aldrich; cat. no. T5648) working solution was prepared at 30mg/mL by dissolving TAM overnight in corn oil (Sigma-Aldrich; cat. no.C8267) on a rotator at 37ºC. TAM was i.p. injected into mice for 5 consecutive days at 100mg/kg/day using a 25-gauge needle.

Acknowledgements for Chapter 4

I would like to thank the UCI transgenic mouse facility for helping design the LMOH DNA construct and creating mice that bare this construct. I would like to thank Dr. Isis Ludwig-Portugall for providing us with the membrane bound OVA-HEL sequence needed to design our ITP mouse model. Iris Wong also has contributed to this mouse model by testing possible ways to detect membrane bound OVA-HEL through flow cytometry.

Supplementary Table S4.1 LMOH DNA CONSTRUCT	
Construct Region	**Base Pair Number**
Left Homology Arm	1-130
Lox-STOP-Lox	131-436
Human Fas Ligand Transmembrane Domain	437-562
Ovalbumin	563-1,306
Hen Egg Lysozyme	1,307-1,695
P2A	1,696-1,780
Right Homology Arm	1,781-1,912

LMOH CONSTRUCT:

AGAGGAAGACTTGGTTGTATCTGAGCGTTCCAAGGCCGTGAGAGTGCTGGCCCAAAAACT
GTGCTTGCAGCAGTGCGTGCAGGGCTCCAGGATATGCTCTGAGCCTTGTTTTTGCTCTTGC
ATTTCAGACataacttcgtatagcatacattatacgaagttatCTGTGCCTTCTAGTTGCCAGCCATCTGTTGTTT
GCCCCTCCCCCGTGCCTTCCTTGACCCTGGAAGGTGCCACTCCCACTGTCCTTTCCTAATAA
AATGAGGAAATTGCATCGCATTGTCTGAGTAGGTGTCATTCTATTCTGGGGGGTGGGGTG
GGGCAGGACAGCAAGGGGGAGGATTGGGAAGACAATAGCAGGCATGCTGGGGATGCGGT
GGGCTCTATGGataacttcgtatagcatacattatacgaagttatagccaccatggccCTGAAGAAGAGAGGGAACCAC
AGCACAGGCCTGTGTCTCCTTGTGATGTTTTTCATGGTTCTGGTTGCCTTGGTgGGATTGGG
CCTGGGGATGTTTCAGCTCTTCCACCTcCAGAAGGAGacaggcGCAGACCAAGCAAGGGAAC
TTATCAATTCTTGGGTCGAGTCCCAAACTAATGGCATTATCAGGAACGTTCTGCAACCCTC
TAGTGTCGACAGCCAGACCGCTATGGTTCTCGTGAACGCTATCGTGTTTAAAGGCCTGTGG
GAGAAGACTTTCAAAGATGAGGATACCCAAGCTATGCCATTCAGGGTGACAGAGCAGGA
GTCCAAGCCTGTCCAAATGATGTACCAGATTGGGCTTTTTAGAGTGGCCAGCATGGCCTCC
GAGAAAATGAAGATCCTGGAGCTGCCATTCGCCTCTGGCACTATGAGTATGCTCGTCCTGC
TTCCTGATGAAGTGTCTGGACTGGAGCAGCTTGAATCCATCATCAACTTTGAGAAGTTGAC
AGAATGGACTTCCTCCAACGTGATGGAGGAGCGCAAGATCAAGGTGTACCTTCCACGGAT
GAAGATGGAAGAGAAATACAATCTCACAAGCGTTCTTATGGCTATGGGGATTACAGATGT
CTTTAGTAGCTCAGCCAACCTGAGTGGCATCTCAAGTGCCGAGAGCCTGAAGATTAGTCA
AGCTGTACATGCCGCACATGCTGAAATCAACGAGGCTGGACGAGAAGTTGTTGGCTCCGC
CGAGGCAGGCGTGGACGCAGCAAGTGTTAGCGAAGAGTTTAGGGCCGATCATCCATTCCT
GTTTTGCATTAAACACATCGCAACCAATGCTGTCCTCTTCTTTGGGCGGTGTGTTTCACCA
GGCAAAGTGTTTGGGCGATGCGAACTTGCAGCAGCAATGAAGCGCCACGGCCTGGATAAC
TATAGAGGCTATTCCCTCGGCAACTGGGTCTGTGCAGCCAAATTCGAGTCTAACTTCAACA
CTCAGGCAACAAATAGGAACACAGACGGCTCCACTGATTATGGGATCCTTCAAATTAACT
CAAGATGGTGGTGCAATGATGGCCGGACCCCAGGAAGTAGGAACCTCTGCAATATACCAT
GCTCTGCCCTCCTTAGCTCAGACATTACAGCATCAGTGAACTGCGCAAAAAAGATCGTAA
GTGATGGGAATGGAATGAACGCTTGGGTGGCTTGGCGGAATAGATGCAAAGGCACAGAT
GTCAGAGCATGGATTAGAGGCTGTAGGCTCGGAAGCGGAGCTACTAACTTCAGCCTGCTG
AAGCAGGCTGGAGACGTGGAGGAGAACCCTGGACCTATGttgAGAtccGCaCTcCTGTCCGCa
GTGCTCGCACTCTTGCGTGCCCAACCTTTTCCCTGCCCCAAAACCTGCAAGTGTGTGGTCC
GCGATGCCGCGCAGTGCTCGGGCGGCAGCGTGGCTCACATCGCTGAGCTAGGTCTGCCTA
CG

Supplementary Table S4.2. List of Antibodies				
Antigen	**Clone**	**Conjugate**	**Source**	**Catalogue #**
TER119	TER119	APC	Tonbo	20-5921
CD42d	1C2	PerCP/Cy5.5	Biolegend	148508
	1C2	PE	Biolegend	148504
CD61	2C9.G2	PE	Biolegend	104308
CD41	MHReg30	PE/Cy7	Biolegend	133916
CD45	30-F11	APC/Cy7	Biolegend	103116

CHAPTER 5: DISCUSSION AND FUTURE DIRECTIONS

Hematopoietic stem cell transplantation (HCT) use has come a long way since the mid 1900's when it stemmed from atomic energy research during and after World War I. There have been many advances in HCT since then which allowed it to be safer and more efficient. In this dissertation, I have explored proof of principle concepts to improve allogeneic HCT by decreasing the severity of GvHD with the glucocorticoid fluticasone propionate (Flonase).

GvHD experiments were conducted using one mouse model of GvHD, or aGvHD. An important aspect of using mouse models for this disease is that there is less variability between the recipients compared to human patients receiving HCT. Most of the existing clinical information and statistics on GvHD varies due to differences in age, existing conditions, conditioning regiments, and donor cell source. This produces inconsistent data especially for calculating GvHD incidence which currently has a large range of about 30-70%. In addition, the criteria for distinguishing aGvHD and cGvHD has changed multiple times making it difficult to discern the two types. Lastly, there has been contradicting data from different clinical sources with some showing that post-transplant cyclophosphamide treatment significantly reduces GvHD and others showing no difference between post-transplant cyclophosphamide treatment and the standard of care. Resource differences between clinics or in patient pool could be responsible for these discrepancies.

For this study, I chose this mouse model based on numerous literature sources suggesting that it displays the most severe form of GvHD by causing lethality around day 10 post transplantation. If the most severe version of this disease could be treated by a method, there is a high likelihood that it could treat less severe versions of GvHD. I would like to note that the mouse

model used is that of severe acute GvHD, and that most patients in the clinic have a low chance of suffering from severe GvHD especially with the rise of the new gold standard treatment post-transplantation cyclophosphamide treatment in haploidentical transplants. Some do consider this mouse model for cGvHD as well; however, I have not tested alloantibody production, nor have I analyzed cGvHD specific tissue damage. Other mouse studies have reduced GvHD severity after allo-HCT with post transplantation drug administration and found that mice are healthy for the first few days then start dying off at later stages.[156,186] Many drugs tested in other studies temporarily suppress donor alloreactive T cells after transplantation, however often times long term tolerance is not achieved. In our study, the 4 remaining mice that belong to the Flonase group have recovered from their mild GvHD symptoms and are still alive 8 months after treatment.

Some might argue that transplanting different cell numbers in the Vehicle group compared to the Flonase group could explain the reduction in GvHD severity. This could indeed be contributing to reduced GvHD, however in a similar study using the same mouse model transplanted small numbers of splenocytes also and found that all mice later succumb to cGvHD at day 60 post transplantation whereas the Flonase mice did not.[187] Initially, our goal was to deplete donor T cells using Flonase to prevent GvHD in allo-HCT. Since T cells are needed for successful HSC engraftment, we aimed to supplement this effect by using Flonase to bolster HSC engraftment since it increases CXCR4 expression. However, we found similar percentages of engrafted donor T cells in the Flonase group and the Vehicle group at day 10 post HCT. This suggests that Flonase pre-treatment did not inhibit allogeneic T cell expansion in recipients. Interestingly, even though Flonase induced a large percentage of apoptosis in the lymphocyte population pretransplant, Flonase group-derived T cells expanded rapidly in the allogeneic recipients. These cells might have undergone homeostatic expansion or non-alloreactive donor cell activation from a cytokine

storm produced by TBI conditioning. Another possibility is that these expanded cells could be alloreactive T cells suppressed by Flonase. On the other hand, T cells treated with Flonase did not activate or expand when cultured with allogeneic splenocytes but did so after stimulation with anti-CD28 and anti-CD3 co-stimulation. Treated cells may have lost their alloreactivity, but still possess the ability to elicit an immune response. It could also mean that CD3 and CD28 co-stimulation is a stronger activation signal compared to the allogeneic mixed lymphocyte reaction. However, vehicle pre-treated cells showed a significant response against the allogeneic environment, therefore the signal was adequate for activation and expansion. There is always the possibility that there are different signals *in vivo* that we have yet explored which expand alloreactive cells after Flonase treatment.

Our secondary transplantation data contradicts the notion that the expanded T cells in the Flonase group are alloreactive when there was almost 100% recipient survival. One would think that any possible Flonase suppressive effects on potential alloreactive cells would have worn off in secondary recipients. Cell numbers injected into the secondary recipients were more closely matched than initial injection into primary recipients between the treated groups. We would have expected increased GvHD in the vehicle group secondary recipients compared to primary recipients, however it was diminished. At day 7, alloreactive cells might have already migrated out of the spleen into the peripheral tissues of the liver, skin and gut which could explain lower overall GvHD in secondary recipients. We could test this by including cells harvested from peripheral tissues in the secondary transplants.

Since Flonase induces apoptosis in CD4+ conventional T cells and CD8+ T cells, but not Foxp3+ cells (Tregs), and there are elevated percentages of Tregs in Flonase group spleens after allo-HCT, our hypothesis is that the increased donor Treg to CD4+ conventional T cell ratio largely

contributes to the decreased GvHD. As mentioned previously, Tregs are known to suppress alloreactive T cells and alleviate GvHD when added to an allo-HCT. To help prove this hypothesis we can remove all Tregs from donor cells prior to transplantation to test if the GvHD phenotype is rescued. For this experiment, we would sort out GFP+ splenocytes from Foxp3-eGFP mice and transplant the Flonase treated negative population.

Donor bone marrow and splenocytes were combined into one culture well per recipient for the entirety of this study to significantly reduce the number of wells used. This also simulates the heterogenicity of human donor mobilized blood which often has CD34+ hematopoietic stem cells along with a large number of mature immune cells like lymphocytes.

If Tregs are partially responsible for reducing GvHD in the Flonase group, we would see an increase in the clinical score or a decrease in overall weight after transplanting cultured cells devoid of Tregs. The Flonase group absent of Tregs could be compared to Flonase and Vehicle groups with Tregs. These control groups would still be subjected to sorting to keep the method consistent between groups. In this way we can rule out the probability that stress caused any discrepancies in data. Another possible experiment would be adding *in vitro* expanded Tregs to match the Treg:Tconv ratio to the Flonase group. Tregs can also be collected from sorted splenocytes from other mice as an alternative source. Combining these 2 experiments would make a convincing argument if they both support the hypothesis that Tregs are responsible for GvHD reduction. If both experiments disprove the hypothesis, then there could be another underlying mechanism we are unaware of.

We have only touched the surface of uncovering the underlying cellular mechanisms involved in our allo-HCT system. We have yet explored the possible GvL responses of Flonase treated allogeneic donor cells. Balancing allo-HCT to favor GvL but prevent GvHD is the preferred

outcome that is difficult to achieve. GvL response can be tested using a mouse tumor model made by injecting recipients with either lymphoma or leukemia murine cell lines post-transplantation. This usually leads to death due to the rapid expansion of tumor cells in recipients. With this, our hypothesis would be that Flonase treated cells can still suppress tumor growth by eliciting an anti-tumor or GvL response. This would test if Flonase prevented T cells from eliciting an anti-tumor response. This hypothesis would be supported by comparable tumor growth and recipient survival among mice receiving vehicle and Flonase treated cells, or if the Flonase group has higher survival and a smaller tumor growth compared to mice only receiving T cell depleted bone marrow. It is debatable whether a complete MHC mismatch allo-HCT mouse model would work to test anti-tumor effects. It might be necessary for the tumor and donor cells to be MHC matched for donor T cells to adequately bind to tumor MHC to kill tumor cells, therefore we might have to switch to a haploidentical mouse model.

It would be highly impactful to replicate Flonase-mediated GvHD reduction with human cells. Obviously, we cannot use human recipients for this experiment, therefore immunocompromised mice like NSGs are needed for human cell recipients to prevent graft rejection. We have preliminary data on whether Flonase induced cell death in human lymphocytes (data not shown). Human PBMCs were purified from whole blood using a ficoll gradient. These cells were then cultured with 1μM of Flonase for 24 hours, a much higher Flonase concentration and culture length compared to splenocytes from mice which were 3nM and 16h respectively. We saw that only 10% more lymphocytes underwent apoptosis after Flonase treatment compared to the vehicle group, meaning that lymphocytes from human PBMCs are more resistant to Flonase induced apoptosis than those from mice. Human lymphocytes could also need longer Flonase treatment to achieve the same level of cell death as mouse splenocytes cultured for 16h. However,

there is still some indication that human cells die after Flonase treatment. Once the concentration and culture time has been optimized, the next step is transplanting cultured human PBMCs into NSG recipients to observe any protection against GvHD. We would then introduce tumor cells to test donor cell GVL response. Unfortunately, more human data was not collected before the completion of this dissertation due to UCI blood donor program closure during the COVID-19 pandemic.

Flonase also induced almost 100% apoptosis in natural killer (NK) cells from mouse spleens (data not shown). We are unsure if this is favorable for reducing GvHD in allo-HCT. NK cells normally contribute to an anti-cancer response by recognizing any irregularities in MHC expression, therefore they would be beneficial for a GVL response. Infusing allogeneic NK cells in NSG mice gave the best results in eradicating engrafted human leukemia cells.[188] One would think that donor allogeneic NKs would lead to an elevated GvHD response due to mismatched immunoglobulin-like receptors (KIR), however, contrarily, clinical data shows reduced GvHD in patients receiving KIR mismatched allogeneic NK cells.[189] Any remaining host NK cells after allo-HCT conditioning can contribute to graft rejection and donor NK cells can help HSC engraftment. There have been inconsistent preclinical findings that show that NK cells both prevent and promote GvHD, so its role in GvHD is unclear. If we wanted to uncover more about NK cells in our allo-HCT system, we can deplete NK cells from our cultured bone marrow and splenocytes prior to transplantation to test any difference in GvHD severity.

Avoiding GvHD is a challenge for the state-of-the-art cancer therapy using chimeric antigen receptor T cells (CAR-T cells) adoptive transfers. CAR-T cells have been a breakthrough in cancer therapy because they can selectively target tumor cells through their engineered T cell receptors. One target for hematological malignancies is IL-3Rα or CD123. Additionally, non-

Hodgkin's lymphoma is treated with anti-CD19 CAR-T cells to eliminate lymphoblastic cancer B cells. CAR-T cells show high tumor cell killing efficiency, so it is a very promising therapy, however about less than half of the patients go into remission after this treatment. Many biotech companies have strived to improve and utilize this technology. These companies are competing against each other to optimize CAR-T cell therapy, however GvHD and graft rejection is still an obstacle that needs to be addressed. Another therapy similar to Car-T cell therapy is allogeneic T cell adoptive transfer, however there is high graft and host rejection. Our method/study can potentially shed light on achieving T cell tolerance for immunotherapy use.

I would like to shift to the other topics in this dissertation such as HSC development, HSC chemotaxis, and HCT use for autoimmune disease treatment. There is a large community of scientists that study HSC development and origin within the embryo. There are great scientists that have helped start and contributed largely to this field including Dr. Irving Weissman, Dr. Hanna Mikkola, Dr. Matthew Inlay, Dr. David Traver, Dr. Elaine Dzierzak and many others. There is a current debate on which embryonic tissue gives rise to HSCs: the aorta-gonad-mesonephros (AGM), yolk sac (YS), or the placenta (PL). Many believe that HSCs originate from only the AGM, however some believe the PL and YS is also included as tissues of origin. Some of the early works studying HSC development in the AGM used zebrafish. After, mouse models were used as the main model for HSC development. Our data in our most recent publication "Absence of CD11a expression identifies embryonic hematopoietic stem cell precursors via competitive neonatal transplantation assay" or Chapter 2 in this dissertation supports the idea that HSCs also originate from the YS since we show long-term engraftment of HSCs when transplanting YS cells into NSG neonates.

Chapter 2 is important for isolating pre-HSCs to phenotype this cell type and distinguish pre-HSCs from HSCs. One of the distinguishing factors is that pre-HSCs cannot engraft to the adult bone marrow whereas HSCs can. This is why we used a neonatal transplantation system to measure pre-HSC engraftment since pre-HSCs first engraft the neonatal liver where they develop into HSCs. The absence of CXCR4 expression on pre-HSCs could be responsible for the difference in bone marrow engraftment between pre-HSCs and HSCs. CXCR4 is important for chemotaxis, so the absence of this receptor could potentially be responsible for a lack of pre-HSC-bone marrow engraftment.

Initially, we were going to induce CXCR4 expression in pre-HSCs using either a transgenic approach or a drug induction approach. We were inspired by the Guo et. al. paper published in 2017 from the Dr. Hal Broxmeyer lab where they used Flonase to increase CXCR4 expression on pre-HSCs, but unfortunately, we did not see any difference in CXCR4 expression in pre-HSCs after Flonase treatment.[20] On the other hand, we did see an increase of CXCR4 on murine bone marrow derived HSCs which was also surprising since Guo et. al. did not see this effect when they looked at mouse cells possibly because they used too high of a Flonase dose. This led us to pursue further experimentation using Flonase to culture HSCs from the bone marrow. Even though it is very important to increase CXCR4 expression on HSCs to increase bone marrow engraftment efficiency, HSCs from mobilized bone marrow already have a high engraftment efficiency without drugs. The circumstances that would need enhanced HSC engraftment would be if donor HSCs are from human cord blood where there are low numbers of harvested HSCs, if T cells are depleted from the donor hematopoietic cell pool before transplantation, or when HSCs lose their CXCR4 expression in culture. These are significant reasons to increase CXCR4 expression, however clinicians are shying away from using cord blood as an HSC source.

Improving the efficacy and safety of allo-HCT could expand the patient pool to include patients with lower risk diseases like autoimmune disease. It will take some time to improve this therapy enough to safely treat other diseases, but if that time comes, autoimmune diseases could in theory be treated with HCT because they are blood disorders. This therapy can essentially eradicate the existing damaging autoimmune system using conditioning regiments and replace it with a healthy one using donor HSCs. Our goal was to test this in an ITP mouse model that we are developing, however it is still a work in progress. There is no cure to ITP except spleen removal to get rid of splenic macrophages that phagocytose platelets. However, spleen removal is a harsh treatment that renders a patient immunocompromised.

As mentioned before there are imperfect existing mouse models for ITP, therefore we decided to develop a more efficient one that allows us to test possible therapies like HCT. With the help of the transgenic mouse facility at UCI, we successfully obtained transgenic mice that had our construct (LMOH) inserted into the correct GPV locus. Earlier we confirmed that GPV was only expressed on platelets, megakaryocytes and megakaryocyte progenitors and no other hematopoietic cell (data not shown). Unfortunately, there were no flow cytometry antibodies that could detect ovalbumin (OVA) or hen egg lysozyme (HEL), therefore using western blotting could be helpful to detect the membrane bound protein in the future. We carried out many different strategies to induce blood platelet loss in mice baring the LMOH construct, however none of them produced preferable results. Nonetheless, immunizing MOH mice (LMOH mice with removed LSL) showed some promise in reducing platelet levels below the average platelet count. The immunizations may be eliciting antibody production against the soluble OVA or HEL which in turn could be binding to the membrane bound OVA-HEL on platelets. In the future, we will be using donor OT-II mice to conduct adoptive transfers into MOH mice. Since OT-II cells are CD4+

T cells specific for ovalbumin, we hypothesize that it will create an immune response against platelets that express MOH to ultimately eliminate platelets. There are other potential donor mice that we can use such as OT-I mice that have CD8+ T cells specific for ovalbumin or IghelMD4 mice that have B cells specific for hen egg lysozyme.

HCT is a very useful technique that allows us to study basic scientific questions about blood cell and HSC development. HCT is also a curative therapy that treats many hematological malignancies, however there are many drawbacks and complications that prevent this therapy from living up to its full potential. We explored possible ways to resolve these issues by preventing GvHD and increasing HSC-bone marrow engraftment. We also dabbled in the possibility of using HCT to treat autoimmune disease. Improving HCT can potentially expand the patient pool to those who have other blood diseases and for those who have less severe cases of hematological malignancies. We have come a long way from the first HCT, and it is just a matter of time where there are little to no complications after performing this curative therapy.

References

1. Till, J. E., & McCulloch, E. A. (1961). A direct measurement of the radiation sensitivity of normal mouse bone marrow cells. *Radiation research*, *14*(2), 213-222.
2. Siminovitch, L., McCulloch, E. A., & Till, J. E. (1963). The distribution of colony-forming cells among spleen colonies.
3. Becker, A. J., McCulloch, E. A., & Till, J. E. (1963). Cytological demonstration of the clonal nature of spleen colonies derived from transplanted mouse marrow cells.
4. Wu, A. M., Till, J. E., Siminovitch, L., & McCulloch, E. A. (1968). Cytological evidence for a relationship between normal hematopoietic colony-forming cells and cells of the lymphoid system. *The Journal of experimental medicine*, *127*(3), 455-464.
5. Spangrude, G. J., Heimfeld, S., & Weissman, I. L. (1988). Purification and characterization of mouse hematopoietic stem cells. *Science*, *241*(4861), 58-62.
6. Morrison, S. J., & Weissman, I. L. (1994). The long-term repopulating subset of hematopoietic stem cells is deterministic and isolatable by phenotype. *Immunity*, *1*(8), 661-673.
7. Tavassoli, M. (1991). Embryonic and fetal hemopoiesis: an overview. *Blood cells*, *17*(2), 269-81.
8. Moore, M. A., & Metcalf, D. (1970). Ontogeny of the haemopoietic system: yolk sac origin of in vivo and in vitro colony forming cells in the developing mouse embryo. *British journal of haematology*, *18*(3), 279-296.
9. Yoshimoto, M., Porayette, P., Glosson, N. L., Conway, S. J., Carlesso, N., Cardoso, A. A., ... & Yoder, M. C. (2012). Autonomous murine T-cell progenitor production in the extra-embryonic yolk sac before HSC emergence. *Blood, The Journal of the American Society of Hematology*, *119*(24), 5706-5714.
10. Yoder, M. C., & Hiatt, K. (1997). Engraftment of embryonic hematopoietic cells in conditioned newborn recipients. *Blood, The Journal of the American Society of Hematology*, *89*(6), 2176-2183.
11. Inlay, M. A., Serwold, T., Mosley, A., Fathman, J. W., Dimov, I. K., Seita, J., & Weissman, I. L. (2014). Identification of multipotent progenitors that emerge prior to hematopoietic stem cells in embryonic development. *Stem cell reports*, *2*(4), 457-472.
12. Wright, D. E., Bowman, E. P., Wagers, A. J., Butcher, E. C., & Weissman, I. L. (2002). Hematopoietic stem cells are uniquely selective in their migratory response to chemokines. *The Journal of experimental medicine*, *195*(9), 1145-1154.
13. Nagasawa, T., Hirota, S., Tachibana, K., Takakura, N., Nishikawa, S. I., Kitamura, Y., ... & Kishimoto, T. (1996). Defects of B-cell lymphopoiesis and bone-marrow myelopoiesis in mice lacking the CXC chemokine PBSF/SDF-1. *Nature*, *382*(6592), 635-638.
14. Ma, Q., Jones, D., Borghesani, P. R., Segal, R. A., Nagasawa, T., Kishimoto, T., ... & Springer, T. A. (1998). Impaired B-lymphopoiesis, myelopoiesis, and derailed cerebellar neuron migration in CXCR4-and SDF-1-deficient mice. *Proceedings of the National Academy of Sciences*, *95*(16), 9448-9453.
15. Nie, Y., Han, Y. C., & Zou, Y. R. (2008). CXCR4 is required for the quiescence of primitive hematopoietic cells. *Journal of Experimental Medicine*, *205*(4), 777-783.
16. Zhang, Y., Dépond, M., He, L., Foudi, A., Kwarteng, E. O., Lauret, E., ... & Wittner, M. (2016). CXCR4/CXCL12 axis counteracts hematopoietic stem cell exhaustion through selective protection against oxidative stress. *Scientific reports*, *6*(1), 1-13.

17. Sugiyama, T., Kohara, H., Noda, M., & Nagasawa, T. (2006). Maintenance of the hematopoietic stem cell pool by CXCL12-CXCR4 chemokine signaling in bone marrow stromal cell niches. *Immunity*, *25*(6), 977-988.
18. Miao, R., Lim, V. Y., Kothapalli, N., Ma, Y., Fossati, J., Zehentmeier, S., ... & Pereira, J. P. (2020). Hematopoietic Stem Cell niches and signals controlling immune cell development and maintenance of immunological memory. *Frontiers in Immunology*, *11*, 3074.
19. Brenner, S., Whiting□Theobald, N., Kawai, T., Linton, G. F., Rudikoff, A. G., Choi, U., ... & Malech, H. L. (2004). CXCR4□transgene expression significantly improves marrow engraftment of cultured hematopoietic stem cells. *Stem Cells*, *22*(7), 1128-1133.
20. Guo, B., Huang, X., Cooper, S., & Broxmeyer, H. E. (2017). Glucocorticoid hormone-induced chromatin remodeling enhances human hematopoietic stem cell homing and engraftment. *Nature medicine*, *23*(4), 424-428.
21. Denning□Kendall, P., Singha, S., Bradley, B., & Hows, J. (2003). Cytokine expansion culture of cord blood CD34+ cells induces marked and sustained changes in adhesion receptor and CXCR4 expressions. *Stem Cells*, *21*(1), 61-70.
22. Phelan, R., Arora, M., Chen, M. **Current use and outcome of hematopoietic stem cell transplantation: CIBMTR US summary slides, 2020.**
23. Chou, S., Chu, P., Hwang, W., & Lodish, H. (2010). Expansion of human cord blood hematopoietic stem cells for transplantation. *Cell stem cell*, *7*(4), 427-428.
24. Kaufman, C. L., Colson, Y. L., Wren, S. M., Watkins, S., Simmons, R. L., & Ildstad, S. T. (1994). Phenotypic characterization of a novel bone marrow-derived cell that facilitates engraftment of allogeneic bone marrow stem cells.
25. Ashwell, J. D., Chen, C., & Schwartz, R. H. (1986). High frequency and nonrandom distribution of alloreactivity in T cell clones selected for recognition of foreign antigen in association with self class II molecules. *The Journal of Immunology*, *136*(2), 389-395.
26. Suchin, E. J., Langmuir, P. B., Palmer, E., Sayegh, M. H., Wells, A. D., & Turka, L. A. (2001). Quantifying the frequency of alloreactive T cells in vivo: new answers to an old question. *The Journal of Immunology*, *166*(2), 973-981.
27. Lee, S. J., Klein, J., Haagenson, M., Baxter-Lowe, L. A., Confer, D. L., Eapen, M., ... & Anasetti, C. (2007). High-resolution donor-recipient HLA matching contributes to the success of unrelated donor marrow transplantation. *Blood, The Journal of the American Society of Hematology*, *110*(13), 4576-4583.
28. Fürst, D., Müller, C., Vucinic, V., Bunjes, D., Herr, W., Gramatzki, M., ... & Mytilineos, J. (2013). High-resolution HLA matching in hematopoietic stem cell transplantation: a retrospective collaborative analysis. *Blood, The Journal of the American Society of Hematology*, *122*(18), 3220-3229.
29. Guillen, F. J., Ferrara, J., Sleckman, B., Burakoff, S. J., & Murphy, G. F. (1986). Cutaneous acute graft-versus-host disease to minor histocompatibility antigens in a murine model: histologic analysis and correlation to clinical disease. *Journal of investigative dermatology*, *86*(4), 371-375.
30. Korngold, R., & Sprent, J. (1978). Lethal graft-versus-host disease after bone marrow transplantation across minor histocompatibility barriers in mice. Prevention by removing mature T cells from marrow. *The Journal of experimental medicine*, *148*(6), 1687-1698.
31. Bachier, C. R., Aggarwal, S. K., Hennegan, K., Milgroom, A., Francis, K., & Rotta, M. (2019). Epidemiology and real-world treatment of chronic graft-versus-host disease post allogeneic hematopoietic cell transplantation: A US claims analysis.

32. Boyiadzis, M., Arora, M., Klein, J. P., Hassebroek, A., Hemmer, M., Urbano-Ispizua, A., ... & Pavletic, S. Z. (2015). Impact of chronic graft-versus-host disease on late relapse and survival on 7,489 patients after myeloablative allogeneic hematopoietic cell transplantation for leukemia. *Clinical Cancer Research*, *21*(9), 2020-2028.
33. Lee, S. J., & Flowers, M. E. (2008). Recognizing and managing chronic graft-versus-host disease. *ASH Education Program Book*, *2008*(1), 134-141.
34. Flowers, M. E., Parker, P. M., Johnston, L. J., Matos, A. V., Storer, B., Bensinger, W. I., ... & Martin, P. J. (2002). Comparison of chronic graft-versus-host disease after transplantation of peripheral blood stem cells versus bone marrow in allogeneic recipients: long-term follow-up of a randomized trial. *Blood, The Journal of the American Society of Hematology*, *100*(2), 415-419.
35. Filipovich, A. H., Weisdorf, D., Pavletic, S., Socie, G., Wingard, J. R., Lee, S. J., ... & Flowers, M. E. (2005). National Institutes of Health consensus development project on criteria for clinical trials in chronic graft-versus-host disease: I. Diagnosis and staging working group report. *Biology of blood and marrow transplantation*, *11*(12), 945-956.
36. Vigorito, A. C., Campregher, P. V., Storer, B. E., Carpenter, P. A., Moravec, C. K., Kiem, H. P., ... & Flowers, M. E. (2009). Evaluation of NIH consensus criteria for classification of late acute and chronic GVHD. *Blood, The Journal of the American Society of Hematology*, *114*(3), 702-708.
37. Nestel, F. P., Price, K. S., Seemayer, T. A., & Lapp, W. S. (1992). Macrophage priming and lipopolysaccharide-triggered release of tumor necrosis factor alpha during graft-versus-host disease. *The Journal of experimental medicine*, *175*(2), 405-413.
38. Xun, C. Q., Thompson, J. S., Jennings, C. D., Brown, S. A., & Widmer, M. B. (1994). Effect of total body irradiation, busulfan-cyclophosphamide, or cyclophosphamide conditioning on inflammatory cytokine release and development of acute and chronic graft-versus-host disease in H-2-incompatible transplanted SCID mice.
39. Cooke, K. R., Hill, G. R., Crawford, J. M., Bungard, D., Brinson, Y. S., Delmonte, J., & Ferrara, J. L. (1998). Tumor necrosis factor-alpha production to lipopolysaccharide stimulation by donor cells predicts the severity of experimental acute graft-versus-host disease. *The Journal of clinical investigation*, *102*(10), 1882-1891.
40. Ferrara, J. L. (1993). Cytokine dysregulation as a mechanism of graft versus host disease. *Current opinion in immunology*, *5*(5), 794-799.
41. Toubai, T., Mathewson, N. D., Magenau, J., & Reddy, P. (2016). Danger signals and graft-versus-host disease: current understanding and future perspectives. *Frontiers in immunology*, *7*, 539.
42. Via, C. S., Rus, V., Gately, M. K., & Finkelman, F. D. (1994). IL-12 stimulates the development of acute graft-versus-host disease in mice that normally would develop chronic, autoimmune graft-versus-host disease. *The Journal of Immunology*, *153*(9), 4040-4047.
43. Yi, T., Chen, Y., Wang, L., Du, G., Huang, D., Zhao, D., ... & Zeng, D. (2009). Reciprocal differentiation and tissue-specific pathogenesis of Th1, Th2, and Th17 cells in graft-versus-host disease. *Blood, The Journal of the American Society of Hematology*, *114*(14), 3101-3112.
44. Nikolic, B., Lee, S., Bronson, R. T., Grusby, M. J., & Sykes, M. (2000). Th1 and Th2 mediate acute graft-versus-host disease, each with distinct end-organ targets. *The Journal of clinical investigation*, *105*(9), 1289-1298.

45. Zeiser, R., & Blazar, B. R. (2017). Acute graft-versus-host disease—biologic process, prevention, and therapy. *New England Journal of Medicine*, *377*(22), 2167-2179.
46. Schwab, L., Goroncy, L., Palaniyandi, S., Gautam, S., Triantafyllopoulou, A., Mocsai, A., ... & Zeiser, R. (2014). Neutrophil granulocytes recruited upon translocation of intestinal bacteria enhance graft-versus-host disease via tissue damage. *Nature medicine*, *20*(6), 648-654.
47. Hill, G. R., Crawford, J. M., Cooke, K. R., Brinson, Y. S., Pan, L., & Ferrara, J. L. (1997). Total body irradiation and acute graft-versus-host disease: the role of gastrointestinal damage and inflammatory cytokines. *Blood, The Journal of the American Society of Hematology*, *90*(8), 3204-3213.
48. Hill, G. R., & Ferrara, J. L. (2000). The primacy of the gastrointestinal tract as a target organ of acute graft-versus-host disease: rationale for the use of cytokine shields in allogeneic bone marrow transplantation. *Blood, The Journal of the American Society of Hematology*, *95*(9), 2754-2759.
49. Wysocki, C. A., Panoskaltsis-Mortari, A., Blazar, B. R., & Serody, J. S. (2005). Leukocyte migration and graft-versus-host disease. *Blood*, *105*(11), 4191-4199.
50. Via, C. S., Nguyen, P., Shustov, A., Drappa, J., & Elkon, K. B. (1996). A major role for the Fas pathway in acute graft-versus-host disease. *The Journal of Immunology*, *157*(12), 5387-5393.
51. Wu, Q., Chen, H., Fang, J., Xie, W., Hong, M., & Xia, L. (2012). Elevated Fas/FasL system and endothelial cell microparticles are involved in endothelial damage in acute graft-versus-host disease: a clinical analysis. *Leukemia research*, *36*(3), 275-280.
52. Shimabukuro-Vornhagen, A., Hallek, M. J., Storb, R. F., & von Bergwelt-Baildon, M. S. (2009). The role of B cells in the pathogenesis of graft-versus-host disease. *Blood, The Journal of the American Society of Hematology*, *114*(24), 4919-4927.
53. Sarantopoulos, S., Stevenson, K. E., Kim, H. T., Bhuiya, N. S., Cutler, C. S., Soiffer, R. J., ... & Ritz, J. (2007). High levels of B-cell activating factor in patients with active chronic graft-versus-host disease. *Clinical Cancer Research*, *13*(20), 6107-6114.
54. van Leeuwen, L., Guiffre, A., Atkinson, K., Rainer, S. P., & Sewell, W. A. (2002). A two-phase pathogenesis of graft-versus-host disease in mice. *Bone marrow transplantation*, *29*(2), 151-158.
55. Blazar, B. R., Carroll, S. F., & Vallera, D. A. (1991). Prevention of murine graft-versus-host disease and bone marrow alloengraftment across the major histocompatibility barrier after donor graft preincubation with anti-LFA1 immunotoxin.
56. Vallera, D. A., Soderling, C. C., Carlson, G. J., & Kersey, J. H. (1981). Bone marrow transplantation across major histocompatibility barriers in mice. Effect of elimination of T cells from donor grafts by treatment with monoclonal Thy-1.2 plus complement or antibody alone. *Transplantation*, *31*(3), 218-222.
57. Panoskaltsis-Mortari, A., Lacey, D. L., Vallera, D. A., & Blazar, B. R. (1998). Keratinocyte growth factor administered before conditioning ameliorates graft-versus-host disease after allogeneic bone marrow transplantation in mice. *Blood, The Journal of the American Society of Hematology*, *92*(10), 3960-3967.
58. Pickel, K., & Hoffmann, M. K. (1977). Suppressor T cells arising in mice undergoing a graft-vs-host response. *The Journal of Immunology*, *118*(2), 653-656.

59. Fowler, D. H., Breglio, J., Nagel, G., Eckhaus, M. A., & Gress, R. E. (1996). Allospecific CD8+ Tc1 and Tc2 populations in graft-versus-leukemia effect and graft-versus-host disease. *The Journal of Immunology*, *157*(11), 4811-4821.
60. Ghayur, T. A. R. I. Q., Seemayer, T. A., Xenocostas, A., & Lapp, W. S. (1988). Complete sequential regeneration of graft-vs.-host-induced severely dysplastic thymuses. Implications for the pathogenesis of chronic graft-vs.-host disease. *The American journal of pathology*, *133*(1), 39.
61. Korngold, R. O. B. E. R. T., & Sprent, J. O. N. A. T. H. A. N. (1987). Variable capacity of L3T4+ T cells to cause lethal graft-versus-host disease across minor histocompatibility barriers in mice. *The Journal of experimental medicine*, *165*(6), 1552-1564.
62. Ito, R., Katano, I., Kawai, K., Hirata, H., Ogura, T., Kamisako, T., ... & Ito, M. (2009). Highly sensitive model for xenogenic GVHD using severe immunodeficient NOG mice. *Transplantation*, *87*(11), 1654-1658.
63. King, M. A., Covassin, L., Brehm, M. A., Racki, W., Pearson, T., Leif, J., ... & Greiner, D. L. (2009). Human peripheral blood leucocyte non□obese diabetic□severe combined immunodeficiency interleukin□2 receptor gamma chain gene mouse model of xenogeneic graft□versus□host□like disease and the role of host major histocompatibility complex. *Clinical & Experimental Immunology*, *157*(1), 104-118.
64. van Rijn, R. S., Simonetti, E. R., Hagenbeek, A., Hogenes, M. C., de Weger, R. A., Canninga-van Dijk, M. R., ... & Ebeling, S. B. (2003). A new xenograft model for graft-versus-host disease by intravenous transfer of human peripheral blood mononuclear cells in RAG2-/-γc-/-double-mutant mice. *Blood*, *102*(7), 2522-2531.
65. Nervi, B., Rettig, M. P., Ritchey, J. K., Wang, H. L., Bauer, G., Walker, J., ... & DiPersio, J. F. (2007). Factors affecting human T cell engraftment, trafficking, and associated xenogeneic graft-vs-host disease in NOD/SCID β2mnull mice. *Experimental hematology*, *35*(12), 1823-1838.
66. Hamilton, B. L., & Parkman, R. (1983). Acute and chronic graft-versus-host disease induced by minor histocompatibility antigens in mice. *Transplantation*, *36*(2), 150-155.
67. Ruzek, M. C., Jha, S., Ledbetter, S., Richards, S. M., & Garman, R. D. (2004). A modified model of graft□versus□host–induced systemic sclerosis (scleroderma) exhibits all major aspects of the human disease. *Arthritis & Rheumatism: Official Journal of the American College of Rheumatology*, *50*(4), 1319-1331.
68. Zhang, C., Todorov, I., Zhang, Z., Liu, Y., Kandeel, F., Forman, S., ... & Zeng, D. (2006). Donor CD4+ T and B cells in transplants induce chronic graft-versus-host disease with autoimmune manifestations. *Blood*, *107*(7), 2993-3001.
69. Srinivasan, M., Flynn, R., Price, A., Ranger, A., Browning, J. L., Taylor, P. A., ... & Blazar, B. R. (2012). Donor B-cell alloantibody deposition and germinal center formation are required for the development of murine chronic GVHD and bronchiolitis obliterans. *Blood, The Journal of the American Society of Hematology*, *119*(6), 1570-1580.
70. Zorn, E., Kim, H. T., Lee, S. J., Floyd, B. H., Litsa, D., Arumugarajah, S., ... & Ritz, J. (2005). Reduced frequency of FOXP3+ CD4+ CD25+ regulatory T cells in patients with chronic graft-versus-host disease. *Blood*, *106*(8), 2903-2911.
71. Edinger, M., Hoffmann, P., Ermann, J., Drago, K., Fathman, C. G., Strober, S., & Negrin, R. S. (2003). CD4+ CD25+ regulatory T cells preserve graft-versus-tumor activity while inhibiting graft-versus-host disease after bone marrow transplantation. *Nature medicine*, *9*(9), 1144-1150.

72. Hoffmann, P., Ermann, J., Edinger, M., Fathman, C. G., & Strober, S. (2002). Donor-type CD4+ CD25+ regulatory T cells suppress lethal acute graft-versus-host disease after allogeneic bone marrow transplantation. *The Journal of experimental medicine*, *196*(3), 389-399.
73. Di Ianni, M., Falzetti, F., Carotti, A., Terenzi, A., Castellino, F., Bonifacio, E., ... & Martelli, M. F. (2011). Tregs prevent GVHD and promote immune reconstitution in HLA-haploidentical transplantation. *Blood, The Journal of the American Society of Hematology*, *117*(14), 3921-3928.
74. Riegel, C., Boeld, T. J., Doser, K., Huber, E., Hoffmann, P., & Edinger, M. (2020). Efficient treatment of murine acute GvHD by in vitro expanded donor regulatory T cells. *Leukemia*, *34*(3), 895-908.
75. Fundación Pública Andaluza para la gestión de la Investigación en Sevill. (2018, September 25-). Donor Regulatory T-cells for Steroid-Refractory Chronic Graft-versus-host-Disease (GvHD-TReG). Identifier NCT03683498. https://clinicaltrials.gov/ct2/show/NCT03683498.
76. Rubtsov, Y. P., Rasmussen, J. P., Chi, E. Y., Fontenot, J., Castelli, L., Ye, X., ... & Rudensky, A. Y. (2008). Regulatory T cell-derived interleukin-10 limits inflammation at environmental interfaces. *Immunity*, *28*(4), 546-558.
77. Collison, L. W., Workman, C. J., Kuo, T. T., Boyd, K., Wang, Y., Vignali, K. M., ... & Vignali, D. A. (2007). The inhibitory cytokine IL-35 contributes to regulatory T-cell function. *Nature*, *450*(7169), 566-569.
78. Andersson, J., Tran, D. Q., Pesu, M., Davidson, T. S., Ramsey, H., O'Shea, J. J., & Shevach, E. M. (2008). CD4+ FoxP3+ regulatory T cells confer infectious tolerance in a TGF-β–dependent manner. *The Journal of experimental medicine*, *205*(9), 1975-1981.
79. Cao, X., Cai, S. F., Fehniger, T. A., Song, J., Collins, L. I., Piwnica-Worms, D. R., & Ley, T. J. (2007). Granzyme B and perforin are important for regulatory T cell-mediated suppression of tumor clearance. *Immunity*, *27*(4), 635-646.
80. Deaglio, S., Dwyer, K. M., Gao, W., Friedman, D., Usheva, A., Erat, A., ... & Robson, S. C. (2007). Adenosine generation catalyzed by CD39 and CD73 expressed on regulatory T cells mediates immune suppression. *Journal of Experimental Medicine*, *204*(6), 1257-1265.
81. Wing, K., Onishi, Y., Prieto-Martin, P., Yamaguchi, T., Miyara, M., Fehervari, Z., ... & Sakaguchi, S. (2008). CTLA-4 control over Foxp3+ regulatory T cell function. *Science*, *322*(5899), 271-275.
82. Huang, C. T., Workman, C. J., Flies, D., Pan, X., Marson, A. L., Zhou, G., ... & Vignali, D. A. (2004). Role of LAG-3 in regulatory T cells. *Immunity*, *21*(4), 503-513.
83. Hossain, M. S., Kunter, G. M., El-Najjar, V. F., Jaye, D. L., Al-Kadhimi, Z., Taofeek, O. K., ... & Waller, E. K. (2017). PD-1 and CTLA-4 up regulation on donor T cells is insufficient to prevent GvHD in allo-HSCT recipients. *PLoS One*, *12*(9), e0184254.
84. Li, J., Semple, K., Suh, W. K., Liu, C., Chen, F., Blazar, B. R., & Yu, X. Z. (2011). Roles of CD28, CTLA4, and inducible costimulator in acute graft-versus-host disease in mice. *Biology of Blood and Marrow Transplantation*, *17*(7), 962-969.
85. Mohty, M. (2007). Mechanisms of action of antithymocyte globulin: T-cell depletion and beyond. *Leukemia*, *21*(7), 1387-1394.
86. Bolaños-Meade, J., Reshef, R., Fraser, R., Fei, M., Abhyankar, S., Al-Kadhimi, Z., ... & Koreth, J. (2019). Three prophylaxis regimens (tacrolimus, mycophenolate mofetil, and cyclophosphamide; tacrolimus, methotrexate, and bortezomib; or tacrolimus, methotrexate,

and maraviroc) versus tacrolimus and methotrexate for prevention of graft-versus-host disease with haemopoietic cell transplantation with reduced-intensity conditioning: a randomised phase 2 trial with a non-randomised contemporaneous control group (BMT CTN 1203). *The Lancet Haematology*, *6*(3), e132-e143.
87. McSweeney, P. A., Niederwieser, D., Shizuru, J. A., Sandmaier, B. M., Molina, A. J., Maloney, D. G., ... & Storb, R. F. (2001). Hematopoietic cell transplantation in older patients with hematologic malignancies: replacing high-dose cytotoxic therapy with graft-versus-tumor effects. *Blood, The Journal of the American Society of Hematology*, *97*(11), 3390-3400.
88. Cines, D. B., Cuker, A., & Semple, J. W. (2014). Pathogenesis of immune thrombocytopenia. *La Presse Médicale*, *43*(4), e49-e59.
89. Liebman, H. A. (2008). Viral-associated immune thrombocytopenic purpura. *ASH Education Program Book*, *2008*(1), 212-218.
90. McKenzie, C. G., Guo, L., Freedman, J., & Semple, J. W. (2013). Cellular immune dysfunction in immune thrombocytopenia (ITP). *British journal of haematology*, *163*(1), 10-23.
91. Li, X., Wang, S. W., Feng, Q., Hou, Y., Lu, N., Ma, C. H., ... & Peng, J. (2019). Novel murine model of immune thrombocytopaenia through immunized CD41 knockout mice. *Thrombosis and haemostasis*, *119*(03), 377-383.
92. Chow, L., Aslam, R., Speck, E. R., Kim, M., Cridland, N., Webster, M. L., ... & Semple, J. W. (2010). A murine model of severe immune thrombocytopenia is induced by antibody- and CD8+ T cell–mediated responses that are differentially sensitive to therapy. *Blood, The Journal of the American Society of Hematology*, *115*(6), 1247-1253.
93. Hagedorn, E. J., Durand, E. M., Fast, E. M., & Zon, L. I. (2014). Getting more for your marrow: boosting hematopoietic stem cell numbers with PGE2. *Experimental cell research*, *329*(2), 220-226.
94. Zovein, A. C., Hofmann, J. J., Lynch, M., French, W. J., Turlo, K. A., Yang, Y., ... & Iruela-Arispe, M. L. (2008). Fate tracing reveals the endothelial origin of hematopoietic stem cells. *Cell stem cell*, *3*(6), 625-636.
95. Lancrin, C., Sroczynska, P., Stephenson, C., Allen, T., Kouskoff, V., & Lacaud, G. (2009). The haemangioblast generates haematopoietic cells through a haemogenic endothelium stage. *Nature*, *457*(7231), 892-895.
96. Palis, J., Robertson, S., Kennedy, M., Wall, C., & Keller, G. (1999). Development of erythroid and myeloid progenitors in the yolk sac and embryo proper of the mouse. *Development*, *126*(22), 5073-5084.
97. Alvarez-Silva, M., Belo-Diabangouaya, P., Salaün, J., & Dieterlen-Lièvre, F. (2003). Mouse placenta is a major hematopoietic organ.
98. Palis, J. (2016). Hematopoietic stem cell□independent hematopoiesis: emergence of erythroid, megakaryocyte, and myeloid potential in the mammalian embryo. *FEBS letters*, *590*(22), 3965-3974.
99. Yoder, M. C., Hiatt, K., Dutt, P., Mukherjee, P., Bodine, D. M., & Orlic, D. (1997). Characterization of definitive lymphohematopoietic stem cells in the day 9 murine yolk sac. *Immunity*, *7*(3), 335-344.
100. Taoudi, S., Gonneau, C., Moore, K., Sheridan, J. M., Blackburn, C. C., Taylor, E., & Medvinsky, A. (2008). Extensive hematopoietic stem cell generation in the AGM region via maturation of VE-cadherin+ CD45+ pre-definitive HSCs. *Cell stem cell*, *3*(1), 99-108.

101. Arora, N., Wenzel, P. L., McKinney-Freeman, S. L., Ross, S. J., Kim, P. G., Chou, S. S., ... & Daley, G. Q. (2014). Effect of developmental stage of HSC and recipient on transplant outcomes. *Developmental cell*, *29*(5), 621-628.
102. Rybtsov, S., Ivanovs, A., Zhao, S., & Medvinsky, A. (2016). Concealed expansion of immature precursors underpins acute burst of adult HSC activity in foetal liver. *Development*, *143*(8), 1284-1289.
103. Zhou, F., Li, X., Wang, W., Zhu, P., Zhou, J., He, W., ... & Liu, B. (2016). Tracing haematopoietic stem cell formation at single-cell resolution. *Nature*, *533*(7604), 487-492.
104. Kumaravelu, P., Hook, L., Morrison, A. M., Ure, J., Zhao, S., Zuyev, S., ... & Medvinsky, A. (2002). Quantitative developmental anatomy of definitive haematopoietic stem cells/long-term repopulating units (HSC/RUs): role of the aorta-gonad-mesonephros (AGM) region and the yolk sac in colonisation of the mouse embryonic liver.
105. Gekas, C., Dieterlen-Lièvre, F., Orkin, S. H., & Mikkola, H. K. (2005). The placenta is a niche for hematopoietic stem cells. *Developmental cell*, *8*(3), 365-375.
106. Müller, A. M., Medvinsky, A., Strouboulis, J., Grosveld, F., & Dzierzakt, E. (1994). Development of hematopoietic stem cell activity in the mouse embryo. *Immunity*, *1*(4), 291-301.
107. Beaudin, A. E., Boyer, S. W., Perez-Cunningham, J., Hernandez, G. E., Derderian, S. C., Jujjavarapu, C., ... & Forsberg, E. C. (2016). A transient developmental hematopoietic stem cell gives rise to innate-like B and T cells. *Cell Stem Cell*, *19*(6), 768-783.
108. Wiesmann, A., Phillips, R. L., Mojica, M., Pierce, L. J., Searles, A. E., Spangrude, G. J., & Lemischka, I. (2000). Expression of CD27 on murine hematopoietic stem and progenitor cells. *Immunity*, *12*(2), 193-199.
109. Kiel, M. J., Yilmaz, Ö. H., Iwashita, T., Yilmaz, O. H., Terhorst, C., & Morrison, S. J. (2005). SLAM family receptors distinguish hematopoietic stem and progenitor cells and reveal endothelial niches for stem cells. *cell*, *121*(7), 1109-1121.
110. Balazs, A. B., Fabian, A. J., Esmon, C. T., & Mulligan, R. C. (2006). Endothelial protein C receptor (CD201) explicitly identifies hematopoietic stem cells in murine bone marrow. *Blood*, *107*(6), 2317-2321.
111. Karlsson, G., Rörby, E., Pina, C., Soneji, S., Reckzeh, K., Miharada, K., ... & Enver, T. (2013). The tetraspanin CD9 affords high-purity capture of all murine hematopoietic stem cells. *Cell reports*, *4*(4), 642-648.
112. Weissman, I. L. (1978). Fetal hematopoietic origins of the adult hematolymphoid system. *Differentiation of Normal and Neoplastic Hematopoietic Cells*, *33*.
113. Akashi K, Weissman IL (2001) Stem cells and hematolymphoid development. In: Zon LI, editor. Hematopoiesis: A developmental approach. Oxford: Oxford University Press. pp. 15–34.
114. Rybtsov, S., Sobiesiak, M., Taoudi, S., Souilhol, C., Senserrich, J., Liakhovitskaia, A., ... & Medvinsky, A. (2011). Hierarchical organization and early hematopoietic specification of the developing HSC lineage in the AGM region. *Journal of Experimental Medicine*, *208*(6), 1305-1315.
115. Hadland, B. K., Varnum-Finney, B., Mandal, P. K., Rossi, D. J., Poulos, M. G., Butler, J. M., ... & Bernstein, I. D. (2017). A common origin for B-1a and B-2 lymphocytes in clonal pre-hematopoietic stem cells. *Stem cell reports*, *8*(6), 1563-1572.

116. Yoder, M. C., Hiatt, K., & Mukherjee, P. (1997). In vivo repopulating hematopoietic stem cells are present in the murine yolk sac at day 9.0 postcoitus. *Proceedings of the National Academy of Sciences*, *94*(13), 6776-6780.
117. Boisset, J. C., van Cappellen, W., Andrieu-Soler, C., Galjart, N., Dzierzak, E., & Robin, C. (2010). In vivo imaging of haematopoietic cells emerging from the mouse aortic endothelium. *Nature*, *464*(7285), 116-120.
118. Cumano, A., & Godin, I. (2007). Ontogeny of the hematopoietic system. *Annu. Rev. Immunol.*, *25*, 745-785.
119. Kinashi, T. (2005). Intracellular signalling controlling integrin activation in lymphocytes. *Nature Reviews Immunology*, *5*(7), 546-559.
120. Shamri, R., Grabovsky, V., Gauguet, J. M., Feigelson, S., Manevich, E., Kolanus, W., ... & Alon, R. (2005). Lymphocyte arrest requires instantaneous induction of an extended LFA-1 conformation mediated by endothelium-bound chemokines. *Nature immunology*, *6*(5), 497-506.
121. Zhang, Y., & Wang, H. (2012). Integrin signalling and function in immune cells. *Immunology*, *135*(4), 268-275.
122. Fathman, J. W., Fernhoff, N. B., Seita, J., Chao, C., Scarfone, V. M., Weissman, I. L., & Inlay, M. A. (2014). Upregulation of CD11A on hematopoietic stem cells denotes the loss of long-term reconstitution potential. *Stem cell reports*, *3*(5), 707-715.
123. Karimzadeh, A., Scarfone, V. M., Varady, E., Chao, C., Grathwohl, K., Fathman, J. W., ... & Inlay, M. A. (2018). The CD11a and endothelial protein C receptor marker combination simplifies and improves the purification of mouse hematopoietic stem cells. *Stem cells translational medicine*, *7*(6), 468-476.
124. Ishikawa, F. (2013). Modeling normal and malignant human hematopoiesis in vivo through newborn NSG xenotransplantation. *International journal of hematology*, *98*(6), 634-640.
125. Verbiest, T., Finnon, R., Brown, N., Finnon, P., Bouffler, S., & Badie, C. (2016). NOD scid gamma mice are permissive to allogeneic HSC transplantation without prior conditioning. *International journal of molecular sciences*, *17*(11), 1850.
126. Dai, H., Friday, A. J., Abou-Daya, K. I., Williams, A. L., Mortin-Toth, S., Nicotra, M. L., ... & Lakkis, F. G. (2017). Donor SIRPα polymorphism modulates the innate immune response to allogeneic grafts. *Science immunology*, *2*(12).
127. De Bruijn, M. F., Ma, X., Robin, C., Ottersbach, K., Sanchez, M. J., & Dzierzak, E. (2002). Hematopoietic stem cells localize to the endothelial cell layer in the midgestation mouse aorta. *Immunity*, *16*(5), 673-683.
128. Kim, K. H., & Sederstrom, J. M. (2015). Assaying cell cycle status using flow cytometry. *Current protocols in molecular biology*, *111*(1), 28-6.
129. Rybtsov, S., Batsivari, A., Bilotkach, K., Paruzina, D., Senserrich, J., Nerushev, O., & Medvinsky, A. (2014). Tracing the origin of the HSC hierarchy reveals an SCF-dependent, IL-3-independent CD43− embryonic precursor. *Stem cell reports*, *3*(3), 489-501.
130. de Bruijn, M. F., Speck, N. A., Peeters, M. C., & Dzierzak, E. (2000). Definitive hematopoietic stem cells first develop within the major arterial regions of the mouse embryo. *The EMBO journal*, *19*(11), 2465-2474.
131. Bowie, M. B., Kent, D. G., Dykstra, B., McKnight, K. D., McCaffrey, L., Hoodless, P. A., & Eaves, C. J. (2007). Identification of a new intrinsically timed developmental

checkpoint that reprograms key hematopoietic stem cell properties. *Proceedings of the National Academy of Sciences*, *104*(14), 5878-5882.
132. Moore, K. A., Ema, H., & Lemischka, I. R. (1997). In vitro maintenance of highly purified, transplantable hematopoietic stem cells. *Blood, The Journal of the American Society of Hematology*, *89*(12), 4337-4347.
133. Martin, M. A., & Bhatia, M. (2005). Analysis of the human fetal liver hematopoietic microenvironment. *Stem cells and development*, *14*(5), 493-504.
134. Chou, S., & Lodish, H. F. (2010). Fetal liver hepatic progenitors are supportive stromal cells for hematopoietic stem cells. *Proceedings of the National Academy of Sciences*, *107*(17), 7799-7804.
135. Khan, J. A., Mendelson, A., Kunisaki, Y., Birbrair, A., Kou, Y., Arnal-Estapé, A., ... & Frenette, P. S. (2016). Fetal liver hematopoietic stem cell niches associate with portal vessels. *Science*, *351*(6269), 176-180.
136. Riddell, J., Gazit, R., Garrison, B. S., Guo, G., Saadatpour, A., Mandal, P. K., ... & Rossi, D. J. (2014). Reprogramming committed murine blood cells to induced hematopoietic stem cells with defined factors. *Cell*, *157*(3), 549-564.
137. Lee, J., Dykstra, B., Spencer, J. A., Kenney, L. L., Greiner, D. L., Shultz, L. D., ... & Rossi, D. J. (2017). mRNA-mediated glycoengineering ameliorates deficient homing of human stem cell–derived hematopoietic progenitors. *The Journal of clinical investigation*, *127*(6), 2433-2437.
138. Sugimura, R., Jha, D. K., Han, A., Soria-Valles, C., Da Rocha, E. L., Lu, Y. F., ... & Daley, G. Q. (2017). Haematopoietic stem and progenitor cells from human pluripotent stem cells. *Nature*, *545*(7655), 432-438.
139. Bair, S. M., Brandstadter, J. D., Ayers, E. C., & Stadtmauer, E. A. (2020). Hematopoietic stem cell transplantation for blood cancers in the era of precision medicine and immunotherapy. *Cancer*, *126*(9), 1837-1855.
140. Ratajczak, M. Z., & Suszynska, M. (2016). Emerging strategies to enhance homing and engraftment of hematopoietic stem cells. *Stem cell reviews and reports*, *12*(1), 121-128.
141. van Os, R., Ausema, A., Dontje, B., van Riezen, M., van Dam, G., & de Haan, G. (2010). Engraftment of syngeneic bone marrow is not more efficient after intrafemoral transplantation than after traditional intravenous administration. *Experimental hematology*, *38*(11), 1115-1123.
142. Iscove, N. N., & Nawa, K. (1997). Hematopoietic stem cells expand during serial transplantation in vivo without apparent exhaustion. *Current Biology*, *7*(10), 805-808.
143. Hendrikx, P. J., Martens, C. M., Hagenbeek, A., Keij, J. F., & Visser, J. W. (1996). Homing of fluorescently labeled murine hematopoietic stem cells. *Experimental hematology*, *24*(2), 129-140.
144. Gluckman, E., Rocha, V., Boyer-Chammard, A., Locatelli, F., Arcese, W., Pasquini, R., ... & Chastang, C. (1997). Outcome of cord-blood transplantation from related and unrelated donors. *New England Journal of Medicine*, *337*(6), 373-381.
145. Bahçeci, E., Read, E. J., Leitman, S., Childs, R., Dunbar, C., Young, N. S., & Barrett, A. J. (2000). CD34+ cell dose predicts relapse and survival after T-cell-depleted HLA-identical haematopoietic stem cell transplantation (HSCT) for haematological malignancies. *British journal of haematology*, *108*(2), 408-414.

146. Peled, A., Petit, I., Kollet, O., Magid, M., Ponomaryov, T., Byk, T., ... & Lapidot, T. (1999). Dependence of human stem cell engraftment and repopulation of NOD/SCID mice on CXCR4. *Science*, *283*(5403), 845-848.
147. Sharma, M., Afrin, F., Satija, N., Tripathi, R. P., & Gangenahalli, G. U. (2011). Stromal-derived factor-1/CXCR4 signaling: indispensable role in homing and engraftment of hematopoietic stem cells in bone marrow. *Stem cells and development*, *20*(6), 933-946.
148. Cashen, A. F., Nervi, B., & DiPersio, J. (2007). AMD3100: CXCR4 antagonist and rapid stem cell-mobilizing agent.
149. Jagasia, M., Arora, M., Flowers, M. E., Chao, N. J., McCarthy, P. L., Cutler, C. S., ... & Hahn, T. (2012). Risk factors for acute GVHD and survival after hematopoietic cell transplantation. *Blood, The Journal of the American Society of Hematology*, *119*(1), 296-307.
150. Khoury, H. J., Wang, T., Hemmer, M. T., Couriel, D., Alousi, A., Cutler, C., ... & Pidala, J. (2017). Improved survival after acute graft-versus-host disease diagnosis in the modern era. *haematologica*, *102*(5), 958.
151. Bashey, A., Zhang, X., Morris, L. E., Holland, H. K., Solh, M., & Solomon, S. R. (2019). Improved Survival of Patients Diagnosed with Severe (Grade 3-4) Acute GVHD or Severe NIH Grade Chronic GVHD in the Current Era Compared to Historic Controls.
152. Cronstein, B. N., & Aune, T. M. (2020). Methotrexate and its mechanisms of action in inflammatory arthritis. *Nature Reviews Rheumatology*, *16*(3), 145-154.
153. Storb, R., Deeg, H. J., Whitehead, J., Appelbaum, F., Beatty, P., Bensinger, W., ... & Thomas, E. D. (1986). Methotrexate and cyclosporine compared with cyclosporine alone for prophylaxis of acute graft versus host disease after marrow transplantation for leukemia. *New England Journal of Medicine*, *314*(12), 729-735.
154. Ruutu, T., Gratwohl, A., De Witte, T., Afanasyev, B., Apperley, J., Bacigalupo, A., ... & Niederwieser, D. (2014). Prophylaxis and treatment of GVHD: EBMT–ELN working group recommendations for a standardized practice. *Bone marrow transplantation*, *49*(2), 168-173.
155. Ho, V. T., & Soiffer, R. J. (2001). The history and future of T-cell depletion as graft-versus-host disease prophylaxis for allogeneic hematopoietic stem cell transplantation. *Blood*, *98*(12), 3192-3204.
156. Luznik, L., Jalla, S., Engstrom, L. W., Iannone, R., & Fuchs, E. J. (2001). Durable engraftment of major histocompatibility complex–incompatible cells after nonmyeloablative conditioning with fludarabine, low-dose total body irradiation, and posttransplantation cyclophosphamide. *Blood, The Journal of the American Society of Hematology*, *98*(12), 3456-3464.
157. Luznik, L., O'Donnell, P. V., Symons, H. J., Chen, A. R., Leffell, M. S., Zahurak, M., ... & Fuchs, E. J. (2008). HLA-haploidentical bone marrow transplantation for hematologic malignancies using nonmyeloablative conditioning and high-dose, posttransplantation cyclophosphamide. *Biology of Blood and Marrow Transplantation*, *14*(6), 641-650.
158. Modi, D., Albanyan, O., Kim, S., Deol, A., Alavi, A., Kin, A. D., ... & Uberti, J. P. (2020). Toxicities after high dose post-transplant cyclophosphamide in haploidentical donor transplants: Risk factors and impact on survival.
159. Irene, G. C., Albert, E., Anna, B. V., Rahinatu, A., Silvana, N., Silvana, S., ... & Rodrigo, M. (2020). Patterns of infection and infectious-related mortality in patients receiving post-

transplant high dose cyclophosphamide as graft-versus-host-disease prophylaxis: impact of HLA donor matching. *Bone Marrow Transplantation*, 1-10.
160. Fuji, S., Byrne, M., Nagler, A., Mohty, M., & Savani, B. N. (2021). How we can mitigate the side effects associated with systemic glucocorticoid after allogeneic hematopoietic cell transplantation. *Bone Marrow Transplantation*, 1-9.
161. Naserian, S., Leclerc, M., Thiolat, A., Pilon, C., Le Bret, C., Belkacemi, Y., ... & Cohen, J. L. (2018). Simple, reproducible, and efficient clinical grading system for murine models of acute graft-versus-host disease. *Frontiers in immunology*, *9*, 10.
162. Beilhack, A., Schulz, S., Baker, J., Beilhack, G. F., Wieland, C. B., Herman, E. I., ... & Negrin, R. S. (2005). In vivo analyses of early events in acute graft-versus-host disease reveal sequential infiltration of T-cell subsets. *Blood*, *106*(3), 1113-1122.
163. Schumann, J., Stanko, K., Schliesser, U., Appelt, C., & Sawitzki, B. (2015). Differences in CD44 surface expression levels and function discriminates IL-17 and IFN-γ producing helper T cells. *PLoS One*, *10*(7), e0132479.
164. Riegel, C., Boeld, T. J., Doser, K., Huber, E., Hoffmann, P., & Edinger, M. (2020). Efficient treatment of murine acute GvHD by in vitro expanded donor regulatory T cells. *Leukemia*, *34*(3), 895-908.
165. Prenek, L., Litvai, T., Balázs, N., Kugyelka, R., Boldizsár, F., Najbauer, J., ... & Berki, T. (2020). Regulatory T cells are less sensitive to glucocorticoid hormone induced apoptosis than CD4+ T cells. *Apoptosis*, *25*(9), 715-729.
166. Sugrue, M. W., Williams, K., Pollock, B. H., Khan, S., Peracha, S., Wingard, J. R., & Moreb, J. S. (2000). Characterization and outcome of "hard to mobilize" lymphoma patients undergoing autologous stem cell transplantation. *Leukemia & lymphoma*, *39*(5-6), 509-519.
167. Gordan, L. N., Sugrue, M. W., Lynch, J. W., Williams, K. D., Khan, S. A., Wingard, J. R., & Moreb, J. S. (2003). Poor mobilization of peripheral blood stem cells is a risk factor for worse outcome in lymphoma patients undergoing autologous stem cell transplantation. *Leukemia & lymphoma*, *44*(5), 815-820.
168. Pavone, V., Gaudio, F., Console, G., Vitolo, U., Iacopino, P., Guarini, A., ... & Liso, A. (2006). Poor mobilization is an independent prognostic factor in patients with malignant lymphomas treated by peripheral blood stem cell transplantation. *Bone marrow transplantation*, *37*(8), 719-724.
169. Moon, J. H., Kim, S. N., Kang, B. W., Chae, Y. S., Kim, J. G., Ahn, J. S., ... & Sohn, S. K. (2010). Early onset of acute GVHD indicates worse outcome in terms of severity of chronic GVHD compared with late onset. *Bone marrow transplantation*, *45*(10), 1540-1545.
170. Gratwohl A., Hermans J., Apperley J., Arcese W., Bacigalupo A., Bandini G., et al. (1995) Acute graft-versus host disease: grade and outcome in patients with chronic myelogenous leukemia. Working Party Chronic Leukemia of the European Group for Blood and Bone Marrow Transplantation. *Blood* 86: 813–818.
171. Handgretinger, R., Klingebiel, T., Lang, P., Schumm, M., Neu, S., Geiselhart, A., ... & Niethammer, D. (2001). Megadose transplantation of purified peripheral blood CD34+ progenitor cells from HLA-mismatched parental donors in children. *Bone marrow transplantation*, *27*(8), 777-783.
172. Aversa, F., Tabilio, A., Velardi, A., Cunningham, I., Terenzi, A., Falzetti, F., ... & Gambelunghe, C. (1998). Treatment of high-risk acute leukemia with T-cell–depleted stem

cells from related donors with one fully mismatched HLA haplotype. *New England Journal of Medicine*, *339*(17), 1186-1193.
173. Benichou, G., Valujskikh, A., & Heeger, P. S. (1999). Contributions of direct and indirect T cell alloreactivity during allograft rejection in mice. *The Journal of Immunology*, *162*(1), 352-358.
174. Pietras, E. M., Lakshminarasimhan, R., Techner, J. M., Fong, S., Flach, J., Binnewies, M., & Passegué, E. (2014). Re-entry into quiescence protects hematopoietic stem cells from the killing effect of chronic exposure to type I interferons. *Journal of Experimental Medicine*, *211*(2), 245-262.
175. Coutinho, A. E., & Chapman, K. E. (2011). The anti-inflammatory and immunosuppressive effects of glucocorticoids, recent developments and mechanistic insights. *Molecular and cellular endocrinology*, *335*(1), 2-13.
176. Wilkinson, A. C., Ishida, R., Kikuchi, M., Sudo, K., Morita, M., Crisostomo, R. V., ... & Yamazaki, S. (2019). Long-term ex vivo haematopoietic-stem-cell expansion allows nonconditioned transplantation. *Nature*, *571*(7763), 117-121.
177. Segal, J. B., & Powe, N. R. (2006). Prevalence of immune thrombocytopenia: analyses of administrative data. *Journal of Thrombosis and Haemostasis*, *4*(11), 2377-2383.
178. Yenicesu, İ., Yetgin, S., Özyürek, E., & Aslan, D. (2002). Virus-associated immune thrombocytopenic purpura in childhood. *Pediatric hematology and oncology*, *19*(6), 433-437.
179. Lippman, S. M., Arnett, F. C., Conley, C. L., Ness, P. M., Meyers, D. A., & Bias, W. B. (1982). Genetic factors predisposing to autoimmune diseases: autoimmune hemolytic anemia, chronic thrombocytopenic purpura, and systemic lupus erythematosus. *The American journal of medicine*, *73*(6), 827-840.
180. Olsson, B., Andersson, P. O., Jernås, M., Jacobsson, S., Carlsson, B., Carlsson, L. M., & Wadenvik, H. (2003). T-cell-mediated cytotoxicity toward platelets in chronic idiopathic thrombocytopenic purpura. *Nature medicine*, *9*(9), 1123-1124.
181. Frederiksen, H., Maegbaek, M. L., & Nørgaard, M. (2014). Twenty□year mortality of adult patients with primary immune thrombocytopenia: a Danish population□based cohort study. *British journal of haematology*, *166*(2), 260-267.
182. Ghanima, W., Godeau, B., Cines, D. B., & Bussel, J. B. (2012). How I treat immune thrombocytopenia: the choice between splenectomy or a medical therapy as a second-line treatment. *Blood, The Journal of the American Society of Hematology*, *120*(5), 960-969.
183. Chow, L., Aslam, R., Speck, E. R., Kim, M., Cridland, N., Webster, M. L., ... & Semple, J. W. (2010). A murine model of severe immune thrombocytopenia is induced by antibody- and CD8+ T cell–mediated responses that are differentially sensitive to therapy. *Blood, The Journal of the American Society of Hematology*, *115*(6), 1247-1253.
184. Li, X., Wang, S. W., Feng, Q., Hou, Y., Lu, N., Ma, C. H., ... & Peng, J. (2019). Novel murine model of immune thrombocytopaenia through immunized CD41 knockout mice. *Thrombosis and haemostasis*, *119*(03), 377-383.
185. O'Connell, K. E., Mikkola, A. M., Stepanek, A. M., Vernet, A., Hall, C. D., Sun, C. C., ... & Brown, D. E. (2015). Practical murine hematopathology: a comparative review and implications for research. *Comparative medicine*, *65*(2), 96-113.
186. Xia, S., Liu, X., Cao, X., & Xu, S. (2020). T-cell expression of Bruton's tyrosine kinase promotes autoreactive T-cell activation and exacerbates aplastic anemia. *Cellular & molecular immunology*, *17*(10), 1042-1052.

187. Wu, T., Young, J. S., Johnston, H., Ni, X., Deng, R., Racine, J., ... & Zeng, D. (2013). Thymic damage, impaired negative selection, and development of chronic graft-versus-host disease caused by donor CD4+ and CD8+ T cells. *The Journal of Immunology*, *191*(1), 488-499.
188. Ruggeri, L., Capanni, M., Urbani, E., Perruccio, K., Shlomchik, W. D., Tosti, A., ... & Velardi, A. (2002). Effectiveness of donor natural killer cell alloreactivity in mismatched hematopoietic transplants. *Science*, *295*(5562), 2097-2100.
189. Murphy, W. J., Bennett, M., Kumar, V., & Longo, D. L. (1992). Donor-type activated natural killer cells promote marrow engraftment and B cell development during allogeneic bone marrow transplantation. *The Journal of Immunology*, *148*(9), 2953-2960.